U.PORTO

INSTITUTO DE CIÊNCIAS BIOMÉDICAS ABEL SALAZAR
UNIVERSIDADE DO PORTO

Universidade do Porto
FEUP Faculdade de Engenharia

Mestrado Integrado em Bioengenharia

Lipid nanoparticles for topical and transdermal application for alopecia treatment

Dissertation

Maria João Bidarra Tavares Gomes

Supervisor:

Prof. Dr. Salette Reis

Faculdade de Farmácia da Universidade do Porto

July 2012

Approved in public trials by the jury:

President: Alexandre Quintanilha (IBMC/UP)

External examiner: Susana Martins (FF/UP)

Supervisor: Salette Reis (FF/UP)

Acknowledgments

This study was carried out in the period between March of 2012 and July of 2012 at the Departamento de Química da Faculdade de Farmácia, under the supervision of Professor Doctor Salette Reis, at the Universidade do Porto.

I would like to express my gratitude to my supervisor Prof. Dr. Salette Reis, for her constant advice, guidance and support, for giving me the opportunity to work on this interesting topic, and also for the kindness and motivation during all the time.

I would like to thank Dr. Susana Martins of Departamento de Tecnologia Farmacêutica da Faculdade de Farmácia da Universidade do Porto, for her help in the analysis and interpretation of some results.

I would like to thank Prof. Dr. Amália Jurado and Catarina Grilo from CNC Coimbra for using the DSC, and also for their help with the DSC experiments.

I would like to thank Prof. Dr. Marcela Segundo of Departamento de Química da Faculdade de Farmácia for her help and guidance during HPLC experiments.

I would like to thank all the people of Departamento de Química da Faculdade de Farmácia, for the excellent working environment provided, it was a great experience.

Finally, I want to thank my family and friends, especially my mother for her support and love, thank you for always being there for me; and my sister that, near or far, always supported me, thank you for giving me strength in the last days.

Abstract

Alopecia is a dermatological disorder characterized by the reduction of visible hair. This abnormality affects the hair follicle and causes its shed. There are different types of alopecia according to its cause, but one of the most common types – androgenic alopecia – affects up to half of the Caucasian male population by middle age, and almost all Caucasian men by old age (95%). Besides, it also affects women. Therefore, and since this disorder also affects psychologically, it is urgent to develop new drug delivery systems able to improve alopecia therapy. The *stratum corneum* (SC) is the main penetration barrier to the access of the majority of the chemicals that come in contact with the skin. Several nanoparticles (e.g. liposomes and lipid nanoparticles) have been developed to penetrate the SC. These nanoparticles have proved to be effective in dermal application of cosmetic and pharmaceutical forms, showing beneficial properties such as: drug delivery and controlled release; increase in skin penetration and skin hydration, and an excellent tolerance.

The present work aims to explore the nanotechnology potential in alopecia therapy, based on the development and optimization of lipid nanocarriers (NLC) that were characterized and evaluated regarding the shelf stability. It was also assessed the suitability of these NLC as carriers for dermal and transdermal delivery of anti-alopecia drugs by the evaluation of several important parameters.

Anti-alopecia drugs: minoxidil and finasteride were encapsulated in NLC prepared by ultrasonication method. NLC for all drugs showed mean particle sizes bellow (some of them around) 200 nm, as desired to achieve the dermis and the hair follicles, and zeta potential values around -20 and -30 mV, which indicates a good physical stability. Over a month of storage little variations in these parameters were observed, which indicates that all nanoformulations are stable in storage. SEM measurements showed that all NLC exhibit a spherical shape and a smooth surface independently of their composition. Differential scanning calorimetry (DSC) studies allowed the determination of phase transition temperatures. A high loading efficiency (around 90%) was achieved for finasteride, while only nearly 30% was achieved for minoxidil NLC over a month. Penetration assays through pig ear skin demonstrated that NLC loaded with minoxidil and finasteride have low levels of penetration.

In conclusion, the proposed novel formulation present several good characteristics which indicate that can be an excellent non-invasive therapy for alopecia.

Key words: nanostructured lipid carriers (NLC), alopecia, anti-alopecia therapy, minoxidil, finasteride

Contents

List of Figures

List of Tables

1 Aims and Organization of the Dissertation

Lipid nanoparticles have features that make them interest for the pharmaceutical and cosmetic technology research groups worldwide. This is the main reason why LNs importance is increasing. Currently, solid lipid nanoparticles (SLN) and nanostructured lipid carriers (NLC) have been already investigated as carrier systems for many applications.

This dissertation aims the development of an innovative nanoformulation based on the combination of two anti-alopecia drugs carried in lipid nanoparticles (NLC). The formulation developed should be able to deliver the drugs specifically to hair follicles where they may act. Given the ease of application, and the probably synergic effect obtained by the combination of two of the most widely used drugs, the formulation developed is promising.

The first part of this dissertation is organized as follows: in the first sections the skin histology and physiology are described, as well as the different types of drug penetration into the skin; also the pharmaceuticals forms and drugs used to treat alopecia are presented, which are important to understand alopecia aetiology and its treatment. This introduction of skin and alopecia led to literature review with respect to the uses of lipid nanoparticles as dermal drug delivery systems. In addition, characteristics of nanosystems in general and the features of LNs in particular, as topical delivery systems, were mentioned.

Secondly, it is presented the work developed aiming the production of such nanosystems with the ability to incorporate and deliver the anti-alopecia drugs into the dermis and hair follicles. These systems were characterized and investigated with regard to physical (size, charge, morphology and polymorphic modifications), chemical (drug loading) properties. The stability of NLC over a month was also assessed. Finally, the penetration profiles of drugs were also analyzed.

2 Introduction and State of the art

2.1 Skin

Skin, the major human organ, is a heterogeneous membrane: lipophilic on its surface and hydrophilic in its deeper layers[1]. Skin is very complex due to its histology and this is translated in multifaceted functions. Those skin roles have an utmost importance to human survival and welfare. Regarding this and also taking into account the need to penetrate skin for therapeutic purposes, this field deserves careful attention in order to progress towards efficient nanomaterials capable of reach and correctly act on their target while maintaining skin integrity. Consequently, drug penetration routes into the skin as well as evaluation of drug release, percutaneous penetration and skin retention are important aspects that need to be studied.

2.1.1 Histology of the skin

Skin has three different layers – epidermis, dermis and hypodermis (**Figure 1**) – that have distinct composition and functions. Usually, epidermis and dermis are considered more important from a penetration perspective[2]. In epidermis, keratinocytes are the most abundant cell phenotype and are organized in five different strata (*stratum basale* (in contact with dermis), *stratum spinosum*, *stratum granulosum*, *stratum lucidum* and *stratum corneum* (SC, in contact with the external environment)), reason why epidermis is histologically classified as a stratified epithelial layer[2]. From the *stratum basale* to the SC, keratinocytes undergo a progressive modification, varying in shape and cytoplasm content, that enables epidermis to keep healthy and defensively competent since this process promotes a continuous regeneration and renewal of its components. According to this, epidermis could be distinguished in viable epidermis (VE) and SC where keratinocytes are completely differentiated into anucleated cells filled with keratin and keratin cross-linked with filaggrin (histidine rich protein, responsible for filament compaction, that binds keratin fibers[3]) – called corneocytes[2,4]. Those corneocytes (diameter 30 to 50 μm and thickness 0,2-0,8 μm) are disposed along 15 to 20 layers that consist SC and are spaced from each other by a gap of approximately 75 nm under air-dried conditions. Thus, corneocytes delimit a tortuous path that is filled with a complex matrix of organized lipid bilayers[1,2,5]. Summarizing, SC is the outermost layer of the skin and is comprised of a 10-20 μm thick matrix of dehydrated and dead corneocytes that are embedded in highly ordered lipid layers, which serve as a cover[5,6]. On the other hand, the VE is approximately 100-150 μm thick and composed of multiple layers of keratinocytes and several other types of cells. The hypodermis or subcutaneous tissue resides below the dermis and is composed of loose textured, white, fibrous connective tissue in which fat and elastic fibres are combined[6].

Regarding hydrophobicity/lipophilicity, SC is lipophilic and contains ≈ 13% of water, while VE is significantly hydrophilic (> 50%). In the dermis the water content reaches 70%, favouring hydrophilic drug uptake[1].

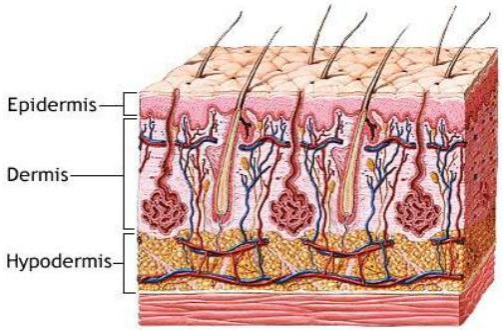

Figure 1: Schematic cross-sectional representation of skin[7].

SC hydration is important to prevent SC mechanical failure and cracking, and assures preservation of SC enzyme activities that supports the terminal differentiation of SC layers and a correct self-assembly of intercorneocyte lipids. Therefore, its regulation (that depends on the proteolysis of corneocyte content, which produces a mixture of osmotically active amino acids that are able to sequestrate water and to act as moisturizing factors) is essential as well[2]. SC microstructure is fundamental to study skin penetration since it involves hydrophobicity concepts as it refers to supramolecular organization of intercorneocyte lipids that are assembled in parallel head-head tail-tail repeating bilayers. As a consequence, repeating hydrophilic and lipophilic regions exists within those bilayers. Regarding SC spatial organization, it depends on the type and amount of intercorneocyte lipids[2]. The most common intercellular lipids (nearly 80% are apolar) may be classified in four categories: cholesterol and its derivatives, ceramides, free fatty acids, and triglycerides[2,5]. Their fluidity is lower on lipid heads in comparison with tails, and tails region is also known as the transdermal intercellular apolar (or lipidic) route of skin absorption. Nevertheless, skin may also contain aqueous pores that contribute to the transdermal intercellular polar (or hydrophilic) route of skin absorption[2] (see section *2.1.3 Skin penetration*). Furthermore, SC chemical composition determines that SC, as a whole, is generally referred as a lipophilic stratum, in contrast to the higher amount of water in VE which contributes to its hydrophilicity. Consequently, hydrophobicity change in epidermis is not homogeneous – hydrophilic-lipophilic gradient. Proving that, it is well known that moderate oil in water (o/w) partition coefficient of a penetrating molecule is one of the key parameters for a successful transcutaneous absorption[2].

Other important skin components are sweat glands and hair follicles. These glands are coiled tubular that extend from SC to dermis or hypodermis (2-5 mm in length) and are involved in thermoregulation and excretion of acids and body wastes. Hair follicles consist of a hair infundibulum (the part between the skin surface and the point of the sebaceous gland duct opening to the hair canal) generally supporting one hair and serving as a route to expel the product of associated sebaceous gland

(sebum)[2,8]. Both components create openings on skin surface, providing breaches that may be used as potential ports of ingress.

The hair follicle, hair shaft, adjoining arrector pili muscle and associated sebaceous gland(s) together form an integrated structure recognized as the pilosebaceous unit (PSU) – a skin appendage (**Figure 2**). This complex 3-D structure within the skin possesses a unique biochemistry, metabolism and immunology[8,9,10]. The hair shaft is composed of the medulla, the cortex with melanosomes, and the cuticula[8].

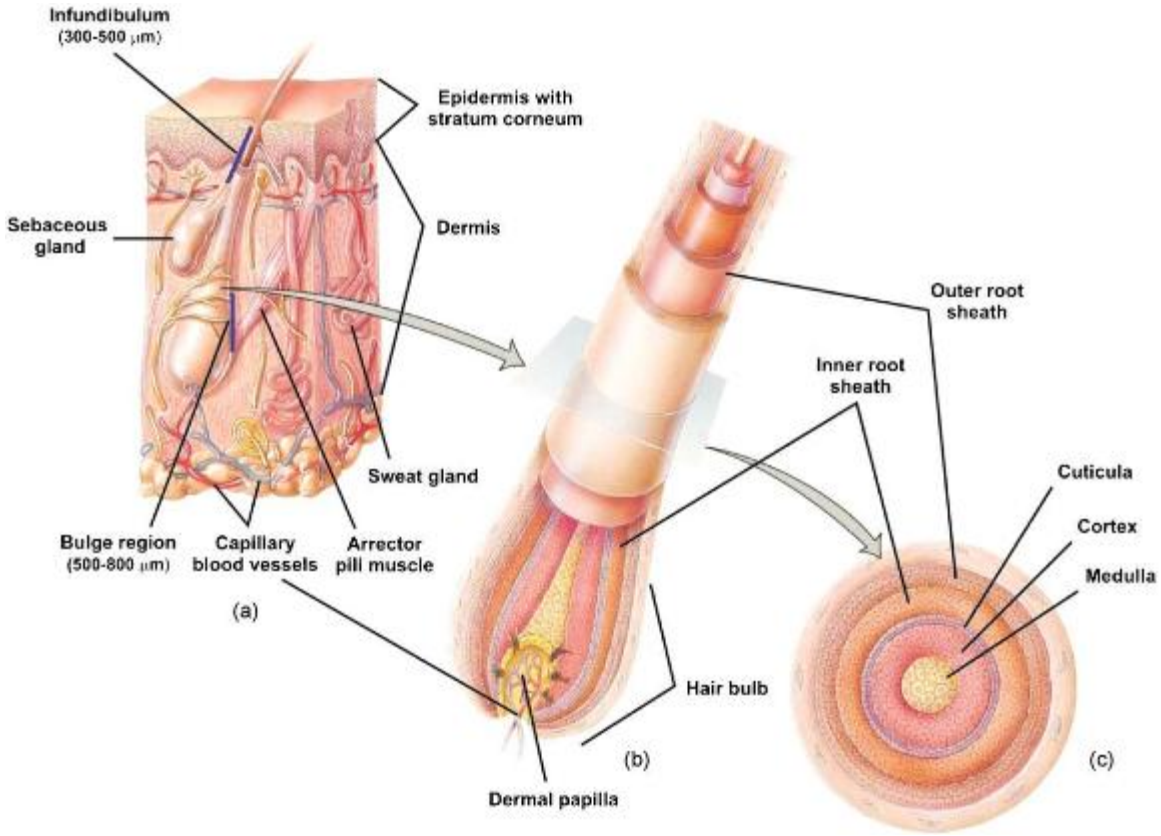

Figure 2: Diagram of the (a) structure of the skin and pilosebaceous unit, (b) structure of the hair follicle, and (c) cross-section of the hair[8].

The hair follicle, apart from contain many cell types that produce highly specialized proteins, consists of a hair bulb and shaft enveloped in an inner root sheath, an outer root sheath, and an outermost acellular basement membrane. The outer root sheath is a keratinized layer continuous with the epidermis[9,10]. Hair follicles are also connected with a network of blood capillaries[8]. A key function of the PSU involves the synthesis and release of sebum – a fungistatic and bacteriostatic mixture of short chain fatty acids produced by sebaceous glands[8,10]. Those glands (androgen-responsive glands), connected to the hair follicle by ducts, are outgrowths of epithelial cells[9].

There are two types of human hairs - terminal hairs and vellus hairs. Terminal hairs are those androgen-independent (eyebrows, lashes) and hormone-dependent (scalp, beard, chest, axilla, pubic region). These hairs are long (> 2 cm), thick (> 0,03 mm), pigmented and usually contain a medullary cavity. These hairs also extend more than 3 mm into the hypodermis. In contrast, the rest of the body in adults is covered

with vellus hairs which are generally short (< 2 cm), thin (< 0,03 mm), unpigmented and typically extend just 1 mm into the dermis[8,10]. Skin follicular density varies between different anatomic regions. On the face and scalp, there are 500-1000 PSU per square centimeter with each follicular opening exhibiting a diameter of some 50-100 μm. The area of these orifices may represent 10% of the total surface area of the face and scalp. In other parts of the body, the follicular openings constitute only about 0,1% of the total skin area. The sole of the foot, the palm of the hand and the lips do not have hair follicles[8,9,10]. Hair shaft diameters have relatively little variation (16-42 μm)[8].

In human, the hair grows cyclically (a continuous cycle) with alternating periods of activity and rest (**Figure 3**). The cycle has an active growth stage with a rapid hair matrix cells division and migration upward to form the hair shaft (anagen), with parallel melanin production[11]. This phase is followed by a regressive stage with cessation of mitosis and the lower portion of the hair follicle is largely resorbed through apoptosis (catagen). Catagen phase conclusion gives rise to a resting follicle (telogen) and finally a lag phase – resulting telogen hair is a quiescent tissue – during which hair shaft is shed (exogen). The cycle then returns to anagen and the lower follicle is reformed. Recently another stage has been described – kenogen – as the lag time between exogen and new anagen. In human scalp hairs the cycle lasts about 4 years, and nearly 90% of the time is spent in anagen (catagen and telogen are relatively short)[8,9,10,12]. This cycle is controlled by locally active inhibitors. The duration of each growth phase as well as the percentage of hair in each growth phase differs between vellus and terminal hairs. In addition, seasonal variations in hair growth are modulated by the endocrine system[10]. Moreover, the rate of scalp hair shaft elongation is between 0,3 and 0,4 mm per day[8].

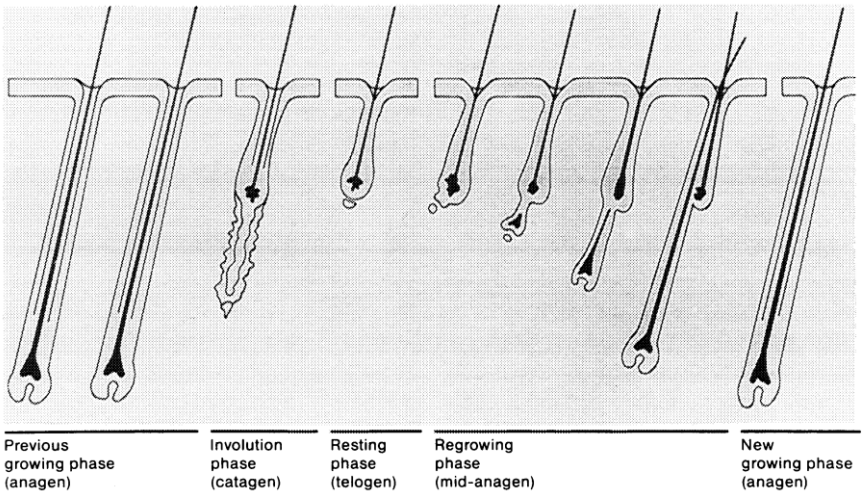

Figure 3: Growth cycle of hair follicle[12].

2.1.2 Major Skin Functions

The skin surface is an ecosystem in equilibrium with precise characteristics. Skin has many different functions, but the main one is to defend the body from the external environment – skin provides a natural barrier against exogenous aggressions and particles penetration[13]. Therefore, skin confers the capability to prevent the entrance of chemical and biological agents due to SC structure and composition[2]. Dermis, which is a more inner layer than epidermis, has capillary anastomoses capable to carry nutrients and oxygen to the epidermis, and also clear the dermis from cell metabolic products and penetrated foreign agents. Otherwise, the outer skin layer epidermis (majority the SC) acts as a defensive layer and, therefore, influence the ingress and diffusion of foreign nanometric agents[2]. Due to that, SC is commonly referred as the main skin barrier, function that results from the cooperation and interactions between SC macro and microstructure, supramolecular organization of SC lipidic matrix, and SC whole composition[2]. The SC constitutes only 10% of the entire skin but contributes to over 80% of the cutaneous barrier function[5]. The SC presents a barrier to most low molecular weight compounds and prevents intact nanoparticle ingress[14]. Therefore, as SC cells, corneocytes represent the first macroscopic physical barrier against the penetration of foreign agents, also assuring impact resistance. Although, besides those defensive functions, foreign agents (like therapeutic nanoparticles and microparticles) can be delivered in diseased skin and to hair follicles openings[13].

Besides this, skin also minimizes the effects of UV and IR radiations by absorbing them (UV), and dissipating associated heat through the regulation of blood flux, perspiration, and/or sweating (IR). In addition, cellular and molecular barriers are also important and all molecular or biological agents that manage to overcome the skin have to face them[2]. Like that, SC acts as a protective barrier thanks to key enzymatic reactions, bacterial flora, immune signalling compounds, and preservation of the acidic pH[5]. On the one hand, key enzymatic reactions play important roles since they are necessary for the desquamation, a protective mechanism that contributes to the elimination of both microorganisms and cells. On the other hand, the resident bacterial flora in the skin constitutes a complex ecosystem that is very important in skin defence against potentially pathogenic organisms. Furthermore, the SC is a biosensor that regulates the responses of the epidermis – SC senses the level of cytokines and growth factors, which are keys to the inflammatory reaction. Finally, pH in SC is acidic (ranges between 5 and 6) which is crucial to integrity and cohesion of the SC, and to enzymatic activities. To maintain the acidic pH, endogenous (such as secretion of sebum) and/or exogenous (originated outside the epidermis) variables cooperate[5]. Therefore, skin protective functions are against external mechanical, chemical, microbial and physical influences[6].

SC structure contributes to its homeostatic function preventing the loss of water from the epidermis. The existence of a water-resistant skin keeping water in and exogenous substances out is a key aspect for living on Earth. As the main function of

the skin is to protect the inner body and this one is rich in water, the protective function is also against the dry environment[1,5]. Therefore, SC allows the maintenance of the body hydration which is needed to maintain flexibility, among other things. Moreover, water permeability is a reason why lipid regions are considered to be great barriers of the skin[1,5].

Additionally, the SC provides protection from the outside environment through its antioxidants – which are capable of protecting against lipid peroxidation and allow the stabilization of lipid bilayers[5]. SC is also responsible for the maintenance of body temperature since it is in charge of isolate the organism from environment, and this barrier acts also as a reservoir for topically applied substances[15].

2.1.3 Skin penetration

The treatment of a local cutaneous dermatologic or pathologic condition could be made using different means, but there is no doubt that directly applying a pharmaceutical formulation is easy, convenient, and generally well accepted by patients. Regarding these reasons, skin has been extensively used for the cutaneous and percutaneous delivery of therapeutic drugs[2]. Also because of large surface area and easy accessibility, skin delivery has potential on application in drug delivery[6]. Besides this, local skin targeting is of interest for the pharmaceutical and the cosmetic industry[9]. A topically applied substance has distinct possibilities to penetrate into the skin since this delivery involves, in addition to the transdermal route (through SC), the transfollicular route through pilosebaceous unit – comprising of hair follicle and sebaceous glands[9].

There are many factors that can affect the cutaneous absorption of a molecule (and consequently a nanoparticle or nanomaterial too), and those may be distinguished in three different classes: (i) location and skin conditions at the application site; (ii) physicochemical properties of the penetrating molecule; and (iii) physicochemical properties of the vehicle dispersing the penetrating molecule[2].

The skin integrity variation (by dermatological and other pathological conditions, damage and trauma...), dimensions of orifices and aqueous pores, and density of appendages are conditions affecting the absorption of any agent (i). Also thickness of SC varies in different body regions and pilosebaceous units are unequally distributed in the body (their density and diameter of hair follicle orifices vary per each body location). Further, age, skin type and sex hormones influence skin permeability. Other factors like SC hydrophilic-lipophilic gradient, skin temperature and methods of application (massaging a formulation on the skin could increase the local temperature) could favour the penetration of particulate formulations. Therefore, depending on body site, skin absorption through the transdermal or transfollicular route may be favoured or limited. Thus, penetration of nanometric agents through hair follicles (transfollicular route) should be anatomically favoured in the forehead, where they represent 1,28% of

skin surface. As well, transdermal route should be favoured in those body locations where SC is less thick, or has been exfoliated or abraded with cosmetics, sand, or similar products[2,5].

Several properties of the molecule influence its permeation (ii). Some of them are: solubility and dissolved amount of the penetrating molecule in its vehicle (the highest solubility of a molecule in its vehicle is correlated with the highest thermodynamic activity of that formulation, and consequently with the greatest probability to transdermally deliver that molecule); pK_a of the penetrating molecule and pH of vehicle (only the unionized fraction of a penetrating molecule will be transported to VE); MW of a penetrating agent (that should be less than 500 Da to significantly permeate skin); and the diffusion coefficient (D) of the penetrating molecule in its vehicle and in the skin. Also very important is the o/w partition coefficient of the penetrating molecule since a very lipophilic molecule will easily partition in SC but will leave it with difficulty, whereas a hydrophilic molecule will suffer poor penetration. Additionally, there are some less important features that, however, should not be underestimated as the potential for binding and metabolism. Particle stability is another important parameter and it includes particle disassembly, rupture, stability against chemical reactions (which is capable to modify its superficial properties), and ability to form micelles after contact with specific structures/components of the skin or to be de-coated. Therefore, particle stability could influence numerous other properties. Probably the most significant parameters of the penetrating nanoparticle are the dimension (size), shape and superficial properties (e.g. charge, polarity) since they influence several aspects such as the ability to enter the skin, the selection of the penetration route, the depth of penetration, the coefficient of diffusion in the dispersing vehicle and in the skin, and the potential to establish interactions with skin components (e.g. charge, dipole, hydrophobic, and/or hydrogen-bond interactions). “Shape deformability” and “dimension versus orientation” should be pondered since rigid or deformable shapes and their orientations may influence nanoparticle/nanomaterial passage across a structure with a defined porosity. Superficial charges (frequently it is the coating which is charged), which may interact differently with various components of skin and routes of penetration, usually prevent nanoparticle/nanomaterial aggregation[2,5].

When a formulation is applied on the skin, all its ingredients are too. Thus, all of them are subjected to skin absorption, although to different extents (iii). As a result, the type of formulation where agents are dispersed (its physicochemical properties), possible synergisms/interactions between vehicle-agent-skin, and the application method will definitely affect the absorption outcomes. It is necessary to take into account that many different things could happen – water and volatile compounds will evaporate, non volatile ingredients will be absorbed to different extents, and skin, sweat, and/or sebum components will diffuse in the applied dose. Therefore, composition and penetration ability of formulation components (besides the agent) should not be underestimated – potential enhancing effects could be provided by the ingredients of applied formulations[2].

Several techniques and formulations have been developed to successfully overcome skin barriers[2]. When penetrating agents are molecules, scientists indicate small (<500 Da) lipophilic and uncharged compounds as the best candidates for a successful percutaneous absorption. Recent studies have shown the importance of hair follicles for the absorption of large molecules and particles, or for small hydrophilic molecules[2]. In general, depending on the lipophilic or hydrophilic properties of a drug, it will accumulate in the SC (lipophilic substances), or stay on the surface (very hydrophilic drugs) or cross the skin (amphiphilic drugs)[1,4]. Therefore, the ingress of foreign agents in the SC (as well as their further progression toward the VE) is limited by their features, SC nanoporosity and gradients[2].

It is important to highlight that skin architecture, composition and metabolism potential differ in different species, and therefore only those studies with a very similar experimental set-up should be compared[2]. Furthermore, parameters that affect nanosystems penetration should be studied using the dispersing medium where nanoparticles/nanomaterials are found, and mixtures mimicking human sebum, sweat and sweat-sebum emulsion of healthy and unhealthy people of various ages[2].

2.1.3.1 Major routes for drug penetration into the skin with a special focus in the transfollicular and transdermal route

Drug delivery through the skin has gained popularity because it avoids first pass metabolism effects, gastrointestinal irritation, and metabolic degradation associated with oral administration – systemic side effects are reduced[8,16]. Beyond this, it offers other advantages over the intravenous dosage form such as minimization of pain (non-invasive)[4,6], and avoidance the major fluctuations of plasma levels typical for repeated administration of rapidly eliminated drugs[15].

It is well known that the micro and macromolecules can enter into the skin through three distinct pathways (**Figure 4**): (A) the intercellular pathway – through the lipid matrix that occupies the intercellular spaces of the corneocytes, (B) the intracellular (transcellular) pathway – through successive bilayers and dead cells, and (C) transappendageal pathway – across skin appendages: hair follicles, sebaceous glands and sweat glands[5,6]. Transdermal route involves pathways A and B, while transfollicular route is equivalent to pathway C.

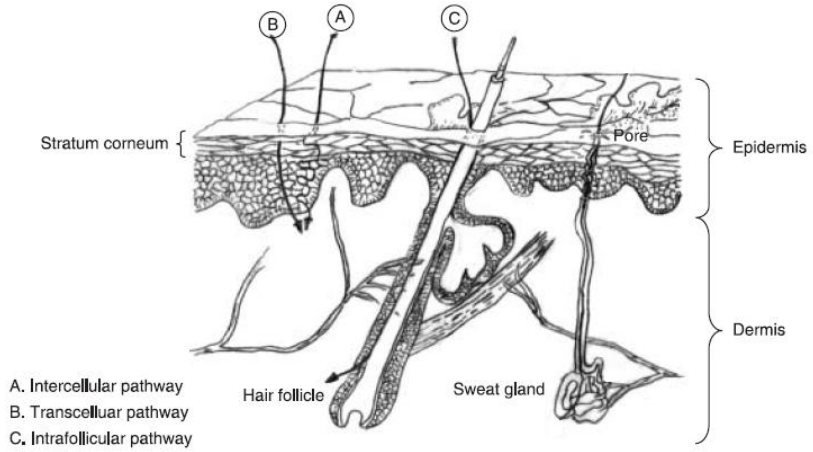

Figure 4: Penetration pathways in the epidermis, through the SC (adapted)[5].

Although it is generally believed that the intercellular route may dominate during steady state penetration of compounds, it has been argued that the skin appendages (hair follicles, pilosebaceous and sweat glands) may offer an alternative pathway for a diffusing molecule, more significant than previously believed[10,17].

Usually, substances smaller than 500 Da, with sufficient oil solubility and high partition coefficient can be absorbed into the skin. In contrast, larger molecules (molecular weight higher than 500 Da) are not able to pass the cutaneous barrier[5,6].

The worldwide transdermal market, in 2000, was worth US$2 billion and represented the most successful non-oral systemic drug delivery system. Nevertheless, transdermal drug delivery is not suited to all drugs and is not justified for all therapies; however there remains a large number of drugs for which it is desirable but presently unfeasible[4].

The transdermal route of administration avoids hepatic first-pass metabolism and allows sustained drug release into the systemic circulation[1]. This route has other advantages as the skin presents a relatively large and readily accessible surface area (1-2 m^2) for absorption[4].

Since skin acts as a natural and protective barrier, transdermal drug delivery is a challenging task for the pharmaceutical scientists. Therefore, in order to increase therapeutic molecules permeability into/across the skin and expand the range of transdermally delivered drugs, several methods/strategies have been examined. A drug penetrates into the skin by a passive diffusion mechanism (according to Fick's Laws), depending on its molar mass and physicochemical properties[1,4]. The simplest approaches to optimize transdermal drug delivery are passive and involve formulation manipulation. One of the most important and extensively investigated strategies is the introduction of reversible structural alterations within the skin (lipidic matrix) by addition of chemical enhancers[4,6]. Another main aspect to reduce skin barrier capability is hydration – using water is the safest method for increasing skin penetration[1,4].

Moreover, other way to do so is changing lipophilicity of the drug/formulation. Also a saturated formulation of the drug will provide the maximal flux[4].

If molecules are large (molar mass bigger than 500 Da), active mechanisms have been developed to overcome the barrier and respond to this challenge[1,4]. Microneedles, jet injectors, iontophoresis, ultrasound (sonophoresis), electroporation, photomechanical waves, magnetophoresis, laser radiation and skin abrasions are some of the main mechanical, physical and active transport techniques available to enhance skin penetration of various drugs[6]. In electroporation (electropermeabilization), high voltage (100-1000 V) electrical impulses are applied during short time intervals (micro- to millisecond) to create temporary pores on the skin. Such pores provide drug penetration routes[1,4,18]. Sonophoresis uses low frequency ultrasonic energy to disrupt lipid packing in the SC creating aqueous pores, which improve drug delivery[1,4]. Iontophoresis is an electrically assisted method where the drug has to be used in an ionic form – it drives charged species into tissue. By applying an small external electrical field to the skin the active ingredient will be accelerated and as a result of electromigration and electro-osmotic forces it will be transported into the skin layers[1,4,18]. Drug penetration through damaged regions of the skin depends on the polarity, valence, mobility of the ions and formulation components[4,18].

After the drug reaches into the skin membrane, it must be sufficiently mobile to diffuse across the SC, which is a complicated diffusion process due to the viscosity of the lipid matrix. This diffusion is extremely sensitive on molecular size[4].

The transfollicular route – generally associated with the lipidic pathway because of the lipophilicity of sebum that is released by sebaceous glands in the hair follicles – has been largely ignored because hair follicles constitute only 0,1% of the total skin[9]. However, the hair follicle has great potential for skin treatment due to its deep extension into the dermis and so it could provide much deeper penetration and absorption of compounds under the skin than seen with the transdermal route. Consequently, there are doubts about transfollicular route and if it plays an important role on the skin absorption of nanoparticles. Scientists have distinct opinions about transfollicular route importance[2,10]. Still, for certain drug delivery systems, hair follicles are privileged penetration pathways. They enter faster into them than through the SC, and then offer the possibility to create high local concentrations of the active compounds within the follicular duct[9]. It has been shown that smaller particles accumulate better and deeper in the hair follicle than larger ones[2]. Furthermore, it was calculated that the storage time of the particle based drug delivery systems in the hair follicles was 10 days compared to short-term storage time in the SC – hair follicles are long term reservoirs[6,8].

In some skin diseases, delivery to sweat glands or to the pilosebaceous unit is essential for the effectiveness of the drug. As an example, there are many diseases of the hair cycle (androgenic alopecia, hair colour loss, alopecia areata ...) that need effective therapeutics which would be more successful if they could be specifically targeted to the hair follicle[10,11]. Within the hair follicles, different target sites of interest have been

defined – the sebaceous gland is of particular interest and is associated with the aetiology of androgenic alopecia; the midfollicle bulge since it has stem cells responsible for follicle reconstitution; and follicular papilla and hair matrix cells, as both have an important role in controlling hair growth (number of matrix cells correlates with the size of the new hair, while melanin concentrations in the matrix cells modulate hair pigmentation)[8,10,13]. In addition, transfollicular route enables the delivery to specific sites of the hair follicle, the increasing of drug concentration within the pilosebaceous units, the possibility to reduce the applied dose of a drug and/or the frequency of its administration, the reduction of hepatic metabolism and drug systemic toxicity. Due to those reasons, transfollicular administration has been increasingly recognised as potentially significant in the percutaneous drug delivery paradigm, and therefore is having more therapeutic interest[10]. Thus, recent studies have focused on the hair follicle as a potential pathway for both localized and systemic drug delivery[9,10]. Therefore, targeted drug delivery to the pilosebaceous compartment may have several therapeutic applications for treating numerous hair follicle associated disease states. Those applications include targeting drugs to the bulge region for gene delivery to facilitate long-term gene correction of congenital hair disorders or genetic skin disorders; PSU utilization as reservoirs for localized therapy or as a transport pathway for systemic drug delivery; and target sebaceous glands to the treatment of acne and androgenetic alopecia[8].

Nevertheless, access to transfollicular route for drug penetration can have some architectural and physicochemical constraints like the membrane that surrounds the entire follicle and the keratinous layers of the inner and outer root sheaths that may physically restrict passage of molecules deep within the follicle. Other barriers include size selectivity of the follicular openings, the sebum flow into the hair follicle (assuming that sebum flow has an upward movement) which may impede drug transport, and the hair growth cycle that also appears to influence pilosebaceous drug delivery[9,10].

Numerous studies have suggested that the enhancement of follicular delivery may be done by applying certain approaches – such as the use of optimised vehicles (use a volatile organic solvent like ethanol – lipophilic – in order to dissolve sebum from the follicular canal); decreasing particle size; or massage following application[8,10]. Furthermore, pre-treatment of the skin with cyanoacrylate skin surface stripping (CSSS) removes the superficial part of the SC and sebum, facilitating penetration[8].

A different method has been introduced – skin sandwich model – to estimate the importance of the transfollicular route[8,10,18].

In summary, transfollicular penetration could be used by those agents whose dimensions are below follicular openings (10-210 μm) and able to disperse themselves into sweat or sebum (lipophilic). Penetrating agents could easily enter the VE or blood stream depending on its penetration depth[2]. In contrast to transdermal route, transfollicular is favourable for high-molecular weight substances[8].

2.1.3.2 *In vitro* evaluation of the release, percutaneous penetration and skin retention

Deliver an active compound transdermally implies the reduction of barrier function of skin and the enhancement of permeation of the active compound through skin. Consequently, several approaches (select an adequate vehicle, chemical modification of an active gradient, among others) were used to enhance the skin permeation of the active ingredient[19].

As formulations remain stable (a characteristic also important to assess), the evaluation of the drug release rates, percutaneous absorption/penetration and skin retention became a crucial step to further validate the possible usefulness of that drug in those formulations[20]. In order to assess nanosystems' drug release, penetration and retention in skin, *in vivo* studies could be made. However, when it is not possible to do them, the equipment and material are not available, or even before their practice, *in vitro* tests could be a possibility. Some of those tests are here described.

For this kind of studies, the first step is done in order to identify a suitable receptor medium for *in vitro* experiments (to create *in vitro* conditions which can replicate the *in vivo* ones). For this, the saturation solubility of the drug in different media (solvents) is analyzed (drug content is analysed by HPLC) and the selected medium should be the one with the highest solubility[20].

The release of the drug from topical preparations depends on the physicochemical properties of the vehicle and the drug employed[16]. In many studies, *in vitro* drug release rates from its formulation is measured through synthetic membranes (of nitrocellulose, cellophane, ...) using vertical Franz diffusion cells setup[16,20,21]. Synthetic membrane is usually sandwiched between the upper donor compartment and the lower receptor compartment of Franz diffusion cells; a quantity (≈ 0,5 to 1 g) of the formulation containing the drug is placed on the surface of the membrane in the donor compartment, while the receptor compartment is filled with the previous selected receptor medium, which is in contact with the membrane. During the experiment, the receptor solution is continuously stirred (at ≈ 100 to 300 rpm) and kept at a proper temperature (37 ± 1 °C). Samples of this receptor medium are taken from the receptor compartment, at predetermined time intervals, and therefore the amount of released drug is analysed by HPLC and its diffusion coefficient (D) is calculated. It is important to note that D reflects the facility by which molecules move through the membrane and through the formulation. All measurements are typically performed, at least, in triplicate and formulations without the drug are used as control[16,20,21].

The drug released from nanocarriers (as solid lipid nanoparticles) into the receptor medium at room temperature could be measured by weighing ≈ 0,5 g samples of nanocarriers into test tubes containing 10 mL receptor medium. Those tubes are

sealed and placed in a rotary tube shaker. After each pre-determined time intervals, the contents of the tubes are filtered and the drug content determined in the filtrate[22].

A drug that is loaded into a topically applied nanoparticle must be released by the particle whilst on the surface of the skin, if it is to penetrate the SC. This requirement to achieve adequate drug release upon application to the skin is counterbalanced by the need of the particles to retain the drug prior to application. Those concepts were taken into account in a study where minoxidil loaded lipid nanoparticles foams and polymeric nanoparticles foams with a lipid core were assessed. In this study, the effect of the premature minoxidil release from nanoparticles on drug permeation across a barrier was assessed using a silicone membrane (an accepted alternative to skin). It was found a limited capability of minoxidil (from PN and LN foams) to cross the silicone membrane – probably because hydrogen bonds formed between minoxidil and silicone[14].

Percutaneous absorption of drugs from topical formulations involves the release of the drug from the formulation and permeation through skin to reach the target tissue[16]. It is important to note that penetration is called permeation if the drug reaches the systemic circulation[1]. Techniques to quantify percutaneous absorption both *in vitro* and *in vivo* have been developed and are continuously improved[15]. As in other fields, studies about skin permeation are more direct, relevant and conclusive if i*n vivo* and in humans. Even so, the advantages of *in vitro* experiments are obvious (as lower cost and the ability to test large numbers of formulations in relatively short time) and many times overcome their disadvantages. Pig ear skin is considered an excellent skin model, since the histological characteristics similarity between pig and human skins. Therefore, pig ear skin model is frequently used for *in vitro* permeation studies of a drug. For the same reasons, rat skin is also commonly used. *In vitro* experiments are performed using human or animal skin, reconstructed human epidermis or perfusion systems such as the perfused bovine udder and pig forelimb model. As mentioned before for drug release studies, Franz diffusion cells are also frequently used to study percutaneous absorption. In this context, usually, a synthetic membrane is used instead of skin. In these absorption studies the skin is mounted on Franz diffusion cells (same setup as release studies) with the dermis facing the receptor compartment (epidermis facing the donor), and a quantity of the formulation containing the drug is placed in the donor compartment, to the skin epidermal surface. The experimental conditions are the same as already described under the release studies. Also, at designated time points, samples of the receptor medium are removed and the amount of drug is analysed by HPLC[15,16,20,21]. Furthermore, another method to evaluate absorption is the tape stripping procedure which determines drug levels in the horny layer (tape stripping cannot give meaningful results for drugs targeted to specific strata of viable skin). Alternatively, for hydrophilic compounds, microdialysis can be used. In this technique, thin (about 100 μm) semipermeable tubes are inserted into the dermis. Then a precision pump provides a continuous flow of a tissue-compatible fluid through the tube. Applied drugs, as well

as other low molecular weight compounds dissolved within the dermis, diffuse into the perfusate which is sampled at regular intervals[15].

In vitro skin retention studies are generally performed after each time point evaluated as described above in the permeation studies[20]. In those cases the skin is removed from the diffusion cell, cleaned with cotton soaked in methanol or with 50% ethanol, and then with water, to remove excess drug from the surface. The solvent is then evaporated with compressed air or absorbent wipes. Then the precipitate deposited on the skin surface is suspended in a medium containing sucrose, KCl and Tris-HCl (pH ≈ 7,4). Instead of this last step, samples could be boiled for 10 minutes in acetic acid (1M) and then centrifuged (≈ 5 minutes at 3000 rpm). As a result, the obtained supernatant is analysed by HPLC. All measurements are also performed, at least, in triplicate and formulations without drug are used as control[16,20,21].

Beside those aspects already mentioned, it is also important to take into account formulation-skin interaction. Usually these studies are done using scanning electron microscope (SEM) with coated skin samples previous subjected to the studied formulation[21]. As well, confocal laser scanning microscope is also generally used to assess depth of penetration[21]. This last microscopy type is a non-invasive methodology (has capacity for *in vivo* application without the need for mechanical sectioning) which gives high resolution images, good time-resolution, and the ability to visualise at multiple depths parallel to the sample surface[8,10]. Further, drug hypersensitivity reactions in skin are significant to future drug compliance and therefore need to be evaluated. T cells (cellular immune response) play an important role in the pathology of those reactions since drugs are presented to them[23].

Studies in this area of skin penetration through different routes have some difficulties as lack of an appropriate and well-characterized animal model to distinguish transfollicular from transdermal percutaneous absorption[9,10,18]. Some studies are based on *in vitro* models and others on *in vivo* (that overcome many of *in vitro* models disadvantages but have ethical constraints)[9]. The scientific community do not have much knowledge about the best animal to be used to mimic specific pathologies/conditions[2,18]. To date, most of the work in this field has been undertaken using a multiplicity of drugs, skin models, application protocols and endpoint evaluation modes. As a result, it has been difficult to discern correlations between penetrating properties, formulation design and the extent of follicular penetration[9,10]. Further, formulations to be applied on diseased skin are generally studied with intact skin, without considering differences in structure and chemical composition between healthy and unhealthy individuals or between different species[2].

2.2 Alopecia and its treatment

2.2.1 Alopecia aetiology and factors that predispose its appearance

There are several dermatological abnormalities and diseases whose aetiologies are related with hair follicle. Acne, androgenetic alopecia, alopecia areata and some skin cancers are among these conditions[9]. Acne – a disease of the pilosebaceous unit – is characterized by hypercornification and hyperkeratosis of outer root sheath and sebaceous duct. Also in pilosebaceous unit, localized cancer may be observed. Other abnormalities included hirsutism which is the growth of coarse terminal hair in female, in part or in whole of the adult male pattern; and hypertrichosis that can occur in a variety of systemic disorders and is defined as the excessive growth of long, often apigmented hair[9]. These two last malformations are a consequence of a prolonged anagen phase with conversion of vellus hair follicles into terminal[8]. The majority of hair growth disorders result from changes in the hair cycle[8]. Some skin disorders such as acne, seborrhea, hirsutism and androgenetic alopecia are consequences of the excess local activity of androgens, more specifically dihydrotestosterone (DHT), in the PSU. DHT is formed from testosterone (T) via the pivotal enzyme, 5α-reductase[17] – as described below.

Alopecia – commonly known as hair loss – results from a reduction of visible hair. This disease has different possible forms according to its distinct causes, and most common clinical patterns are androgenetic alopecia (AGA) or common baldness, telogen effluvium, chemotherapy-induced alopecia, and alopecia areata (AA)[9]. Beyond those, there are other less important alopecia types like neonatal occipital alopecia[24].

Androgenic alopecia is a common form of hair loss in both men and women[13]. It affects up to half of the Caucasian male population by middle age, and almost all (95%) Caucasian men by old age (80 years)[25]. This type of alopecia is caused by a shortening of the anagen stage, with the clinical consequence of increased hair loss, accompanied by a transformation of terminal to cosmetically unsatisfactory vellus hair – eventually, about a third of the total follicles may disappear[8]. Therefore, this process of hair loss is progressive, and related to a perturbation of the hair follicle cycle – shortening of the anagen phase, coupled with a lengthening of the telogen phase. Over time, as the follicle moves through several cycles, the length of the hair that can be grown shortens. As a consequence, with each hair cycle, the hair is shorter, finer and less pigmented. Eventually, the follicle becomes incapable of producing a hair that reaches the skin surface, and the region is recognised as bald[25]. The name AGA reflects the importance of both androgens and genes in this disorder aetiology. The role of androgens is demonstrated by a lack of AGA in pseudohermaphrodites who lack a functional 5α-reductase type II enzyme – which, along 5α-reductase type I, is responsible for the conversion of T to DHT. Both T and DHT bind to the androgen receptor and effect transcription of androgen-dependent genes. Also, AGA is recognised as a genetically multifactorial trait. Proving the relation AGA disorder-androgens, is known that both

the 5α-reductase enzymes and the androgen receptor were more highly expressed in balding follicles compared to non-balding follicles on the same scalp. In addition, it is known that a sequence variation in androgen receptor differed significantly between young balding men (high genetic predisposition) and older men with full heads of hair (low genetic predisposition). This finding reveals androgen receptor as a gene responsible for increased risk of AGA, and it has been estimated that it may confer up to 40% of total genetic risk for this disorder[25].

Telogen effluvium, another common form of alopecia, manifests as excessive shedding of hair and is the result from the synchronous entry of many follicles into exogen phase[9].

Alopecia could be induced by chemotherapy which disrupts the proliferation of matrix keratinocytes in the anagen bulb that produce the hair shaft[9].

Alopecia areata affects almost 0,1% of the general worldwide population and is characterized as a chronic, inflammatory disease resulting in an unpredictable, non-scarring form of hair loss[26,27]. This relapsing disorder can affect any hair-bearing surface, however many areas of irregular baldness are observed on scalp, whereas other body hairs are not so affected[9,27]. AA affects all ages (however it has a peak of incidence between 20 and 30 years), both sexes (though men more often have more severe forms than women), and all ethnic groups[26,27]. The cause and pathogenesis of AA are poorly understood, this complex disorder is thought to be determined by genetic and environmental factors that remain unknown[27]. However, it is also hypothesized to have an autoimmune aetiology mediated by T cells. This hypothesis is supported by the fact that activated CD4 and CD8 T lymphocytes have been found in anagen hair follicles of affected individuals[26]. As a consequence, AA – which is considered a polygenic disease that depends on the additive action of several major genes – could be related to immunogenetics. Various genes that have a role in regulating immunity (as human leukocyte antigens (HLA) genes) have also been associated with susceptibility to AA[26,27]. Further, atopic diseases are thought to be related to AA (risk factors for AA) since they have been associated with 10-60% of AA patients, and the prognosis for hair re-growth is worse in atopic patients than in non-atopic ones[26,27]. Therefore, there is a relationship between AA and some clinical characteristics (which raises AA patients clinical heterogeneity), including a history of atopy, autoimmune disease (12% of AA patients develop co-existing autoimmune diseases), and nail disease (up to 2/3 of AA patients have nail abnormalities). This relation enables the identification of several deregulated chromosomal regions and genes that represents an enriched set of biomarkers relevant to AA pathogenesis – since those regions/genes susceptibility is associated with autoimmunity and atopy[27].

Beyond those forms, complete (or near complete) facial and scalp hair loss (alopecia totalis) and loss of terminal hair from whole body (alopecia universalis) are less prevalent forms of alopecia[9,26].

2.2.2 Drugs used in the treatment of alopecia

For the treatment of alopecia and other diseases that affect hair follicle, there are several target sites within the hair follicle which may be studied for the topical delivery of compounds. These potential target sites could be: outer root sheath (the major target site); the sebaceous glands (desirable target site for some skin disorders, such as acne and androgenetic alopecia); regulatory receptors for retinoic acid, epidermal growth factor and transforming growth factor; the mid-follicle bulge area (this population of cells, found just below the sebaceous gland, possesses one of the fastest rates of cell division in mammals – they are related, for that reason, to cancer); immunocompetent cells for autoimmune diseases. Furthermore, gene therapy may also have great potential as many genes which control hair growth are identified[9].

Several drugs could be used for the treatment of alopecia, as well as for other dermatological diseases. Androgens (as DHT) are steroids involved in hair growth (see section *2.2.1 Alopecia aetiology and factors that predispose its appearance*) and sebaceous gland secretions, reasons why they are involved in skin disorders such as acne, alopecia and hirsutism. Therefore, some antiandrogens are drugs used, by the oral route, to treat these skin disorders. However, they have undesirable systemic side effects which limit their therapeutic use. As an example, RU 58841 and Cimetidine are two antiandrogens. The first one is a new non-steroidal antiandrogen which exhibits a strong topical efficacy, in animal models, on sebaceous gland activity while producing minor systemic effects in the treatment of androgenetic alopecia and hirsutism. The second is a known antiandrogen and is expected to pharmacologically stimulate the pilosebaceous unit, resulting in antiandrogenic activity[9]. Regarding diseases associated with DHT (and 5α-reductase), the possibility to target, to the PSU, 5α-reductase inhibitors in order to alleviate the disease states has been implicated in a number of studies[17]. Finasteride (**Figure 5**), another example of an antiandrogen, is a synthetic steroid that selectively inhibits the action of the type II 5α-reductase enzyme[17,25]. This enzyme, that converts T to DHT, is predominant in prostate, and a 5 mg daily oral dose of finasteride is already approved for the treatment of benign prostatic hyperplasia[25]. Regarding the lack of balding in pseudohermaphrodites, who are naturally deficient in type II 5α-reductase, it was predicted that finasteride would also affect male pattern balding. FDA approved AGA treatment with daily oral dose of 1 mg, and it has been demonstrated to reduce concentrations of DHT in scalp significantly. This treatment is well tolerated by patients, with rare side effects that may include some loss of libido and erectile function. However, the cessation of treatment recommences the balding process, indicating that the effects of finasteride are not curative[25]. Finasteride also has been used topically. In this last case, a preparation is desirable to improve penetration into the skin (especially in sebaceous gland-containing zone), while reducing systemic absorption[17]. Topical application of finasteride loaded vesicular systems (liposomes and niosomes) was already investigated to determine the enhance drug concentration at the PSU.

Studies demonstrate the potentials of liquid-state liposomes and niosomes for successful delivery of finasteride to the PSU[9].

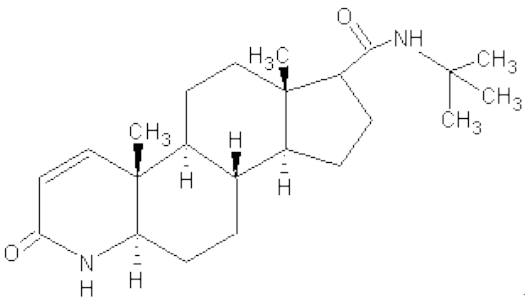

Figure 5: Chemical structure of finasteride[28].

Another drug widely used to alopecia (AGA) treatment is minoxidil[19] (**Figure 6**), a pyridine-derivative[13]. Minoxidil is an ionisable (pKa of 4,6) – soluble in the aqueous nanoparticle dispersing medium – and hydrophilic compound. It is a small molecule with a molecular weight of 209. The aqueous solubility of minoxidil decreased dramatically as the pH of the aqueous vehicle in which it was dissolved increased due to the suppression of drug ionisation[14]. This compound is a vasodilator initially approved as a drug to control hypertension. As hypertensive patients taking minoxidil showed increases in hair growth, a 2% topical solution, and later a 5% topical solution of minoxidil were approved by the FDA for use as a treatment for AGA[25]. Minoxidil appears to halt hair shedding; however, the biological basis for this effect remains unknown. Originally, it was thought that it could be related to the minoxidil vasodilatory properties; later, it was considered that minoxidil actions include stimulation of cell proliferation, and of prostaglandin synthesis[25]. Nevertheless, as finasteride, it is known that minoxidil does not permanently inhibit hair loss processes – cessation of minoxidil treatment is followed by rapid shedding of hairs returning the scalp to an untreated state[25]. Moreover, minoxidil solution has some undesirable consequences as pruritus and scaling of the scalp, caused by irritant contact dermatitis, allergic contact dermatitis or an exacerbation of seborrheic dermatitis – reasons why patients complaint. When studying the effectiveness of minoxidil loaded liposomes as hair growing products, the reduction of telogen period was used as the index of hair growing effects[9]. Despite some mentioned factors, minoxidil has become a mainstay in clinical management of AGA[25].

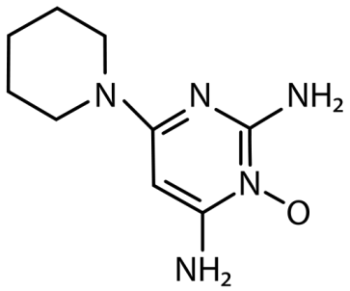

Figure 6: Chemical structure of minoxidil[28].

These most common treatments are not based on knowledge of the underlying molecular aetiology of the hair loss process, but rather hair regrowth was identified as a beneficial side effect when these pharmaceutical agents were used to treat other conditions. Consequently, besides minoxidil and finasteride, there are treatments under development that are more firmly based on aetiological understanding that provide hope for more well targeted and more highly efficacious pharmacological options. One of these treatments is based on dutasteride, which is a dual type I and type II 5α-reductase inhibitor that is approximately 3 times as potent as finasteride at inhibiting type II enzyme action, and 100 times as potent at inhibiting type I enzyme action[25]. If the goal of the treatment is block DHT production, a dual 5α-reductase inhibitor should be preferable to a selective inhibitor. Another studied treatment is with latanoprost, a prostaglandin analogue, which was originally introduced as a treatment for glaucoma and ocular hypertension to reduce intraocular pressure. The effects of this compound were reported on eyebrow and eyelash hair growth and pigmentation – thus the potential for the use of latanoprost as a hair growth stimulant was quickly touted[25].

Moreover, a side effect of anti-cancer treatment with doxorubicin (chemotherapy) is alopecia occurrence. Monoclonal antibodies could be, therefore, capable to prevent alopecia as it was already seen with topical treatment with liposome formulations containing MAD-11 (monoclonal antibody anti doxorubicin). Liposomal delivery of antibody into the epidermal layers resulted in protection against alopecia by forming drug-antibody complexes. The possibility of targeting monoclonal antibodies and other large protein drugs, without loss of biological activity, to the hair follicle may have profound effects on therapies for follicular diseases and abnormalities[9].

As our understanding of the molecular genetics aetiology of alopecia gains speed, it is reasonable to expect that development of more targeted pharmaceuticals based on new knowledge will similarly accelerate.

2.2.3 Commercial pharmaceutical dosage forms and strategies for alopecia treatment

Advancements in new drugs and strategies to treat alopecia are coupled with a growing understanding of the hair loss process and, in particular, the molecular mechanisms through which the process acts. Moreover, as alopecia affects so many people, the baldness treatment industry is worth billions of dollars worldwide annually[25]. Although none of the currently available options are highly efficacious.

The mixture solvent of propylene glycol/water/ethanol (20/30/50, v/v/v) is the composition of the vehicle for commercially-available minoxidil solution (Rogaine, Pfizer). Propylene glycol and ethanol were included not only to solubilise minoxidil, but also to enhance its skin permeation and percutaneous absorption. That is because it is thought that propylene glycol permeates into hairy skin and helps the skin absorb

minoxidil; and ethanol could increase the thermodynamic activity of minoxidil in the vehicle due to its volatile property[19]. Most of commercial products containing minoxidil are solutions with high percentage of alcohol (ethyl alcohol and/or propylene glycol) which recommended frequency of application is twice-daily. As it is deductible, repeated applications of high ethyl alcohol and/or propylene glycol content products lead to severe adverse effects (e.g., scalp dryness, irritation, burning, redness, allergic contact dermatitis). Therefore, new dermatological formulations free of organic solvents are needed to minimize adverse effects and optimize androgenic alopecia treatment[13].

Some traditional strategies for alopecia treatment include various herbal remedies[25]. Several of the available unapproved agents commonly used to treat alopecia are described here. *Serenoa repens*, used in commercial forms Saw Palmetto and Permixon, is a very commonly known product by patients as it is widely available in most nutritional food stores. *Serenoa repens* berries grow naturally and are capable to inhibit DHT production. To be effective the extract of the berries must be taken, not the berries themselves. The product comes in capsule form with 2 to 6 capsules as the recommended daily dose. The cost can range from $12 to $40 per month, U.S. dollars[29]. Kevis is another product, available to men and women, which bind and block androgen receptors by creating a cell-wall barrier to keep DHT out of the follicle. Its active ingredients are a composition of mucopolysaccharides and glycoproteins associated with substances that favour their bioavailability. For this product, a 12 month supply is 216 vials (each vial contains 2 tablespoons of Kevis lotion to be applied topically to the scalp) and 8 bottles of shampoo – and this costs between $650.00 and $975.00. It is uncertain whether there are any side effects with Kevis. Some studies have shown true increases in hair counts[29]. Zinc sulphate was found to be an inhibitor of DHT production and Fabao 101D is an herbal concoction that claims to come from medicinal plants to treat alopecia[29]. Another type of products are Shampoo and Revitalizers. There are hundreds of these, but they all follow a similar structure in making claims to grow hair if patients use the "entire program", which involves revitalizer (that is the one controlling the hair loss), shampoo and conditioner, and powder gelatin. Patients should apply revitalizer during the night and it must be left on the scalp for 6 hours, followed by the shampoo and conditioner. After this, the patient uses the powder gelatine orally. The cost of such a program can be between $124.00 and $214.00, per month[29]. Further, ViviScal, a food supplement incorporating special marine extracts and a silica compound is also used to treat alopecia[29]. As well, Aminexil is a product developed by L'Oreal that acts as an antifibrotic agent, preventing collagen formation around the hair follicle and increasing survival of the follicle. Its aim is the prevention of further hair loss[29]. All of those products need more rigorous testing to be approved, in the future, by the FDA.

2.3 Nanosystems designed for drug delivery through the transfollicular and transdermal route

Over the past decades, the number of nanometric agents with skin penetration potential (transfollicular and transdermal) had a marked increase. Nowadays, several types of nanosystems exist in order to satisfy drug delivery needs (mainly penetration through SC)[2]. One great aim in this field is to understand the interactions between the SC lipid membranes and the different nanocarriers, thereby creating the most efficient drug transporters and causing the least damage on the SC barrier[30]. Another goals of using drug delivery systems is to provide a sufficient dose of a drug to a specific site[9].

Loading dermatologically active therapeutic agents in nanosystems (micro- and nano-encapsulation) is a technology used to cover substances with materials that completely or partially isolate them from the environment[22]. It acts as an useful tool to deliver therapeutic agents to the skin and may offer a number of benefits including: enhancement of product aesthetics; protection of chemically unstable agents against degradation; sustained/controlled release and follicular targeting; possibility to do not use of irritant organic solvents or surfactants. However, despite their advantages, the use of nanocarriers to administer active agents to the skin in clinic remains low[14], it is still necessary to balance drug-vehicle interactions, to ensure adequate drug loading and to allow efficient drug release[14].

Nanoparticles are unique due to their size-dependent physical and chemical properties, feature that can be advantageous in delivery of drugs to the skin. They can be composed of lipids, sugars, degradable or non-degradable polymers, metals and organic or inorganic compounds. As it was already mentioned before (see section *2.1.3.1 Major routes for drug penetration into the skin with a special focus in the transfollicular and transdermal route*), following topical application of nanoparticle formulations, absorption of active compounds can follow different pathways[6]. The purpose of nanocarriers – which are colloidal systems having structures with a size below 500 nm[30] – when applied to the skin, could be the local effect within the skin (dermal drug delivery) or a systemic effect accompanied by the permeation through the skin (transdermal and transfollicular drug delivery)[30].

Nanoparticle dispersions include formulations as lipidic vesicles (liposomes), solid lipid nanoparticles (SLN), nanostructured lipid carriers (NLC) and polymeric microparticles and nanoparticles. Particles dispersed generally are charged to improve dispersion stability against aggregation and their dimensions normally range above 100 nm. Liposomes – known as vesicular drug carrier systems and colloidal lipid aggregates – are largely used vesicles formed by one or multiple lipid bilayers that enclose an aqueous environment. There are several distinct vesicle types, depending on the additives used for their preparation: transfersomes, flexosomes, ethosomes, niosomes, vesosomes, invasomes and polymerosomes[30]. Therefore, formulations could have different compositions that would affect their penetration. Polymeric microparticles and

nanoparticles (spheres or capsules) have the characteristic advantage to control the release of entrapped/encapsulated drug. Spheres are in general rigid and more resistant to rupture than capsules[1,2,6,9]. Nanoparticles are often used in dermatopharmaceutics and in cosmetics. As other nanocarriers, their use could have two main aims: dermal application and follicular application[30]. The development of SLNs and NLCs for dermal application in combination with occlusion is an interesting research topic[30]. The penetration of nanoparticles into the hair follicles, where a high increase in penetration depth was observed, is improved with massage after their application – which pumps nanoparticles deeper into the hair follicles[30]. On a regular application particles penetrate into the hair follicle to a depth of around 300 μm, while after massage they penetrate up to 1500 μm^2.

Other types of nanosystems are dispersions of particles that range between 100 and 1 nm which are inorganic and metallic nanometric agents – microemulsions or nanoemulsions, magnetic nanoparticles (generally made of iron derivates), titanium oxide- and zinc oxide-based nanomaterials (used in the cosmetic industry as sunscreens due to their ability to scatter the UV light), quantum dots and carbon nanotubes and fullerenes[2,6,9]. Microemulsions are colloidal formulations which diameters range between 20-100 nm. Usually they have low viscosity and consist of surfactant, co-surfactant, oil and water. Microemulsions have high solubilisation capacity for hydrophilic and lipophilic drugs, which is an advantage for pharmaceutical use[30].

Those nanosystems above could be used for transdermal or transfollicular route for penetration into skin. Usually, among other factors, by decreasing the size an increased penetration should be expected[2].

In this field is important to note the drug release by nanoparticles during storage and upon application to the skin, which is dependent on the physicochemical properties of the drug and its vehicle and has a significant effect on product performance. If the drug is not well retained in the particle during storage this negates the advantages of using the nanoparticle carrier – reducing the effect of premature drug release is needed. In this way, dynamic foams, a new paradigm in topical drug delivery, are systems capable to trigger the release of agents from nanocarriers only after application to the skin[14].

2.3.1 Lipid nanoparticles: definition and main features

Lipid nanoparticles, besides liposomes already mentioned above, may be distinguished between SLNs and NLCs[2]. Both SLN and NLC have been developed to increase the physicochemical stability of both incorporated drug molecules and particulate system, they have been mainly introduced as an alternative carrier system for pharmaceutical, cosmetic and dermatological uses[6,9]. Therefore, lipid particles have been proposed as an substitute to colloidal delivery systems, emulsions and liposomes,

since they present flexibility with respect to adjusting the size of the desired particle[22,31]. SLN and NLC are composed of physiological (biocompatible) and biodegradable lipids[13], which possess a low cytotoxicity and low systemic toxicity – good tolerability[6,9,31]. Therefore, potential toxicity of nanosized materials, an important point of awareness, is considered to be negligible since LNs are regarded as a nanosave carrier[31]. Amongst the lipids that can be used to produce LNs, phospholipids, triacylglycerols, waxes, fatty acids or their mixtures are some examples[22].

The main difference between those two types of LNs is their solid matrix organization. SLNs are produced with lipid(s) that is (are) solid at body temperature (solid lipid cores[13]), their matrices are perfect crystalline lattices and they are covered with a surfactant that stabilizes their dispersion. SLNs are composed of 0,1% (w/w) to 30% (w/w) solid lipid dispersed in an aqueous medium; and 0,5% (w/w) to 5% (w/w) surfactant. On the other hand, as the second generation of LNs, NLCs are produced with solid and liquid lipids (oils), whose mixture is macroscopically solid at body temperature (solid matrix). This mixture is preferably used in a ratio from 70:30 to 99,9:0,1. Their matrix structural organization, which entraps liquid lipidic nanocompartments, could be a distorted crystalline lattice, or an amorphous lipidic blend, or a solid lipidic matrix. Like SLNs, NLCs also have a superficial surfactant stabilizer. Both particles are rigid and are found dispersed in aqueous solutions or incorporated in o/w formulations. Their average particle size ranges between 50 and 1000 nm[2,9,31]. Usually, the drug can be located between the fatty acid chains, or between the lipid layers, or even in imperfections of the lipid matrix[31].

SLNs and NLCs with a size above 100 nm should penetrate skin through hair follicles (transfollicular) since they should not be able to (deeply) penetrate into the SC through the transdermal route because their dimensions and rigidity[2].

The SLNs and NLCs combine advantages of fat emulsions (good tolerability, large and easy scale production by high pressure homogenization) with advantages of solid polymeric particles (controlled drug release to supply the skin over a prolonged period of time, protection of incorporated drugs against chemical degradation, slower metabolism)[9]. Regarding this, LNs have numerous advantages over conventional formulations. For this reason, increasing attention has been paid on them as possible carriers for skin drug delivery, for dermal application of cosmetics and pharmaceutics[13,31]. Besides those already mentioned, some of the advantages are: LNs have occlusive properties which can increase the water content of the skin (skin hydration) and favour drug penetration into the skin; they also reduce systemic absorption; act as a UV sunscreen system; reduce irritation improving *in vivo* toleration; improve physical stability; and they are low cost compared to phospholipids[9,31]. Also, the use of triglycerides in SLN formulations is an advantage in terms of toxicity[13]. Furthermore, lipidic nanoparticles, unlike polymeric nanoparticles, readily interact with skin lipids[19]. LNs allow drug targeting to the skin or even to its substructures. Thus they might have the potential to improve the benefit/risk ratio of topical drug therapy[31].

The main disadvantage of SLN is related to a change in the lipid conformation to a lower energy crystal state that occurs during storage (probably due to high temperature, light, or shear stress[15]). This transformation from polymorphic to perfect crystals (with a reduction in the amorphous regions of the carrier matrix, and an increase degree of order) does not allow guest molecules in the structure and this leads to expulsion of drug entrapped[1,9,22,31]. To overcome this problem NLC were developed. In NLCs, solid and liquid lipid are mixed in such a combination that the particle solidifies upon cooling but does not recrystallize, remaining in amorphous state (is less ordered). This does not allow the occurrence of the problem mentioned above, so the drug could be accommodated in the particle for a longer time which will increase the drug loading capacity of the systems. The potential of these carriers is variable and must be studied specifically for the follicular drug delivery system[1,6,9,22,31].

Lipidic nanoparticles loading capacity, incorporation efficiency, morphology, mean diameter, release behaviour and skin absorption are features related with LN lipidic composition and encapsulated molecules[15,22]. Frequently, SLNs have low loading capacity which is limited to about 10% of the amount of lipid to ensure stability of the system[15]. Incorporation efficiency is the ratio between the amount of material effectively encapsulated and the initial amount added to the emulsion; and it could be measured by heating LN containing drug (in water at 70 °C for 10 min) to break them and release the drug which is then quantified. A response used to identify the best conditions for molecule retention is the time for 50% release of the core material (i. e. encapsulated molecule)[22].

Lipid nanoparticles production could be made using different methods and has the possibility of industrial scale manufacture[22]. Initially, spray chilling was used and, subsequently, the techniques of precipitation from a microemulsion (emulsification-solvent evaporation) and high-pressure homogenisation were employed to produce LNs[22]. LNs production is easily done by melt emulsification followed by a homogenization step either with high pressure homogenizer or ultrasonic processor[13,31]. Further, emulsification-solvent diffusion, solvent injection, phase inversion, multiple emulsion and membrane contractor are other techniques used for the same purpose[31]. High pressure homogenization technique is the most advantageous compared to other methods – due to its easy scale up, avoidance of organic solvents and short production time. This technique can be considered as being industrially the most feasible one[31]. High pressure homogenization could be hot or cold, and LNs can be produced by both methods from the same technique[15,31]. Briefly, the active compound (drug) is first dissolved or dispersed in melted solid lipid (for SLN) or in a mixture of liquid lipid and melted solid lipid (for NLC). In the hot homogenization method, the lipid melt containing the active compound is dispersed in a hot surfactant solution at the same temperature (5-10 °C above the melting point of the solid lipid or lipid mix) by high speed stirring. The obtained emulsion (called pre-emulsion) is then passed through a high pressure homogenizer at adjusted temperature. On the other hand, in the cold homogenization method, the mixture of active compound and lipid melt is cooled down

for solidification and to obtain lipid microparticles. Those are then dispersed in a cold surfactant solution generating a cold pre-suspension of micronized lipid particles. This suspension is passed through a high pressure homogenizer at room temperature. Finally, for both methods, after cooling lipid nanoparticles are produced[31].

There are different models for drug incorporation in LNs, differentiated by the distribution of the drug within the LNs[15,31]. Drugs may homogeneously distribute within the lipid matrix, or may be enriched in the core or the particle shell, or even may adhere to the particle surface or form clusters (**Figure 7**)[15]. The chemical nature and concentration of any ingredient (active agent, lipid, surfactant) influence the structure of LNs, as do the production conditions (hot or cold homogenisation, for example)[15]. Therefore, distinct release profiles are expected – burst release as well as sustained release have been reported for SLN and NLC dispersions. For dermal application both profiles are of interest, according to the desired effect. While burst release might improve the penetration of active compounds, sustained release becomes important for active ingredients that are irritated or when the compound is needed to be supplied to the skin over a prolonged period of time[31].

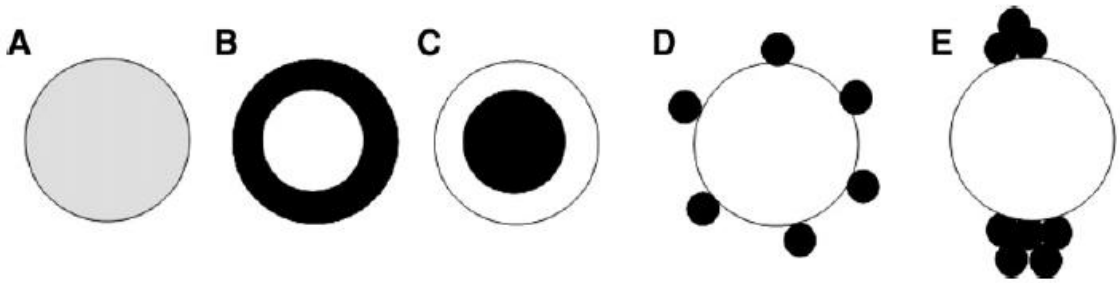

Figure 7: Models of incorporated compounds in lipid nanoparticles: homogeneous matrix (A), compound enriched within the shell (B), compound enriched within the core (C), compounds adhering to the particle surface (D), and clustered compounds adhering to the particle surface (E)[15].

When SLN and NLC are applied on the skin, they show adhesiveness, occlusion and skin hydration effects[1,31]. Adhesiveness is manifested by forming a monolayer on the skin – a hydrophobic monolayer film. As a result, it shows occlusive action on the skin and retards the loss of moisture as a result of evaporation (reduced water loss). This can result in reduction of corneocyte packing and opening of inter-corneocyte gaps, facilitating the drug penetration into deeper layers of skin[6,15,31]. Epidermal lipids interact with lipid carriers which attach to the skin surface allowing lipid exchange between the outermost layers of the SC and the carrier[15]. This interaction rate of the LNs with the skin lipids and sebum is dependent on the lipophilicity of the incorporated molecule, formulation type (if the drug is incorporated into lipid matrix or if it is on the nanoparticle surface) and type of interaction skin-lipid. The highly lipophilic molecules can penetrate easily, while no diffusion occurs when a hydrophilic molecule is used[6].

2.3.2 Patented lipid nanoparticles applied in dermatology and cosmetic

LNs formulations are used to be incorporated into topical products. This incorporation can be obtained by distinct forms: the addiction of SLN/NLC to existing products (as cream or lotion); or adding viscosity enhancers to the aqueous phase of SLN/NLC to obtain a gel; or even by the direct production of a final product containing only nanoparticles in a one-step process (this form uses high lipid concentrations and the final product has high consistency)[31]. Instabilities (aggregation or dissolution) of lipid nanoparticles might occur in cosmetic or pharmaceutical creams or lotions. For hydrogel formulations containing SLN or NLC, a good physical stability was reported[31].

Comparing LNs formulations for dermal application in the pharmaceutical and the cosmetics fields, the technological aspects are very similar. However, the time for product development and market introduction for cosmetic products is much shorter due to the more complex regulations (and tests) for the development of a pharmaceutical product. Therefore, the first LNs product on the market was a cosmetic product[31]. Some cosmetic products currently on the market are made of/incorporated with lipid nanoparticles[31]. An overview of what already exists and is patented is provided here (**Table 1**).

In cosmetic products field, it is important that the cosmetic active penetrate into the skin, but systemically absorption should not occur[31]. In general lipid nanoparticles do not penetrate the horny layer but a follicular uptake by the hair follicles has been reported.

Perfumes and perfumes incorporated into products are cosmetic products where LNs are incorporated. For these examples, a prolonged release is usually desired. It was already found that SLN loaded with the perfume Allure (Chanel) yield a prolonged release of the perfume from the solid lipid matrix of SLN[31]. As well, prolonged release of the perfume Kenzo from NLC was reported[31]. It is important to note that select a solid lipid that can enclose the perfume in its solid matrix contributes to a controlled perfume release (as it had been seen for the perfume CA from two different lipid nanoparticle formulations – Preifac and Apifil)[31]. Furthermore, the release of perfume depends on the lipid matrix composition, the perfume load and the surfactant type.

As it was already mentioned here, LNs can act as a physical UV blocker, they are able to improve the UV protection in combination with organic sunscreens. For that reason, encapsulation of inorganic sunscreens into LNs is a promising approach to obtain well tolerable sunscreens with high protection level[15,31].

Table 1: Cosmetic products containing NLC currently on the market[31].

Product name	Market introduction date	Main active ingredients
Cutanova Cream Nano Repair Q10	10/2005	Q10, polypeptide, hibiscus extract, ginger extract, ketosugar
Intensive Serum NanoRepair Q10	10/2005	Q10, polypeptide, mafane extract
Cutanova Cream NanoVital Q10	06/2006	Q10, TiO_2, polypeptide, ursolic acid, oleanolic acid, sunflower seed extract
SURMER Crème Legère Nano-Protection	11/2006	Kukuinut oil, Monoi Tiare Tahiti®, pseudopeptide, milk extract from coconut, wild indigo, noni extract
SURMER Crème Riche Nano-Restructurante		
SURMER Elixir du Beauté Nano-Vitalisant		
SURMER Masque Crème Nano-Hydratant		
NanoLipid Restore CLR	04/2006	Black currant seed oil containing ω-3 and ω-6 unsaturated fatty acids
Nanolipid Q10 CLR	07/2006	Coenzyme Q10 and black currant seed oil
Nanolipid Basic CLR	07/2006	Caprylic/capric triglycerides
NanoLipid Repair CLR	02/2007	Black currant seed oil and manuka oil
IOPE SuperVital	09/2006	Coenzyme Q10, ω-3 and ω-6 unsaturated fatty acids
Cream		
Serum		
Eye cream		
Extra moist softener		
Extra moist emulsion		
NLC Deep Effect Eye Serum	12/2006	Coenzyme Q10, highly active oligo saccharides
NLC Deep Effect Repair Cream		Q10, TiO_2, higly active oligo saccharides
NLC Deep Effect Reconstruction Cream		Q10, acetyl hexapeptide-3, micronized plant collagen, high active oligosaccharides in polysaccharide matrix
Regenerationscreme Intensiv	06/2007	Macadamia ternifolia seed oil, avocado oil, urea, black currant seed oil
Swiss Cellular White Illuminating Eye Essence	01/2007	Glycoproteins, panax ginseng root extract, equisetum arvense extract,
Swiss Cellular White Intensive Ampoules		Camellia sinensis leaf extract, viola tricolor extract
SURMER Creme Contour Des Yeux Nano-Remodelante	03/2008	Kukuinut oil, Monoi Tiare Tahiti®, pseudopeptide, hydrolized wheet protein
Olivenol Anti Falten Pflegekonzentrat	02/2008	Olea europaea oil, panthenol, acacia senegal, tocopheryl acetate
Olivenol Augenpflegebalsam		Olea europaea oil, prunus amygdalus dulcis oil, hydrolized milk protein, tocopheryl acetate, rhodiola rosea root extract, caffeine

Cutanova Cream NanoRepair Q10 was the first LN based cosmetic product introduced to the market in 2005. This product is a NLC containing cream which provides an increase in skin hydration, as well as an increase in its occlusive factor, by comparison with other nanocarriers. Furthermore, the penetration of coenzyme Q10

(from this cosmetic product) into the SC was found to be higher for this NLC dispersion than for a o/w emulsion[31]. NanoLipid Restore CLR is another cosmetic product based on lipid nanoparticles which was used in the prestigious cosmetic product line IOPE (Amore Pacific, Seoul, South Korea), introduced to the market in September 2006. Furthermore, LNs were used in the cosmetic products line Surmer due to their occlusive properties. The aim was to increase the occlusion of a day cream without changing its light character/without having the glossy skin appearance associated with the high occlusive night creams[31].

It might be difficult to find a nanoparticulate delivery system for which so many regulatory accepted excipients (lipids, surfactants and stabilizers) are available than for the lipid nanoparticles[31].

In 2009, about 30 cosmetic products containing lipid nanoparticles were in the market[31]. Currently, there are several drugs (glucocorticoids, retinoids, non-steroidal anti-inflammatory drugs, COX-2 inhibitors, antimycotics, among others) under investigation for dermal application by using LNs[15,31].

2.3.3 Nanosystems developed for alopecia treatment: composition and preparation methods

In recent years, many attempts have been made to enhance drug deposition in the PSU using delivery systems[17]. It is important to highlight that all the drug delivery systems studied must be effective *in vitro*, as well as effective and selective *in vivo*[11]. Regarding alopecia, several nanosystems were prepared to study possibilities to treat it, and vehicles for minoxidil were largely studied to try to enhance its percutaneous absorption[19].

Studies with minoxidil loaded liposomes reported that they reduce the period of telogen (accelerating hair growth) significantly as compared with ethanolic minoxidil[9].

Copolymer nanoparticles entrapping minoxidil have been investigated to deliver this drug through the skin in a size dependent form, in hairy rats[9]. This study evaluates the effect of hydrodynamic size of self-assembled nanoparticles (biodegradable block copolymer) on skin penetration of minoxidil *in vitro* and *in vivo*. Those nanoparticles (40 nm and 130 nm) were prepared by solvent evaporation of poly-caprolactone-block-poly-ethyleneglycol. It was shown that these nanoparticles can deliver minoxidil to skin very effectively, mainly through shunt routes (like hair follicles) and the permeation behaviour of these nanoparticles was promoted when the size of the nanoparticles was decreased[9].

Minoxidil loaded in ethosomes (which are lipid vesicular systems with relatively high concentrations of ethanol) enhance the skin permeation of minoxidil when

compared with either ethanolic or hydroethanolic solution or phospholipid ethanolic micellar solution of minoxidil. It is confirmed that ethosomes potentiates the penetration of drugs like minoxidil to reach deeper skin structures, such as pilosebaceous follicles. Therefore, these nanosystems constitute a promising approach for the topical delivery of minoxidil in hair loss treatment[9,19].

The mixture solvent propylene glycol/water/ethanol (vehicle for minoxidil solution available in the market) can solubilise enough amount of drug for hair growth promotion, but may cause an irritation to skin and eyes. Therefore, non alcohol-based vehicles having the same high skin permeation-enhancing potency need to be developed[19]. *In vitro* skin permeation and the skin retention of minoxidil loaded in monoolein nanoparticles and of minoxidil solutions (in propylene glycol/water/ethanol (20/30/50, v/v/v), propylene glycol/water (5/95, v/v) and ethanol/water (5/95, v/v)) were observed in diffusion cells, in mice. Whatever the vehicles were, the fluxes of minoxidil increased with time. That happens probably because the components of those vehicles – known as skin permeation enhancers – accumulate within the skin so that the transfer rate is accelerated with time. One of the reasons why the skin retention of minoxidil was the highest when the solution propylene glycol/water/ethanol was applied could be that propylene glycol and ethanol act as co-solvents for minoxidil in skin[19].

Monoolein cubic phases containing hydroxypropyl β-cyclodextrin/minoxidil complex were prepared in order to overcome the poor solubility in the suspension of lipid nanoparticles and keep the high percutaneous absorption. This preparation was done by hydrating molten monoolein with the complex solution, and the nanoparticles were obtained from the cubic phases by a sonication method. The degree of release of minoxidil from cubic phases increases in a saturation manner and the rate of release seemed to be a first-order release[19].

In a study, SLNs suspension made of semi-synthetic triglycerides, stabilized with a mixture of polysorbate and sorbitan oleate, were loaded with 5% of minoxidil (**Table 2**)[13].

Table 2: SLN suspension composition[13].

Components	Content (g)
Minoxidil	5
Suppocire® NAI50	10
Montane® 80PHA	6
Montanox® 20PHA	4
Phosal® 50PG	4
Water	71

In this study, these lipid nanoparticles were compared to solutions already on the market whose compositions are described on **Table 3**.

Table 3: Commercial solutions compositions (g/100 mL)[13].

Components	Commercial solutions	
	Alopexy 5%	**Minoxidil Bailleul 5%**
Minoxidil	5	5
Ethyl alcohol (96%)	25	58,6
Propylene glycol	50	20
Water	Quantity sufficient to 100 mL	Quantity sufficient to 100 mL

For the SLN suspension preparation, components were mixed and heated at 40±2 °C. Minoxidil was added to the mixture under stirring at 100 rpm. This mixture was maintained under stirring at 40±2 °C during 5 h. Then, water was heated at 40±2 °C and added to the lipid-drug mixture under stirring at 500 rpm. Stirring was maintained during 1 h at the same temperature. The obtained pre-emulsion was homogenized at the melting temperature using a high pressure homogenizer (applying 100 000 kPa and three homogenization cycles)[13]. As a result, SLN particle size (an important parameter in order to target the hair follicles) was measured – mean particle size of the SLN was about 190 nm (particles of this size range are qualified for penetrating into the sebaceous gland region of porcine terminal hair follicles). Also zeta potential values are essential and those were just below the critical value of -30 mV, which is required for a good physical stability. Moreover, pH of SLN suspensions was close to skin pH, whereas pH of studied commercial products was over 7,00. Further, SLNs display a biphasic release profile: a burst effect due to the minoxidil contained in the water phase and a prolonged released due to the encapsulated minoxidil[13].

Ex vivo skin penetration of minoxidil entrapped in SLN suspension studies were also performed using diffusion cells and pig ear skin. Permeation of minoxidil through porcine skin was never detected during 24h experiment. In contrast, minoxidil penetration is seen through excised human epidermis with a lag time of 6 h – which suggests that the dermis is leading to a longer lag time for penetration that is not detected at 24 h. Results from this study showed that the SLN suspension penetration into skin layers was statistically non-different from commercial products. In addition, *ex vivo* skin corrosion studies were realized in order to evaluate and compare the corrosive factor of the studied SLN suspension and commercial products. It was concluded that SLN suspension was non-corrosive, while the tested commercial products have potential to be. It is important to verify that this corrosive factor of commercial products can explain their low treatment compliance. According to these results, SLN are found to be as efficient as commercial solutions for skin penetration and also capable to decrease or eliminate skin irritation (non-corrosive)[13]. This novel SLN formulation represents a promising alternative for topical treatment of androgenic alopecia with minoxidil. SLN suspensions would constitute a promising formulation for hair loss treatment[13].

Another study with minoxidil involves loading of this drug into two nanoparticles with different physicochemical properties: lipid nanoparticles (LN) and polymeric nanoparticles with a lipid core (PN). They were produced and suspended in

water to produce aqueous suspensions which were emulsified using pluronic surfactant to generate foams. Minoxidil loaded LNs (minoxidil 1,4 mg/mL) were prepared using a phase inversion method, whereas PNs with a lipid core (minoxidil 0,6 mg/mL) were prepared by solvent displacement. Then, nanoparticle-loaded dynamic foams were prepared. After the preparation process, nanoparticles were assessed – PNs were much larger (≈ 260 nm) compared to LNs (≈ 50 nm) and the polydispersity index was very low for all the particles produced (< 0,2). LNs were neutral, whilst PNs were found to be negatively charged (probably due to the surfactants used in the production methods). Furthermore, LNs release more drug more rapidly compared to PNs (since drug affinity was low with LN)[14].

A study was made where finasteride-containing vesicles (liposomes and niosomes) to topical application were assessed. Liposomes consisted of phospholipid:cholesterol:dicetylphosphate (8:2:1, mole ratio), while niosomes were comprising non-ionic surfactant:cholesterol:dicetylphosphate (7:3:1, mole ratio). Multi Lamellar Vesicles (MLVs) were prepared by the film hydration technique. Finasteride solution (0,53 mM) was spiked with ^{3}H-finasteride and added to the lipid solution, and the solvents were removed using a rotary evaporator at a reduced pressure. The dried thin film was then hydrated with PBS for 30 min at 10 °C above the phase transition temperature of the amphiphiles while shaking. The dispersion was left for 4 h at room temperature to complete hydration and then stored at 4 °C overnight before use. Following this preparation steps all of the vesicles formed were multilamellar with mean diameter ranging from 1,9 to 4,4 μm[17]. Those vesicles were also studied in order to assess the extent of finasteride permeation through and deposition into the different strata of the hamster flank and ear skin. Those permeation studies were assessed using vertical Franz diffusion cells and demonstrated that the total amount of finasteride penetrated into and permeated through hamster skin 24 h after topical application of liposomes and niosomes ranged from 5,5 to 13% of the initial dose. Both *in vitro* permeation and *in vivo* deposition studies confirmed the potentials of liquid-state liposomes and niosomes for successful delivery of finasteride to the PSU[17].

3 Dissertation work plan

Lipid nanoparticles, especially NLC, present different and interesting features that made them promising for the incorporation of anti-alopecia drugs, which include: protection of the skin, enhancement of chemical stability of actives, release properties and skin penetration, film formation on the skin and controlled occlusion, skin hydration, enhanced skin bioavailability of actives and skin targeting and physical stability in topical formulations. Therefore, these nanoparticles were chosen to develop a new nanoformulation for alopecia therapy.

The first part of this work consisted in the selection of the appropriate lipids and in the optimization of the method of production of NLC. Different factors were tested and assessed, such as times of sonication and formulation characteristics, to establish the best conditions for a reproducible NLC production.

Afterwards, the drugs against alopecia (finasteride and minoxidil) where incorporated in the lipid nanoparticles and were characterized according to particle size and shape, the surface charge (zeta potential), the type of lipid modification and loading efficiency. To assess the stability of these nanocarriers, they were characterized at different times after their production (in the day of production, 7 days, 18 days and 28 days after).

These nanoformulations were optimized regarding their size, composition and charge to obtain nanoparticles with the required size (50-200 nm and polydispersity index below 0,25) to achieve the dermis and hair follicles and to have a good drug loading capacity.

Penetration studies through pig ear skin at physiological conditions correspondent to pH and temperature of the plasma (7,4 and 37 °C) were performed, in vertical Franz diffusion cells, to evaluate the drug penetration profile after dermal application.

The next sections describe the results obtained for each part of the work developed.

3.1 Development of lipid nanoparticles (NLC) for alopecia treatment

3.1.1 Optimization of the method of production of lipid nanoparticles

The first aspect assessed was the drug solubility in different lipids (solids and liquids) – in order to select suitable lipids for the NLC production. It is intended to select lipids in which finasteride/minoxidil are soluble so that the drug could be incorporated in NLC. For that, several lipids were tested with increasing percentages of finasteride and minoxidil – these mixtures were macroscopically evaluated for solubility (**Table 4**).

Table 4: Drugs solubility in different lipids. The symbol ✓ means that the drug is soluble in the lipid, in that percentage. The symbol × means that is not soluble. The - means that it was not done.

Lipids	Finasteride									Minoxidil							
	1%	2%	3%	4%	5%	6%	7%	8%	9%	1%	2%	3%	4%	5%	6%	7%	8%
Cetyl palmitate	✓	×	-	-	-	-	-	-	-	×	-	-	-	-	-	-	-
Miglyol 812	×	-	-	-	-	-	-	-	-	✓	×	-	-	-	-	-	-
Precirol ATO 5	✓	✓	✓	✓	✓	✓	✓	✓	×	✓	✓	×	-	-	-	-	-
Dynasan 116	✓	✓	×	-	-	-	-	-	-	✓	✓	×	-	-	-	-	-
Imwitor 308	-	-	-	-	-	-	-	-	-	✓	✓	✓	✓	✓	✓	✓	×
Softisan 100	-	-	-	-	-	-	-	-	-	×	-	-	-	-	-	-	-
Lipocire CM	-	-	-	-	-	-	-	-	-	×	-	-	-	-	-	-	-
Witepsol S58	-	-	-	-	-	-	-	-	-	×	-	-	-	-	-	-	-
Softisan 645	-	-	-	-	-	-	-	-	-	×	-	-	-	-	-	-	-
Compritol HD5 ATO	-	-	-	-	-	-	-	-	-	×	-	-	-	-	-	-	-
Gelucire 33/01	-	-	-	-	-	-	-	-	-	×	-	-	-	-	-	-	-
Compritol E ATO	-	-	-	-	-	-	-	-	-	×	-	-	-	-	-	-	-
Apifil	-	-	-	-	-	-	-	-	-	×	-	-	-	-	-	-	-
Witepsol E85	-	-	-	-	-	-	-	-	-	×	-	-	-	-	-	-	-
Oleic acid	-	-	-	-	-	-	-	-	-	✓	✓	✓	✓	✓	✓	×	-

As it was not found an unique lipid in which both drugs are soluble, two different types of NLC had to be made, one for each drug. Therefore and according to these results, Precirol ATO 5 was the lipid solid chosen for the NLC of finasteride. As well, Oleic acid was the lipid liquid chosen for the NLC of minoxidil. The lipid Imwitor 308, initially, was also assessed for the NLC of minoxidil, but following experiments (see **Table 18**) proved that this hypothesis is not viable.

Consequently, lipid liquid chosen for NLC of finasteride was Miglyol 812; while lipid solid chosen for NLC of minoxidil was Cetyl palmitate.

3.1.1.1 Materials and methods

Materials

A. Cetyl palmitate

Cetyl palmitate is a wax produced by catalytic esterification of fatty alcohol (cetylic alcohol) and fatty acid (palmitic acid) (see **Figure 8**)[32]. Besides palmic acid, cetyl palmitate may contain myristin acid and stearic acid. Cetyl alcohol may be partly replaced by myristyl alcohol or stearyl alcohol. Cetyl palmitate is a white wax which is supplied as pellets or flakes. Pure cetyl palmitate crystallizes in two modifications melting at 52,4-52,9°C and at 53,2-53,8°C. According to the composition of the ester mixture the melting point is increased or decreased[33]. Cetyl palmitate is insoluble in water and paraffin whereas it is soluble in chloroform and acetone.

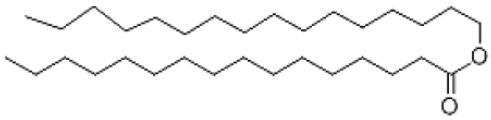

Figure 8: Chemical structure of cetyl palmitate[34].

B. Oleic acid

Oleic acid is the (Z)Octadec-9-enoic acid that usually also contains varying amounts of saturated and other unsaturated fatty acids. This oily liquid lipid is yellowish or brownish and is practically insoluble in water, miscible with alcohol and with methylene chloride[33].

C. Precirol ATO 5

Glyceryl palmitostearate, known as Precirol ATO 5, is a mixture of mono-, di- and triglycerides of C_{16} and C_{18} fatty acids. It is manufactured, without a catalyst, by the direct esterification of palmitic and stearic acids with glycerol. This lipid is a fine white powder with a weak odor, and its melting point is between 52-55 °C. Precirol is freely soluble in chloroform and dichloromethane, practically insoluble in ethanol (95%), mineral oil, and water[35].

D. Miglyol 812

Medium chain triglyceride is a synonym for Miglyol 812. It is produced from the oil which is extracted from the solid and dried part of the endosperms of Cocos mucifera L. and Elaeis guineensis JACQ. Miglyol 812 consists of a mixture of triglycerides, mainly caprylic acid and capric acid. It consists of at least 95% saturated fatty acids with 8 or 10 carbon atoms. Miglyol 812 is a colorless till light yellowish oily liquid which is insoluble in water but miscible with dichloromethane, ethanol, petroleum ether and fatty oils[33].

E. Tween 60 (Polysorbate 60)

The Tween series of surfactants are polyoxyethylene (POE) derivatives of the Span series products produced by Uniqema (Everberg, Belgium). Tween surfactants are hydrophilic, generally soluble or dispersible in water, and soluble to varying degrees in organic liquids. They are used for o/w emulsification, dispersion or solubilisation of oils and wetting. These products are widely used in pharmaceutical and cosmetic products as well as in detergents and food industry. Tween 60 (Polysorbate 60 – **Figure 9**) is a viscous yellow liquid and common nonionic emulsifier, used in a variety of applications[36]. Polysorbates are typically nonirritating to the skin, lubricant and environmentally readily biodegradable[36].

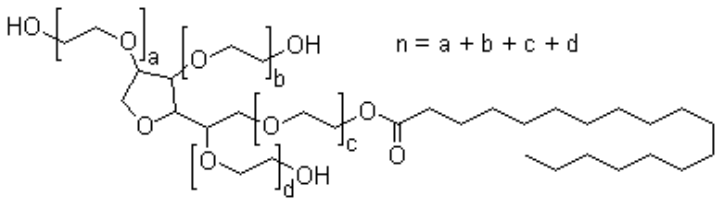

Figure 9: Chemical structure of polysorbate 60[37].

Cetyl palmitate was kindly offered by Gattefossé (France) and Miglyol 812 was purchased from Acofarma (Spain). Polysorbate 60 (Tween 60) was obtained from Merck (Germany). All chemicals and solvents were of analytical grade, and were used without further purification. Aqueous solutions were prepared with ultra pure water MilliQ (conductivity less than 0,1 μS cm^{-1}).

Methods

A. Preparation of NLC

There are many different techniques for the production of lipid nanoparticles described in the literature. These methods are high pressure homogenization[38,39], microemulsion technique[40], emulsification-solvent evaporation[41,42], emulsification-

solvent diffusion method[43], solvent injection (or solvent displacement) method[44], phase inversion[45], multiple emulsion technique[46], ultra-sonication[47] and membrane contractor technique[48].

The method of production used in this work was the **ultrasonication method**[49] and is presented in **Figure 10**. Briefly, after selecting the appropriate lipids and surfactant (**Table 5** and **Table 6**) the compounds (lipids, surfactant and active) were weighted together and kept at temperature above the lipids melting point (70 °C) to promote their mixture. The melted lipid phase (containing both lipids) was dispersed in a hot aqueous phase (containing the stabilizer Polysorbate 60) to obtain a microemulsion by high speed stirring using an ultra-turrax T25 (Janke & Kunkel IKA-Labortechnick). This microemulsion was homogenized with sonication (SONICS Vibra cell), to obtain a nanoemulsion, which was cooled at room temperature allowing the inner oil phase to solidify and forming NLC dispersed in an aqueous phase.

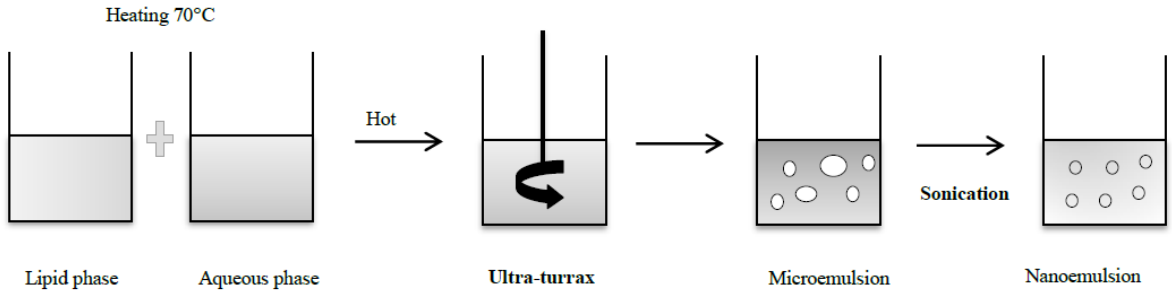

Figure 10: Schematic representation of lipid nanoparticles preparation method.

The nanoparticles obtained dispersed in an aqueous medium were passed through 200 nm filter (MiniSart® NML syringe filters, Sartorius Stedim Biotech S.A., France) to remove aggregates and were transferred to aluminum sealed screw neck vials of 20 mL (*La-Pha-Pack*®GmbH, Germany) for sample storage purposes before posterior analyses.

Table 5: Composition of NLC placebo to produce 5 g of formulation of minoxidil.

Composition	NLC
Cetyl palmitate	671,5 mg
Oleic acid	288 mg
Polysorbate 60	50,5 mg
Water	3,99 g (3,99 mL)

Table 6: Composition of NLC placebo to produce 5 g of formulation of finasteride.

Composition	NLC
Precirol ATO 5	350 mg
Miglyol 812	150 mg
Polysorbate 60	100 mg
Water	4,4 g (4,4 mL)

Several combinations of times of sonication were used (**Table 7** and **Table 8**), to establish the best conditions for both NLC production. From the different combinations, formulations were selected as presenting adequate conditions to obtain reproducible batches, with the required size and with an unimodal distribution. For NLC of minoxidil, only one combination was tested since its size, polydispersity and zeta potential were the intended ones.

Table 7: Time of sonication tested for minoxidil formulation (NLC placebo).

Formulation	Ultra-turrax (7000rpm)	Sonication (70%)
M1	60 sec	10 min

Table 8: Times of sonication for different formulations (NLC placebo of finasteride).

Formulation	Ultra-turrax (7000rpm)	Sonication (70%)
F1	60 sec	10 min
F2	60 sec	15 min
F3	60 sec	20 min

B. Characterization

After preparation of NLC placebo, the nanoparticles were characterized according to particle size and the surface charge (zeta potential).

Dynamic light scattering (DLS) (**Figure 11 A**) is a techniques based on the scattering of light that allow determining the size of the nanoparticles produced. The particles move or diffuse in consequence of collisions with solvent (Brownian movements), causing the scattering of light in all directions and fluctuation in the intensity over time. The correlation of intensity fluctuations in a short time scale allows determining the diffusion coefficient and the hydrodynamic radius (see **Figure 11 B**).

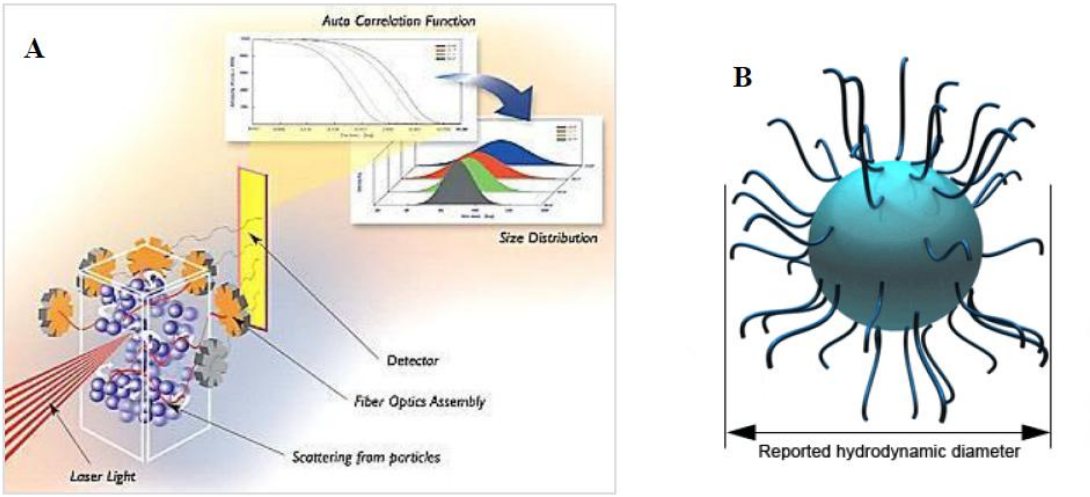

Figure 11: **A**. Schematic representation of DLS[50]; **B**. Hydrodynamic diameter of a nanoparticle[51].

Since within the same suspension, nanoparticles with different hydrodynamic diameters can be present, what is obtained with the measurements is not a unique value of the nanoparticles' size, but a size distribution. The size distribution obtained is a plot of the relative intensity of light scattered by particles in various size classes and is therefore known as an intensity size distribution. From this intensity size distribution it is possible to obtain the mean size (position of the peak maximum in the distribution) which is considered to be the size of the nanoparticles and an estimate of the width of the distribution (polydispersity index). The polydispersity index (PI) is thus related with the size distribution peak width and it is also a very important parameter when evaluating nanoparticles. High PI indicates the existence of particles of different sizes, i.e. aggregates. Low PI indicates a monodisperse population of nanoparticles.

By another technique, also based on the scattering of the light - electrophoretic light scattering (ELS) it is possible to determine the zeta potential. Zeta potential is the electric potential of a particle in a suspension (see **Figure 12**). The measurement of the zeta potential allows predictions about the storage stability of colloidal dispersions[15]. In suspensions, the surfaces of particles develop a charge due to ionization of surface groups or adsorption of ions. This charge depends on both the surface chemistry of the particles and the media around these particles. In general, particle aggregation is less likely to occur for charged particles (i.e. high zeta potential) due to electric repulsion[15]. However, this rule cannot strictly apply to systems which contain steric stabilizers, because the adsorption of steric stabilizer will decrease the zeta potential due to the shift in the shear plane of the particle[15].

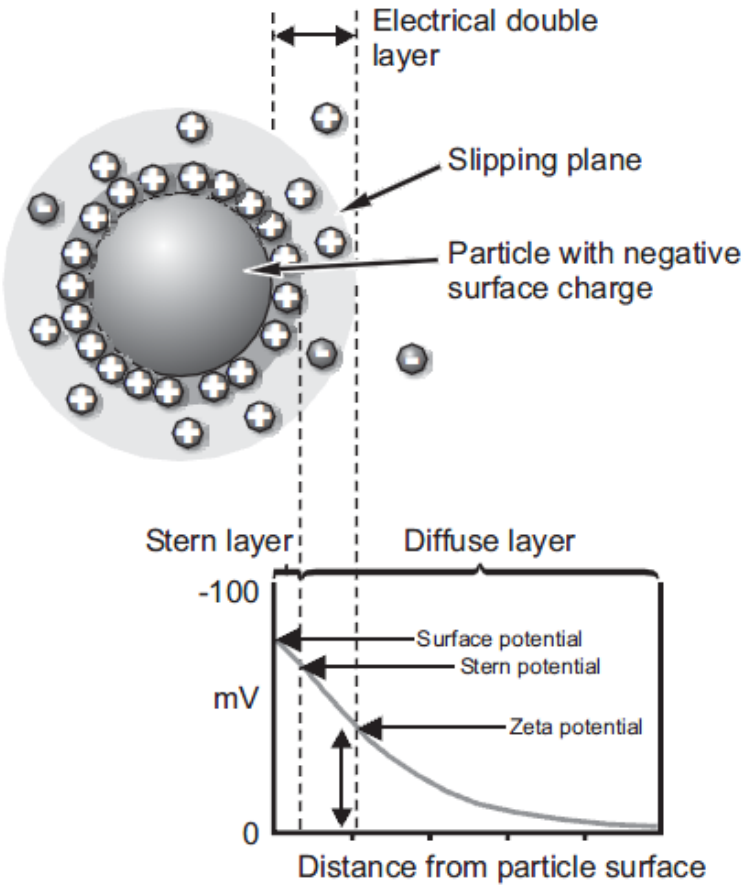

Figure 12: Electric potential of a nanoparticle[52].

Indeed, the particle size analysis is of major importance for colloidal carriers intended for dermal and transdermal route and should generally be below 200 nm. The particle charge determination is also important to predict the stability of the formulation (highly charged nanoparticles will be more stable, given that electric repulsion avoids nanoparticle aggregation).

The lipid nanoparticles characterization was done using a Brookhaven™ BI-MAS and Zeta-Pals on the day of production and 7, 18 and 28 days later. All the formulations were diluted to 400 folds in ultra pure water MilliQ (conductivity less than 0,1 μS cm^{-1}) and tested at 25 ºC, both for size and zeta potential measurements.

For size analysis, the real refractive index and the imaginary refractive index were set at 1,590 and 0, respectively. For each sample, the mean diameter ± standard deviation of six determinations was calculated applying multimodal analysis.

For zeta potential analysis, the samples were placed in polystyrene cuvets with platinum electrodes and then it was applied an electric field across the dispersion of the nanoparticles. Surface charged particles within the dispersion migrated toward the electrode of opposite charge and the velocity of particles migration was converted in zeta potential values by using the Smoluchowski's equation. The zeta potential results

reported are the mean ± standard deviation of six runs of 6 cycles each, from one sample.

Results of size and zeta potential for the placebo formulations are reported in the graphs presented in the next section.

3.1.1.2 Results and discussion

The aim of this initial part of the work developed is to optimize the method of production of the lipid nanoparticles, where several factors are tested. In the first place, it was established a time (60 sec) and a frequency of rotation (7000 rpm) of ultra-turrax, and different times of sonication (10, 15 and 20 min) at 70% were experimented. As it was already mentioned, for NLC of minoxidil, only 10 min of sonication was tested since its size and polydispersity were the intended ones. The mean particle sizes and standard deviation (SD), as well as the polydispersity index (PI) of both NLC placebo at these conditions are presented in **Figure 13** and **Figure 14**.

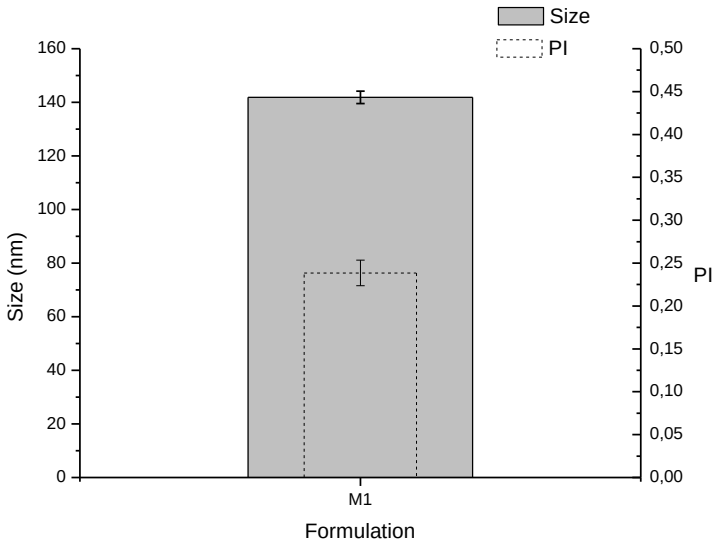

Figure 13: Relation between the size and PI for the formulation made – NLC of minoxidil.

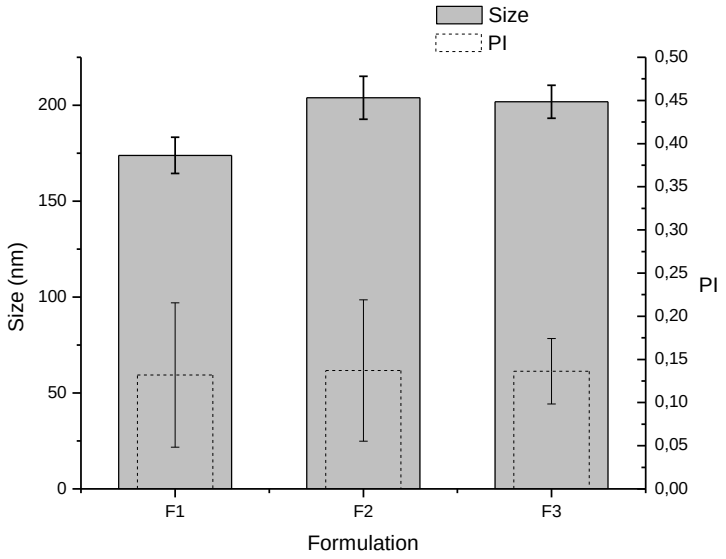

Figure 14: Relation between the size and PI for different formulations made – NLC of finasteride – with different times of sonication.

The results suggested that the size and quality of the nanoparticles are dependent of the production method, since there are significant variations in the size values with time of sonication. It is possible to observe that the best combination is for F1 formulation: 60 seconds of ultra-turrax (7000 rpm) and 10 minutes of sonication (at 70%), because it is the one that produces the smaller lipid nanoparticles.

The values of zeta obtained for both NLC placebo only differ slightly with the different factors tested. Despite the slight differences in zeta values, all the lipid nanoparticles are negatively charged which assures a good physical stability of the formulation by electrostatic repulsion, avoiding the occurrence of particle aggregation or coalescence.

Gathering all the information obtained in these experiments, it is possible to conclude that the best combination of time and intensity of ultra-turrax and time and frequency of sonication is: 60 seconds at 7000 rpm, and 10 minutes at 70%, respectively, for both NLC placebo (for minoxidil and finasteride). These conditions constituted the established method of production of all the lipid nanoparticles presented from this point forward. It is important to note that the reproducibility of these NLC with these characteristics was tested (three batches were prepared and evaluated) and guaranteed.

It is important to highlight that, for the NLC of minoxidil, before its characterization, a substantial number of experiments were made, where numerous

nanoformulations were assessed, in order to select the most reliable one, which should combine the best characteristics as loading efficiency and absence of phase separation. For these experiments different lipids (solid and liquid) were used, as well as distinct quantities of NLC constituents (lipids, surfactant and water) – results are summarized in **Table 18**, in **Appendix I**. Some strategies applied to obtain better nanoformulations include: increase the total lipid quantity to 30%, increase the polysorbate quantity, and add another solid lipid (use a mixture of two solid lipids).

3.1.2 Preparation of drug-loaded lipid nanoparticles

Before the preparation of the drug-loaded LN, it is important to define a linear working range of drug concentrations where according to the Beer-Lambert law we can guarantee that there is a correlation between concentration and absorption. This is necessary because the encapsulation efficiency of the drugs will be assessed by measuring the absorption spectra of the non-encapsulated drugs that stay in aqueous phase. Therefore, for a fixed wavelength, UV/Vis spectroscopy can be used to determine the concentration of the drug absorber in a solution. Furthermore, for the penetration studies of minoxidil this approach was also applied. To establish the linear working range where drug concentrations are proportional to absorbance, for each drug, several standards were rigorously prepared to obtain a calibration curve and the linear part of the curve was fitted to a straight line, using linear regression analysis. The next sections show the calibration curve for each drug in study.

After determining the best conditions for nanoparticles production, the different drugs (finasteride and minoxidil) where incorporated into the lipid nanoparticles. The method used was the same described in section *3.1.1.1* for LN placebo. As so, solid and liquid lipids, polysorbate 60 and drug were weighed in appropriate quantities and warmed up to 70 °C. Ulta pure MilliQ water was warmed up to the same temperature and added to the lipid mixture. The resultant lipid-water emulsion was homogenized in ultra-turrax during 60 seconds at 7000 rpm in order to obtain a microemulsion. Then, the emulsion was sonicated during 10 minutes at 70 % and the resultant nanoemulsion was cooled down to room temperature. The quantities used of each compound, for each nanoformulation prepared, are presented in the **Table 9** and **Table 10**.

Table 9: Composition of the different NLC formulations loaded with minoxidil.

Composition	NLC Placebo	NLC 2% Minoxidil	NLC 3% Minoxidil
Minoxidil	0 mg	20 mg	30 mg
Cetyl palmitate	671,5 mg	651,5 mg	641,5 mg
Oleic acid	288 mg	288 mg	288 mg
Polysorbate 60	50,5 mg	50,5 mg	50,5 mg
Water	3,99 g (3,99 mL)	3,99 g (3,99 mL)	3,99 g (3,99 mL)

Table 10: Composition of the different NLC formulations loaded with finasteride.

Composition	NLC Placebo	NLC 0,8% Finasteride	NLC 2% Finasteride
Finasteride	0 mg	5 mg	12,5 mg
Precirol ATO 5	350 mg	345 mg	337,5 mg
Miglyol 812	150 mg	150 mg	150 mg
Polysorbate 60	100 mg	100 mg	100 mg
Water	4,4 g (4,4 mL)	4,4 g (4,4 mL)	4,4 g (4,4 mL)

Moreover, based on the literature, different drug concentrations were encapsulated in the lipid nanoparticles. The aim of testing various concentrations was to understand the drug effect in the lipid nanoparticles.

3.1.2.1 Preparation of minoxidil-loaded lipid nanoparticles

The UV spectra of standard minoxidil solutions allowed delineate two calibration curves for minoxidil, corresponding to two different wavelengths, which are presented in **Figure 15** and **Figure 16**. The wavelength of maximum absorbance of minoxidil in water is at 230 nm (**Figure 15**); but it has another maximum (at 288 nm – **Figure 16**), further from the range of 200-250 nm, that was used for the penetration studies.

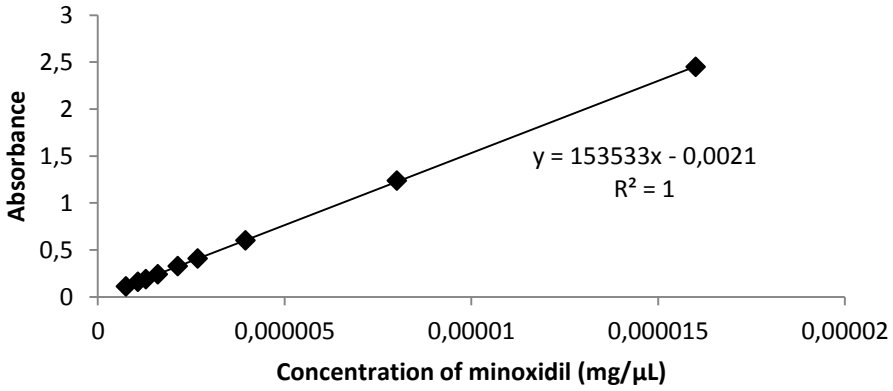

Figure 15: Calibration curve of minoxidil, at 230 nm.

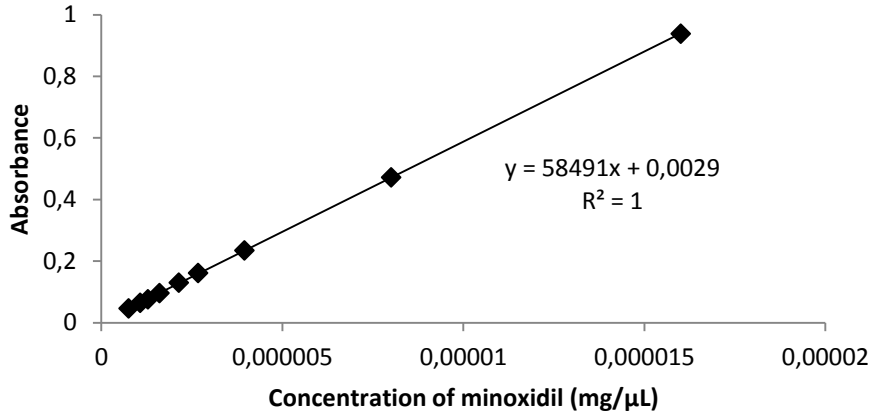

Figure 16: Calibration curve of minoxidil, at 288 nm.

According to the literature[13,25], minoxidil is normally used in anti-alopecia formulations at a concentration of 2% to 5% of the total formulation volume. As so, and according to the difficulties to solubilise this drug, minoxidil was incorporated in NLC in concentrations of 2 and 3% of the total volume of lipids and surfactant.

3.1.2.2 Preparation of finasteride-loaded lipid nanoparticles

The UV spectra of standard finasteride solutions allowed delineate the calibration curve for finasteride, which is presented in **Figure 17**. The wavelength of maximum absorbance of finasteride in water is at 210 nm.

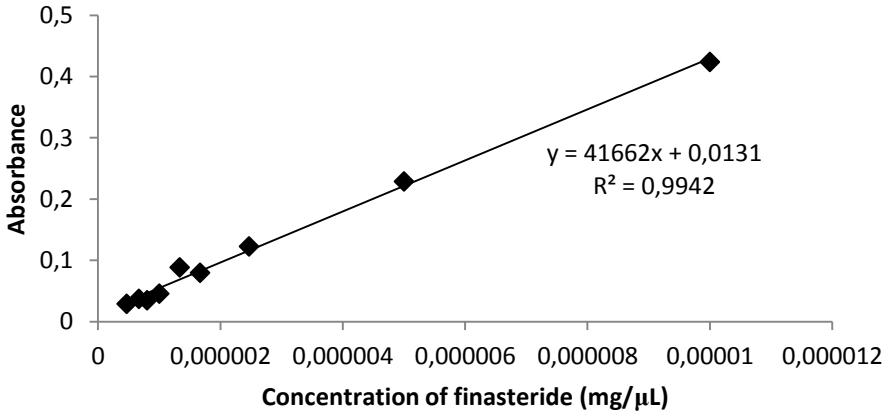

Figure 17: Calibration curve of finasteride, at 210 nm.

According to the literature[17], finasteride is normally used in anti-alopecia formulations at a concentration of 0,02% of the total formulation volume. As so, finasteride was incorporated in NLC in concentrations of 0,8 and 2% of the total volume of lipids and surfactant.

It is important to point that stability with temperature and time were verified for both drugs – by measuring absorbance of a standard solution after exposure to 70 °C (temperature) and after one week and one month (time) with consequent comparison to the absorbance obtained to do the calibration curves.

3.2 Characterization of the lipid nanoparticles

After producing the formulations, the nanoparticles were characterized according to their size and charge (inferred from the values of zeta potential). These features were assessed by DLS and ELS, respectively. Both techniques are described in section *3.1.1.1*. The mean particle size and PI, and zeta potential values obtained were calculated from the triplicate samples done for each concentration of drug tested. The next sections present the results obtained for the different nanoformulations prepared, namely minoxidil and finasteride.

3.2.1 Size

3.2.1.1 Minoxidil

The mean size, PI and SD of NLC loaded with minoxidil, of triplicate samples, are presented in **Figure 18**.

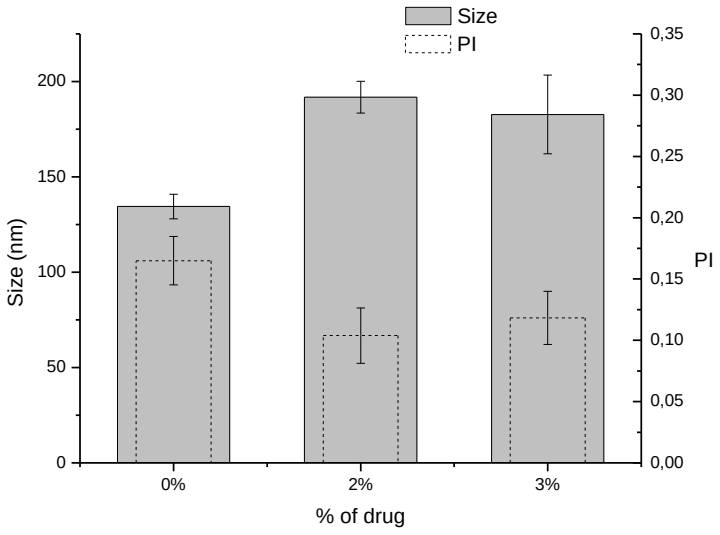

Figure 18: Mean size distribution and PI with increasing concentrations of minoxidil, of triplicate samples of minoxidil-loaded NLC.

The results show that the nanoparticles loaded with minoxidil, present a mean size and PI below the 200 nm and 0,250, respectively, as desired to achieve the dermis and the hair follicles. The polydispersity values obtained for all the lipid formulations were reasonably small (< 0,250) suggesting a fairly narrow and monomodal particle size distribution.

It is possible to observe that the nanoparticles with minoxidil have a larger size than those who have not drug. Thus, minoxidil possibly has an influence on the size of

the particles. However, within minoxidil-loaded nanoparticles there is not a clear tendency of the variation of size with concentration of the drug. Probably if the distribution of the drug was by adsorption at the surface of the nanoparticles, the effect on the size would be more evident. The differences observed in the nanoparticles' size could also be due to the size variability of the formulation, due to the manual method of production.

3.2.1.2 Finasteride

The mean size, PI and SD of NLC loaded with finasteride, of triplicate samples, are presented in **Figure 19**.

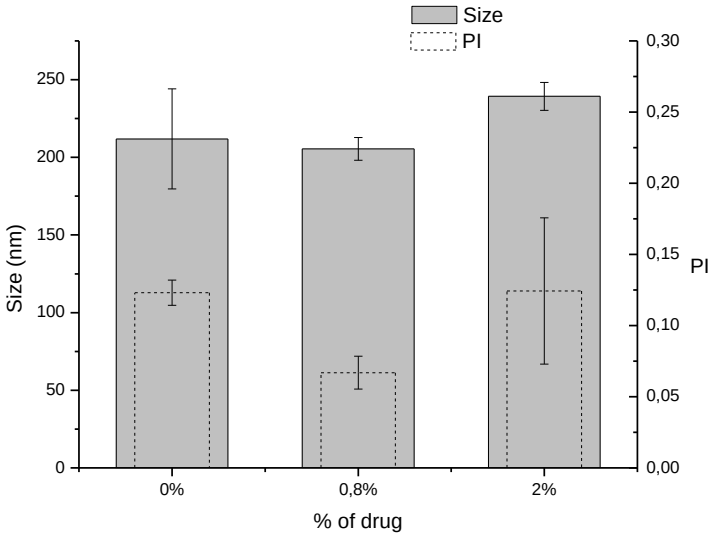

Figure 19: Mean size distribution and PI with increasing concentrations of finasteride, of triplicate samples of finasteride-loaded NLC.

The results show that the lipid nanoparticles present a mean size of almost 200 nm and a PI below the 0,250, as desired. It is important to note that all formulations have two populations – the main one, which is the one that mostly exists, has its mean size around 150 nm; the other population is present in a very low quantity but is the reason why nanoparticles' mean size increases to 200 nm.

There is not a clear tendency of the variation of size with concentration of finasteride. This indicates that finasteride is possibly homogenously distributed and incorporated in the matrix of the nanoparticles, and thus, does not have a great influence on the size of the particles. The slight differences observed in the nanoparticles' size could be only due to the size variability of the formulation, due to the manual method of production.

3.2.2 Zeta Potential

3.2.2.1 Minoxidil

The mean zeta potential values and SD of NLC loaded with minoxidil, of triplicate samples, are presented in **Figure 20**.

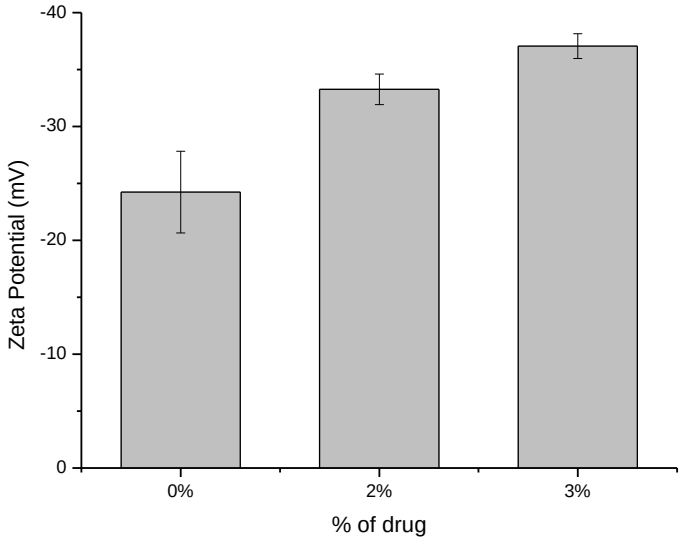

Figure 20: Mean zeta potential distribution and SD with increasing concentrations of minoxidil, of triplicate samples of minoxidil-loaded NLC.

Zeta potential measurements were employed as a useful tool to predict the physical stability of colloidal systems. The results obtained from zeta potential measurements revealed that the lipid nanoparticles are negatively charged. According to the literature, when the absolute value of zeta potential is higher than 30 mV for colloidal formulation, the particles are likely to be electrochemically stable under the investigated condition because the surface charge prevents aggregation of the particles[53,54]. Minoxidil-loaded NLC present particles with charge around 30 mV, in absolute value, which indicates that the nanoformulation in study have a good physical stability.

These values suffered variations (increase, in absolute value) with the increase of the minoxidil concentration, which means that the zeta potential of the nanoparticles is affected by the encapsulation of this drug.

3.2.2.2 Finasteride

The mean zeta potential values and SD of NLC loaded with finasteride, of triplicate samples, are presented in **Figure 21**.

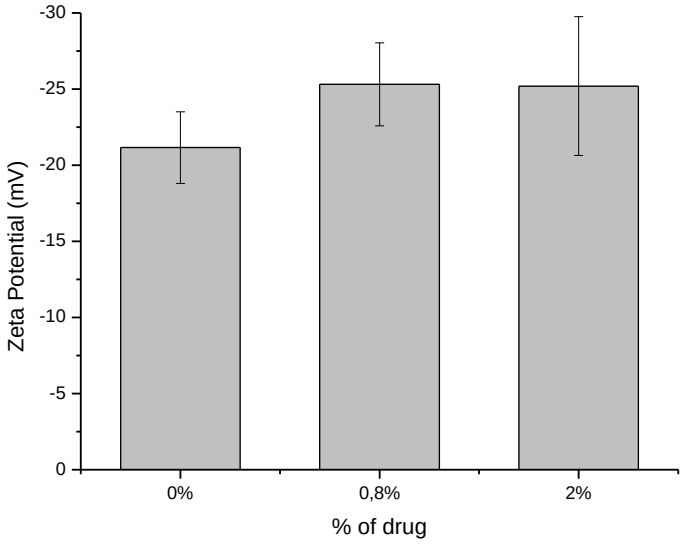

Figure 21: Mean zeta potential distribution and SD with increasing concentrations of finasteride, of triplicate samples of finasteride-loaded NLC.

The results obtained for finasteride-loaded NLC showed that the nanoparticles are negatively charged, and the values of zeta potential are between 20 and 30 mV, in absolute value. Once more, this fact indicates that the nanoformulation in study has a good physical stability.

These values suffered slight variations with the increase of the finasteride concentration, which means that the zeta potential of the nanoparticles was not significantly affected by the encapsulation of drug.

To sum up, all drug (minoxidil and finasteride) loaded lipid nanoparticles have a good size, polydispersity, as desired to achieve the dermis, and negative charge (around 30 mV, in absolute values), which assures a good physical stability for the formulation. As so, all formulations present the features intended, in terms of size and charge, for dermal and transdermal application.

3.2.3 DSC

Particle size and charge analysis is just one aspect of LN quality. The same attention has to be paid on the characterization of lipid crystallinity and modification, because these parameters are strongly correlated with drug incorporation, release rates and drug expulsion during storage[55]. Drug expulsion from lipid nanoparticles is caused by polymorphic modifications of the lipid during storage, and this problem is more pronounced in SLN compared to NLC due to the fact that SLN are only composed by solid lipids. Therefore, after SLN preparation, at least one part of the lipid particles crystallizes in a higher energy modification (α or β')[31]. During storage, these polymorphic forms can be converted into a more ordered modification (β), which is characterized by a lower energy modification and a higher degree of crystallinity[56]. Due to its high degree of order, the number of imperfections in the crystal lattice is reduced leading to drug expulsion. By creating a less ordered solid lipid matrix, i.e. by blending a solid lipid with a liquid lipid (as in NLC), a higher active load of the particles can be achieved and it might be possible to avoid or minimize the expulsion of the active compound during storage[57].

Differential Scanning Calorimetry (DSC) is the technique commonly used to assess the polymorphic status of the lipid (see **Figure 22**). The rational behind the use of this technique is that different lipid transitions into different polymorphic states possess a different thermodynamic behavior[55]. The lipid polymorphic forms are different according to their stability and crystallinity. As mentioned above, there are several types of lipid interconvertible forms (represented in **Figure 22**): supercooled melts; α-form; β' and β-form. Supercooled melts are not lipid nanosuspensions, but emulsions of lipid droplets, while the other forms are crystallized lipid forms, being α-form less ordered, and β'-form, highly ordered with a dense crystal structure. Thermodynamic stability and lipid packing density increase, and drug incorporation rates decrease in the following order: super-cooled melt < α-modification < β'-modification < β-modification (stable)[55].

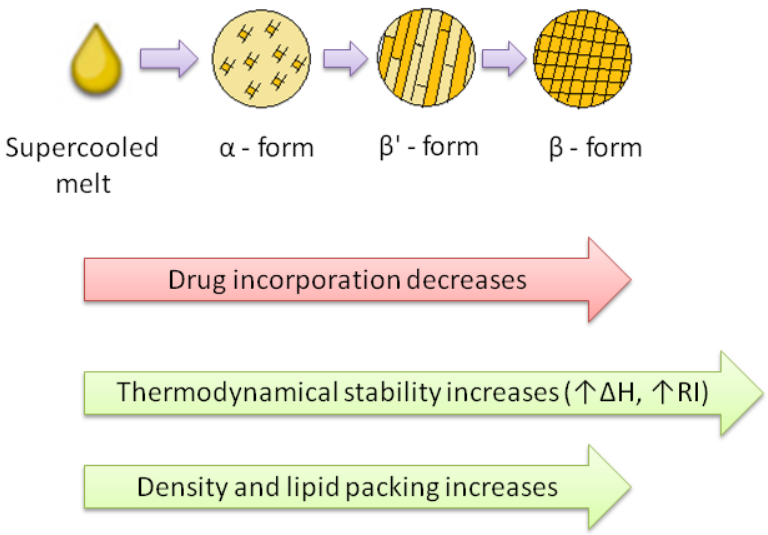

Figure 22: Schematic representation of the polymorphic forms of the lipids in lipid nanoparticles. Arrows indicate the influence of the polymorphic transitions in: the drug incorporation; thermodynamic stability and lipid packing.

DSC analysis is one of the methods used to access the type of polymorphic form, and their transitions in a lipid nanoparticle suspension and how these transitions are affected by the presence of drugs encapsulated in the nanoparticles. Indeed the breakdown of the crystal lattice by heating the sample yields inside information on, e.g., polymorphism, crystal ordering or eutectic mixtures[58]. The physical state of the particles is very important from the technological as well as from the biopharmaceutical point of view. Hence, this analysis is particularly important to observe the crystallization behaviour of nanoparticles, which influences the expulsion of the drug (**Figure 22**) and assess the influence of the incorporated drug on the structure of the lipid matrix. The calorimetric method measures the amount of energy absorbed (endothermic process) or released (exothermic process) of a sample when it is heated or cooled. DSC analysis also provides the determination of the melting temperature and the enthalpy of the lipids that constitute the nanoparticles. Typically, a DSC thermogram representing the phase transitions between the different polymorphic forms would be similar to the one represented in **Figure 23**.

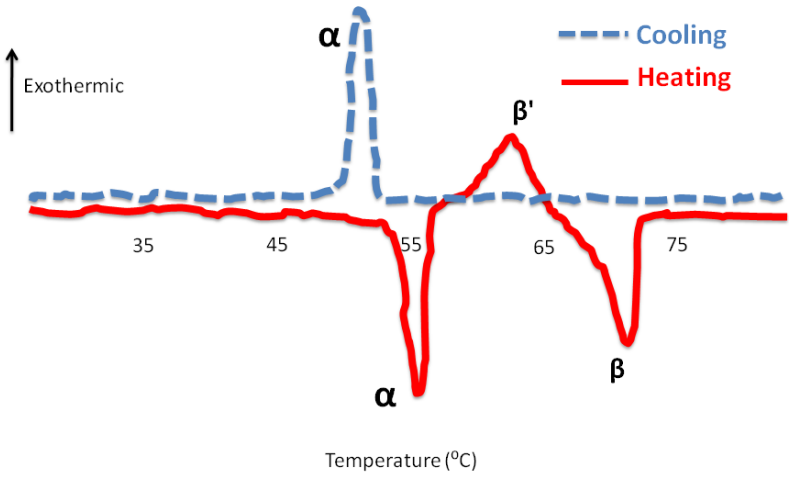

Figure 23: DSC thermogram showing the phase transitions to the different polymorphic forms.

In **Figure 23** it is possible to observe that the heating and cooling thermograms present different peaks correspondent to different polymorphic lipid forms. Several parameters can be evaluated in this thermogram. The temperature from which the peak starts is called **onset temperature**; the maximum of the peak gives the **melting temperature**, and the integration of the peak allows determining the **melting enthalpy (Δ*H*)**. A high value for the melting enthalpy suggests a high level of organization in the crystal lattice, because the fusion of a highly organized crystal (perfect crystal) requires more energy to overcome the forces of cohesion in the crystal lattice.

According to the above mentioned, DSC measurements were performed to obtain information about the melting behaviour, the polymorphism and the degree of crystallinity of the lipid nanoparticles under investigation, as well as, of the bulk materials used in the preparation of the nanoparticles. DSC measurements were carried out using a Perkin-Elmer Pyris 1 differential scanning calorimeter and a software provided by Perkin Elmer for data analysis. The samples were weighed (2-11 mg) directly in aluminum pans and scanned between 30 °C and 60 °C at a heating rate of 5 °C/min and cooling rate of 40 °C/min, under nitrogen gas. An empty aluminum pan was used as reference (**Figure 24**). These measurements were performed for only one determination.

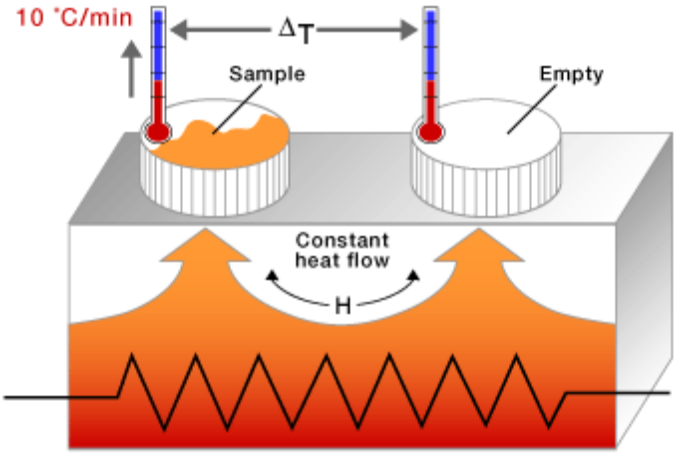

Figure 24: Schematic representation of DSC[59].

The onset and the melting point (peak maximum) were evaluated to describe the melting behaviour. The melting enthalpy (Δ*H*) was evaluated to get more information about the recrystallization of the lipid. Furthermore, the degree of crystallinity or recrystallization index (RI), i.e. percentage of re-crystallized solid lipid related to initial solid lipid concentration (not total lipid concentration of solid and liquid lipid) was calculated using the following equation[60]:

$$RI\ (\%) = \frac{\Delta H\ SLN\ or\ NLC\ dispersion\ (J/g)}{\Delta H\ bulk\ material\ (J/g) \times Concentration\ \ lipid\ phase\ (\%)} \times 100$$

The results of DSC measurements obtained are presented in the next figures and tables.

3.2.3.1 Characterization of bulk material and drugs

The first part of DSC measurements consisted in the characterization of the melting points of the bulk material used in this work – Cetyl palmitate, Precirol ATO 5, Miglyol 812, Oleic acid and Polysorbate 60, as well as the influence of minoxidil and finasteride. After that, NLC unloaded and loaded formulations were also assessed.

The obtained thermogram of Cetyl palmitate bulk material is shown in **Figure 25**. The corresponding DSC data is depicted in **Table 11**.

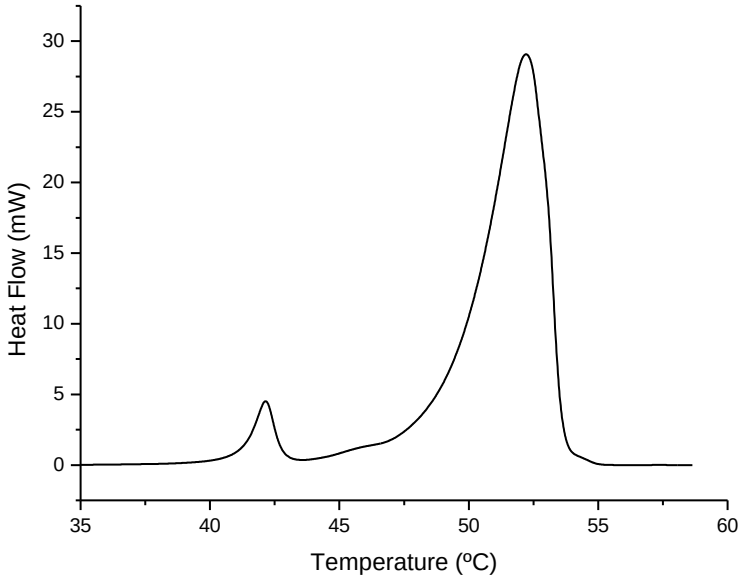

Figure 25: DSC melting curve of cetyl palmitate bulk material (second heating).

The heating curve of cetyl palmitate revealed two distinct polymorphic modifications with melting points at 42,14 °C (first peak) and 52,21 °C (second peak). According to *Saupe et al.* [58], the first peak with lower melting point is attributed to the α-polymorphic form (thermodynamic instable modification) whereas the second peak belongs to the β-polymorphic form (stable modification).

To produce the LN, the mixture of solid and liquid lipids, the drug and surfactant are melted. This mixture is dispersed in hot water to yield a pre-emulsion. This pre-emulsion is homogenized to obtain a hot o/w nanoemulsion. Cooling leads to crystallization of the lipid and formation of LN. This process means that, when analyzing the lipid nanoparticles by DSC, the lipid has been melted before, i.e., DSC analysis of the lipid nanoparticles is a second melting process. Therefore, to imitate the production conditions and to be possible to compare, the bulk cetyl palmitate was heated a second time in the DSC and this heating is the one evaluated (**Figure 25**).

Table 11: Melting point (peak maximum), onset and enthalpy of cetyl palmitate obtained from the second heating in the DSC analysis.

Sample	Peak	Onset (°C)	Melting point (°C)	Enthalpy (J/g)
Cetyl palmitate	First	41,25	42,14	11,19
	Second	49,30	52,21	213,07

The bulk mixture of Cetyl palmitate, Oleic acid and Polysorbate 60 (produced in the same proportions as used to produce NLC), was investigated in order to obtain information about the inclusion of the liquid lipid in the solid lipid and its influence on the melting behaviour, as well as the effect of the surfactant (Polysorbate 60) on the melting points. The influence of minoxidil in this bulk mixture was also tested – this mixture was produced in the same ratio used in NLC 2% Minoxidil. This was the

chosen percentage due to its higher loading efficiency. The obtained thermogram is shown in **Figure 26** and the corresponding DSC data is presented in **Table 12**.

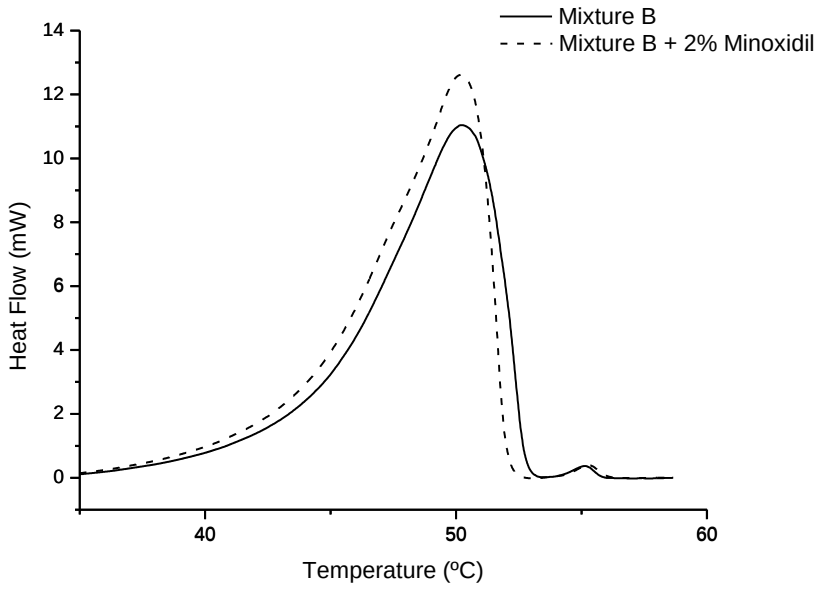

Figure 26: DSC melting curves of bulk mixtures of Cetyl palmitate, Oleic acid and Polysorbate 60 (Mixture B); and this mixture with minoxidil.

In both cases (bulk mixtures with and without addition of minoxidil) DSC thermograms revealed only a β-endotherm (**Figure 26**). Comparatively with Cetyl palmitate, the bulk mixture of the solid and liquid lipids and surfactant revealed a decrease of the melting point from 52,21 °C to 50,23 °C. This indicates that Oleic acid (a liquid lipid) being melted with Cetyl palmitate reduces the order in the crystal structure of Cetyl palmitate. The melting point of this mixture of bulk materials with minoxidil decreased slightly (50,20 °C). However, these values difference is not significant in terms of polymorphic modifications.

As for the values of enthalpy, it is possible to observe a decrease from 213,07 J/g to 147,56 J/g between the solid lipid and the mixture of bulk materials. The presence of minoxidil in the mixture caused an increase of the enthalpy (147,56 J/g to 155,29 J/g). However, these last values are not so different, which allow the conclusion that probably the drug does not change significantly the nanoparticles structure and chemical/physical properties.

Table 12: Melting point (peak maximum), onset and enthalpy of bulk mixture of Cetyl palmitate, Oleic acid and Polysorbate 60; and this mixture with minoxidil.

Sample	Onset (°C)	Melting point (°C)	Enthalpy (J/g)
Mixture B	44,20	50,23	147,56
Mixture B + 2% Minoxidil	44,31	50,20	155,29

The obtained thermogram of Precirol ATO 5 bulk material is shown in **Figure 27**. The corresponding DSC data is depicted in **Table 13**.

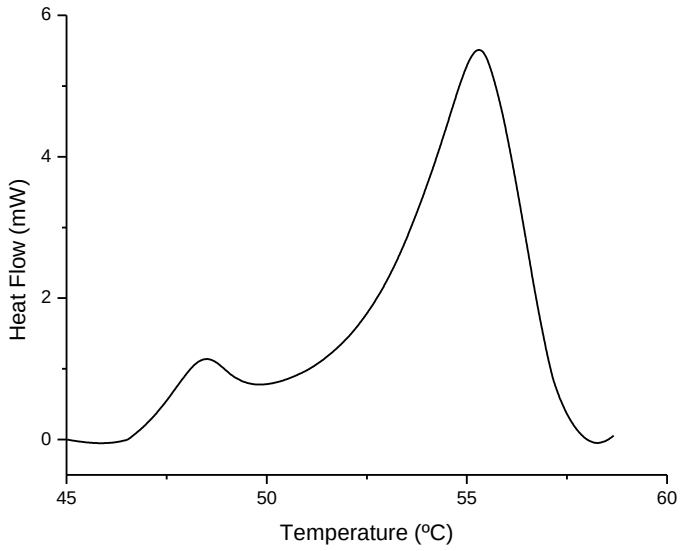

Figure 27: DSC melting curve of Precirol ATO 5 bulk material (second heating).

The heating curve of Precirol ATO 5 revealed two distinct polymorphic modifications with melting points at 48,87 °C (first peak) and 55,02 °C (second peak). Such as Cetyl palmitate, the first peak with lower melting point is attributed to the α-polymorphic form (thermodynamic instable modification) whereas the second peak belongs to the β-polymorphic form (stable modification)[61]. Since the two peaks were not clearly divided, their deconvolution had to be made. Consequently, the all the data here presented is related to the separated peaks – reason why some values as onset temperature were not possible to calculate and therefore are not presented.

Table 13: Melting point (peak maximum) and enthalpy of Precirol ATO 5 obtained from the second heating in the DSC analysis.

Sample	Peak	Melting point (°C)	Enthalpy (J/g)
Precirol ATO 5	First	48,87	7,81
	Second	55,02	55,77

The bulk mixture of Precirol ATO 5, Miglyol 812 and Polysorbate 60 (produced in the same proportions as used to produce NLC), was investigated in order to obtain information about the inclusion of the liquid lipid in the solid lipid and its influence on the melting behaviour, as well as the effect of the surfactant (Polysorbate 60) on the melting points. The influence of finasteride in this bulk mixture was also tested – this mixture was produced in the same ratio used in NLC 2% Finasteride. This was the chosen percentage due to its higher loading efficiency. The obtained thermogram is shown in **Figure 28** and the corresponding DSC data is presented in **Table 14**.

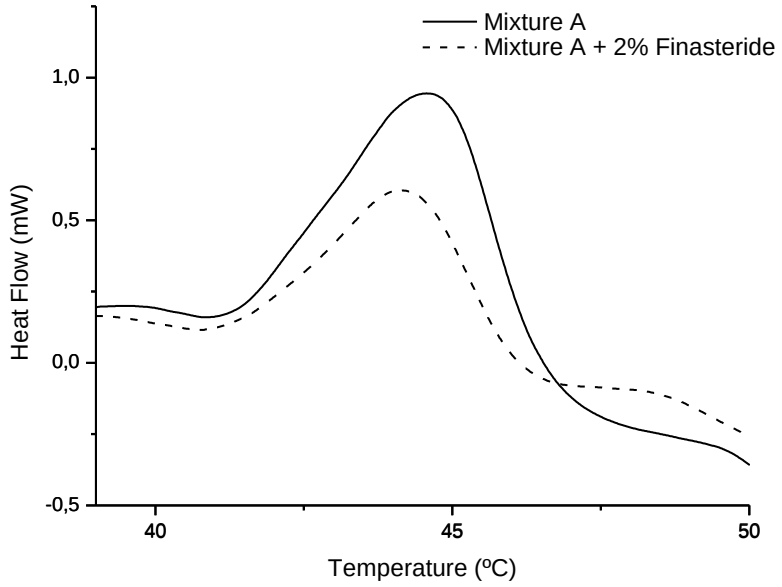

Figure 28: DSC melting curves of bulk mixtures of Precirol ATO 5, Miglyol 812 and Polysorbate 60 (Mixture A); and this mixture with finasteride.

In both cases (bulk mixtures with and without addition of finasteride) DSC thermograms revealed only a β-endotherm (**Figure 28**). Comparatively with Precirol ATO 5, the bulk mixture of the solid and liquid lipids and surfactant revealed a decrease of the melting point from 55,02 °C to 44,67 °C. This indicates that Miglyol 812 (a liquid lipid) being melted with Precirol ATO 5 reduces the order in the crystal structure of Precirol ATO 5. The melting point of this mixture of bulk materials with finasteride decreased slightly (44,22 °C). However, these values difference is not significant in terms of polymorphic modifications.

As for the values of enthalpy, it is possible to observe a decrease from 55,77 J/g to 5,95 J/g between the solid lipid and the mixture of bulk materials. The presence of finasteride in the mixture caused a decrease of the enthalpy (5,95 J/g to 3,89 J/g). However, these last values are not so different, which allow the conclusion that probably the drug does not change significantly the nanoparticles structure and chemical/physical properties.

Table 14: Melting point (peak maximum), onset and enthalpy of bulk mixture of Precirol ATO 5, Miglyol 812 and Polysorbate 60; and this mixture with finasteride.

Sample	Onset (°C)	Melting point (°C)	Enthalpy (J/g)
Mixture A	41,56	44,67	5,95
Mixture A + 2% Finasteride	41,59	44,22	3,89

3.2.3.2 NLC of minoxidil characterization

Although a crystalline lipid (Cetyl palmitate) was used for the production of NLC dispersions, the final physical state of the nanoparticles could be other than solid, due to the presence of the liquid lipid (Oleic acid) and to the well-known supercooling effect. Supercooled melts (emulsions) are produced instead of nanoparticles dispersions when the melting point of the formulation is well below to the room temperature[62,63]. For that reason, the determination of the physical state of the lipid matrix is essential for the development of nanoparticles based on solid lipids. According to this, NLC particles containing or not 2% of minoxidil and prepared in a similar way as described previously, were analyzed by DSC. The obtained thermogram is shown in **Figure 29** and the corresponding DSC data is depicted in **Table 15**.

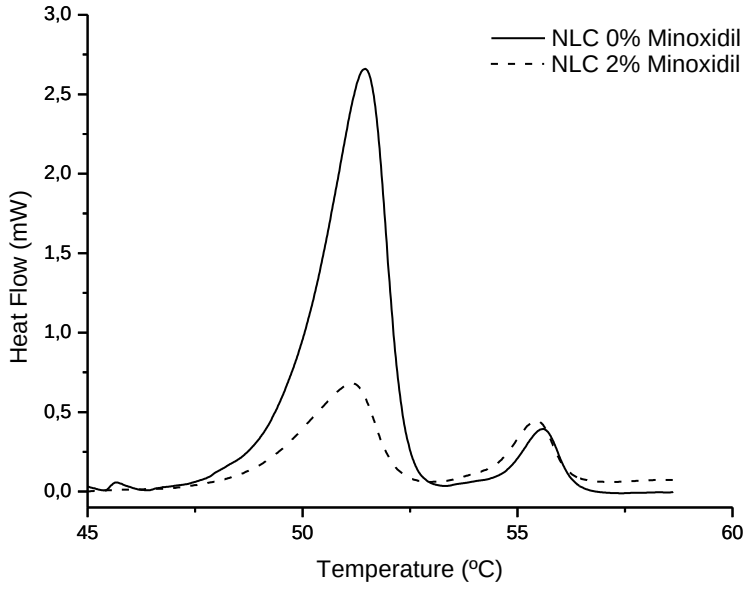

Figure 29: DSC melting curves of NLC placebo and NLC loaded with minoxidil.

The enthalpy obtained for the bulk lipids is much higher than the enthalpy of NLC, meaning that there is a loss of crystallinity of the lipids after their incorporation into NLC. However, the lipids in these formulations still possess some degree of crystallinity as observed by the presence of β-form (first peak) in the DSC thermograms. Indeed, the melting enthalpy in NLC placebo has decreased from 147,56 J/g (bulk mixture) to 6,89 J/g, indicating a slower recrystallization and a crystal order disturbance which might influence the loading capacity. This is expected to happen, since oil incorporation lowers the crystallization and melting temperatures of the particle matrix and accelerates the transition of the wax into the stable β-polymorph after crystallization[58]. Additionally, surfactants distributed in the melted lipid phase can interfere with lipid crystallization, resulting in a lower melting enthalpy. Generally, the presence of guest molecules in the lipid matrix also influences its crystallization degree,

decreasing the lipid layer organization[64]. Thus, the enthalpy of NLC also decreased with the presence of minoxidil.

Solid state was confirmed for both body (37 ºC) and room temperatures (25 ºC) since the onset temperature and the melting peak were above these temperatures (see **Table 15**).

The instable lower melting modification observed in the melting curve of Cetyl palmitate was not observed in drug-loaded NLC. This is caused by the fact that polymorphic transitions can occur more rapidly in lipid nanoparticles than in bulk state[65]. On the other hand, the DSC measurements were not done in the same day of NLC production, but some days after. During storage, the peak corresponding to the α-modification becomes smaller, which can also explain the fact that the lower melting modification is not observed. The melting point obtained for the more stable modification was slightly greater (not significant) than the melting point of this modification in the bulk mixture. For all NLC formulations two maximum peaks occurred – revealing that the drug is not well dissolved in the lipid matrix[66].

Table 15: Melting point (peak maximum), onset, enthalpy and crystallinity index (RI) of NLC minoxidil formulations.

Sample	Onset (°C)	Melting point (°C)	Enthalpy (J/g)	RI (%)
NLC 0% Minoxidil	49,53	51,46	6,89	0,23
NLC 2% Minoxidil	48,82	51,16	1,74	0,06
Bulk mixture (Mixture B)	44,20	50,23	147,56	100

3.2.3.3 NLC of finasteride characterization

As already mentioned, although a crystalline lipid (Precirol ATO 5) was used for the production of NLC dispersions, the final physical state of the nanoparticles could be other than solid, due to the presence of the liquid lipid (Miglyol 812) and to the well-known supercooling effect[62,63]. Therefore, NLC particles containing or not 2% of finasteride and prepared in a similar way as described previously, were analyzed by DSC. The obtained thermogram is shown in **Figure 30** and the corresponding DSC data is depicted in **Table 16**.

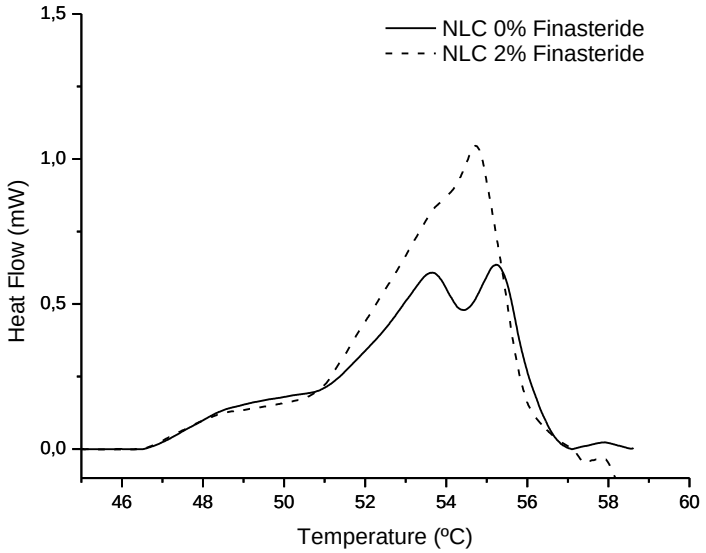

Figure 30: DSC melting curves of NLC placebo and NLC loaded with finasteride.

The enthalpy obtained for the bulk lipids is higher than the enthalpy of NLC, meaning that there is a small loss of crystallinity of the lipids after their incorporation into NLC. However, the lipids in these formulations still possess some degree of crystallinity as observed by the presence of β-form (second peak on NLC 0% Finasteride) in the DSC thermograms. Indeed, the melting enthalpy in NLC placebo has decreased from 5,95 J/g (bulk mixture) to 1,01 J/g, indicating a slower recrystallization and a crystal order disturbance which might influence the loading capacity. This is expected to happen, since oil incorporation lowers the crystallization and melting temperatures of the particle matrix and accelerates the transition of the solid lipid into the stable β-polymorph after crystallization[58]. Additionally, surfactants distributed in the melted lipid phase can interfere with lipid crystallization, resulting in a lower melting enthalpy. Generally, the presence of guest molecules in the lipid matrix also influences its crystallization degree, decreasing the lipid layer organization[64]. However, the enthalpy of NLC increased with the presence of finasteride.

Since the two peaks of NLC 0% Finasteride curve were not clearly divided, their deconvolution had to be made. Consequently, all the data here presented is related to the separated peaks – reason why some values as onset temperature were not possible to calculate and therefore are not presented. These two peaks could correspond to different polymorphic forms that, with the drug presence and due to its probably induced changes in nanoparticles structure or chemistry, is attenuated or disappears.

Solid state was confirmed for both body (37 ºC) and room temperatures (25 ºC) since the onset temperature and the melting peak were above these temperatures (see **Table 16**).

The instable lower melting modification observed in the melting curve of Precirol ATO 5 was not observed in drug-loaded NLC. This is caused by the fact that

polymorphic transitions can occur more rapidly in lipid nanoparticles than in bulk state[65]. On the other hand, the DSC measurements were not done in the same day of NLC production, but some days after. During storage, the peak corresponding to the α-modification becomes smaller, which can also explain the fact that the lower melting modification is not observed. The melting point obtained for the more stable modification was greater than the melting point of this modification in the bulk mixture.

Table 16: Melting point (peak maximum), onset, enthalpy and crystallinity index (RI) of NLC finasteride formulations.

Sample	Onset (°C)	Melting point (°C)	Enthalpy (J/g)	RI (%)
NLC 0% Finasteride	-	55,27	1,01	1,41
NLC 2% Finasteride	52,24	54,72	3,30	7,22
Bulk mixture (Mixture A)	41,56	44,67	5,95	100

3.2.3.4 Comparison with DLS

The phase transition temperatures of NLC (minoxidil and finasteride) were also assessed using DLS. This equipment described on section *3.1.1.1* also measures the mean count rate, which is the average number of photons detected per second[67] – a frequency data given in cps units. This parameter proved to be a method of phase transition temperature determination (considered much more reliable than size). As the temperature is altered, the discontinuity in the mean count route corresponds to a change in optical properties of the material studied. These changes are related with phase transitions in the phospholipids from initial state to another one. Therefore, the basis of this method is that changes in the measured scattering intensity reflect changes in the optical properties of the material during temperature variations[67].

The NLC samples used to these measurements have the same preparation as the others used in DLS (dilution 1:400 and filtration through 200 nm filter). The DLS equipment was set at the measurement automation, with starting temperature at 30 °C and increment of 1 °C between measurements until reaches 70 °C; 2 min was the time defined to temperature stabilization. At each temperature, a measurement of mean count rate (and size) is done – at the end, those count rate values were related to temperature in a plot. All NLC (placebo and with the two percentages of drug tested) were assessed in duplicate – the values of count rate presented were calculated by a normalization and mean of the two sets of data (duplicate).

The inflection point of the obtained plots corresponds to the phase transition temperature (*Tm*), which was calculated based on this following equation already described[68]:

$$r_s = r_{s_1} + p_1 T + \frac{r_{s_2} - r_{s_1} + p_2 T - p_1 T}{1 + 10^{B(1/T - 1/T_m)}}$$

where r_s are steady-stat anisotropy values, T is the absolute temperature, Tm is the midpoint of the phase transition (phase transition temperature), B is a measure of the cooperativity of the transition, p_1 and p_2 correspond to the slopes of the straight lines at the beginning and at the end of the plot, and r_1 and r_2 are the anisotropy intercepting values at the y axis for both lines mentioned[68].

For minoxidil, NLC placebo and loaded with 2 and 3% of drug were assessed using this *Tm* determination method and the results indicate a mean *Tm* of 47 °C – there was no significant differences between formulations. This value is different (4 to 5 °C less) from the ones obtained using DSC – 51,46 °C (NLC placebo) and 51,16 °C (NLC 2%).

For finasteride, NLC placebo and loaded with 0,8 and 2% of drug were assessed using this *Tm* determination method and the results are shown in **Figure 31**. The plot obtained to NLC 0,8% was very similar to NLC placebo. For NLC placebo *Tm* was 49,57 °C, while for NLC 2% finasteride it was 49,19 °C. These values are different (5 to 6 °C less) from the ones obtained using DSC – 55,27 °C (NLC placebo) and 54,72 °C (NLC 2%).

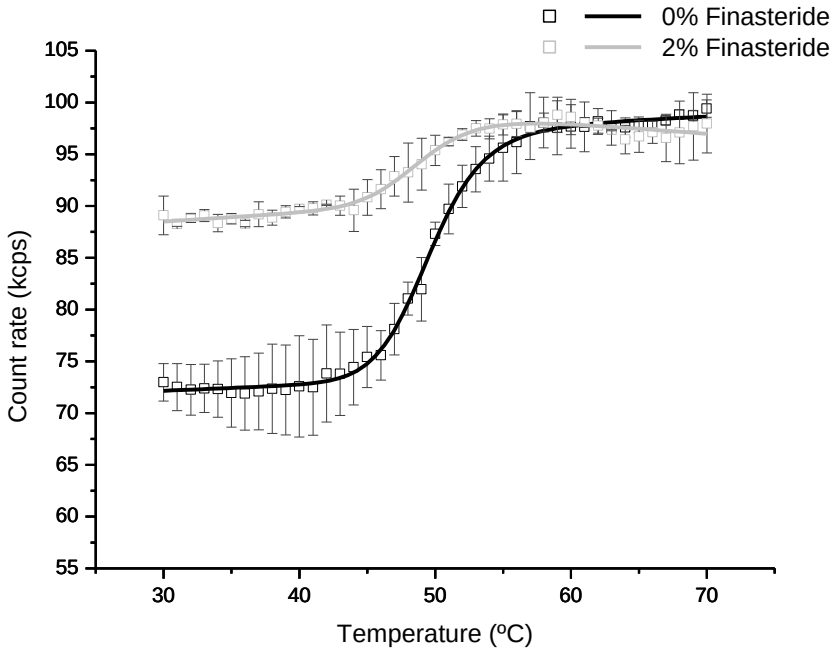

Figure 31: Determination of phase transition temperature of NLC of finasteride.

One possible explanation to this constant difference on results is that the temperature on DLS and/or DSC was not so well adjusted.

In addition, the curve of NLC 2% finasteride has its initial straight line with higher count rate values than NLC 0% – this could be explained due to drug addition, since it could cause an increase of nanoparticles fluidity and this difference in optical properties could be the reason why count rate values increase.

3.2.4 Morphology

Morphological evaluation (shape and size) of the nanoparticles prepared was performed using Scanning Electron Microscopy (SEM) (see **Figure 32**). This method uses the electrons reflected to create a 3D image of the sample surface. Aqueous nanoparticles dispersions were applied and spread on a thin carbon film. An electron gun emits a beam of high energy primary electrons. The beam of the electrons will pass through the lens which concentrates the electrons to a fine spot and scan across the specimen row by row. As the focused electron beam hits a spot on the sample, secondary electrons are emitted by the specimen through ionization. A detector counts these secondary electrons. The electrons are collected by a laterally placed collector and these signals are sent to an amplifier.

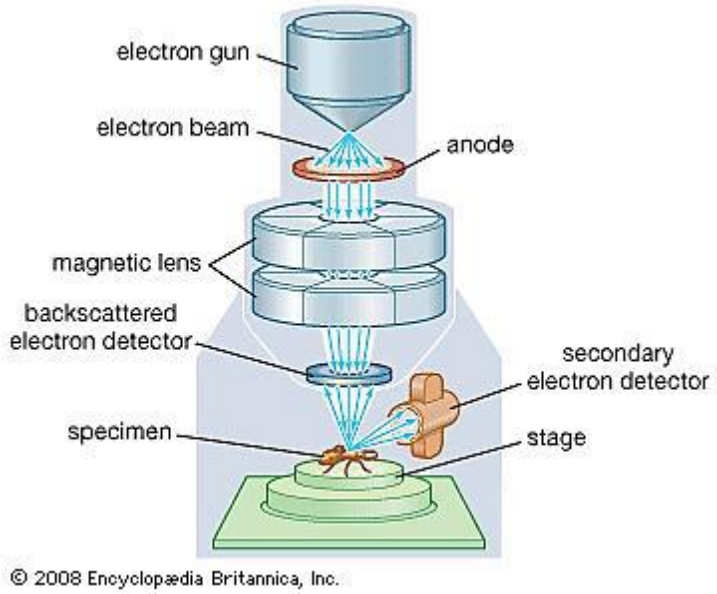

Figure 32: Schematic representation of SEM[69].

Nanoformulations assessed were diluted (1:400) and filtrated (200 nm filter). Measurements done in this work used cryo-SEM technique. In this technique, measurements were prepared by dropping the dispersions of the nanoparticles on a copper grid supported Formvar Films. The samples were frozen in liquid N_2 (-210 °C), cryo-fracture was made (-150 °C) and then samples were subjected to sublimation for 4 minutes (-90 °C). In the end, coating of the samples with an alloy of gold/palladium (-150 °C) were made. Cryo system used is called GATAN ALTO 2500. Finally, samples

were observed using a microscope JEOL JSM 6301F (-150 °C), and analyzed with INCA ENERGY 350, at CEMUP facilities.

3.2.4.1 Results and discussion

Electron microscopy provides, in contrast to DLS, direct information on the particle shape. All nanoparticles exhibit a spherical shape (see **Figure 33**) and a smooth surface independently of their composition. The sizes of the nanoparticles observed by SEM have shown to be similar than the analyzed by DLS; however it has been reported that solvent removal may cause modification changes which will influence the particle shape and size. Points that can be seen on the images obtained are probably due to the coating.

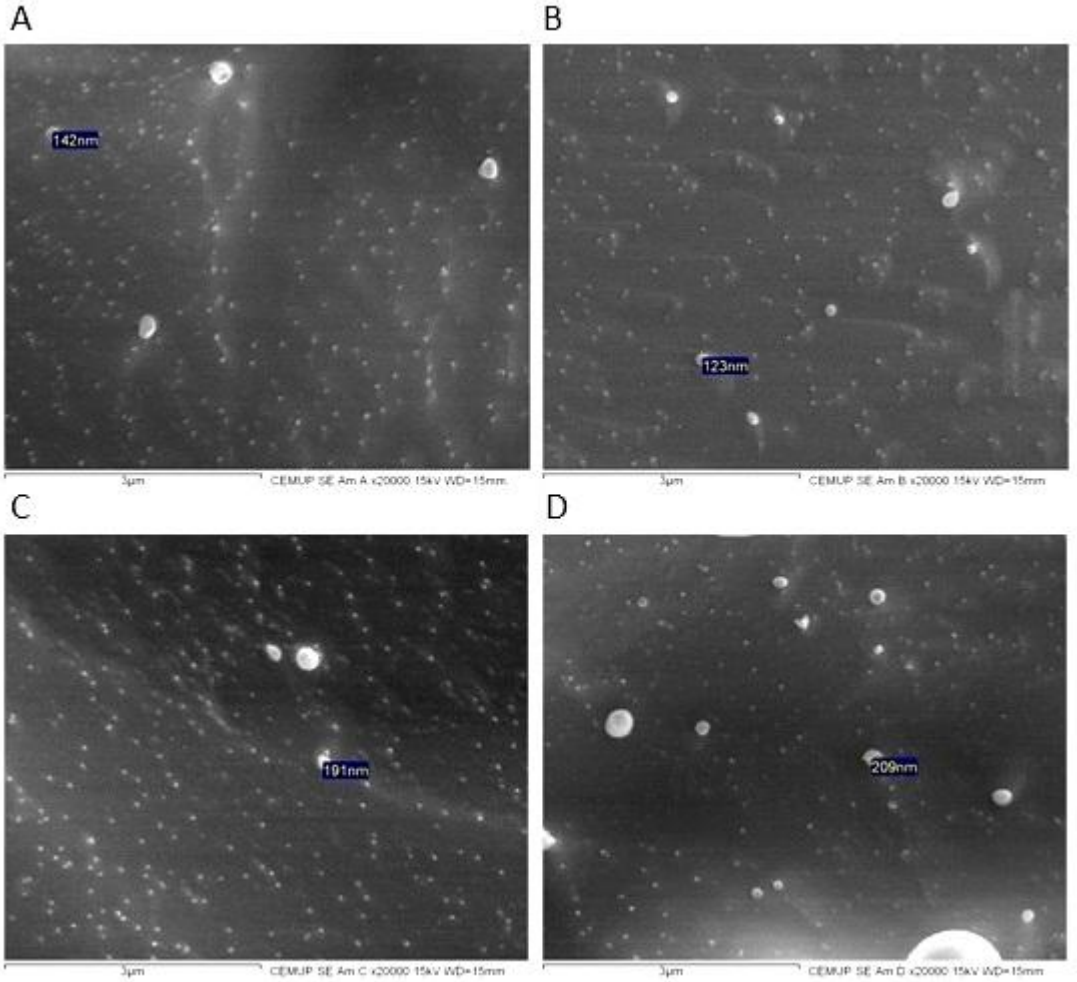

Figure 33: SEM images of NLC placebo finasteride (A), 2% finasteride (B), placebo minoxidil (C) and 2% minoxidil (D). The scale indicated below the images is of 3µm. Size indicated in image A is 142 nm; in B is 123 nm; in C is 191 nm; in D is 209 nm.

3.3 Loading efficiency

In general, loading efficiency (LE) should be high enough to avoid losing drugs during the production and also to avoid the need of using higher concentration of drugs. The nanoformulations were centrifuged (Jouan BR4i, Multifunction centrifuge) through centrifugal filter units (Amicon Ultra-4, PLGC Ultracel-PL Membrane, 10 kDa, Milipore) at 4000 rpm (3300×g) at 25 °C for 5 minutes (to NLC of minoxidil) and for 15 minutes (to NLC of finasteride) or until complete separation between the nanoparticles (pellet retained in the filter unit) and the aqueous phase (supernatant). The supernatant containing the dissolved free drug was analyzed in a PerkinElmer Lambda 45 UV/VIS Spectrometer. Spectra were taken in the range of 200-800 nm for both drugs. Spectra of the nanoparticles without the drug incorporated (placebo) were also analyzed to establish the absorbance baseline. As so, using the equation obtained for the calibration curve it was possible to determine the drug concentration present in the supernatant. Considering the initial concentration of drug used in the formulation ([Drug used in formulation]) and subtracting the free drug concentration present in the supernatant (concentration of drug that was not incorporated in the LN), it is possible to obtain the concentration of drug that was incorporated in the LN ([Drug incorporated in LN]) and thus determine the drug loading efficiency by the following equation:

$$Loading\ Efficiency\ (\%) = \frac{[Drug\ incorporated\ in\ LN] \times 100}{[Drug\ used\ in\ formulation]}$$

This study was conducted over 28 days, and measurements of loading efficiency were performed, in the day of production, 13 and 28 days after, to analyze possible drug expulsion from the lipid nanoparticles during storage. The results obtained for each drug-loaded formulation are presented in the next graphs.

3.3.1 Minoxidil

The percentages of minoxidil loaded into NLC (**Figure 34**) were of 34,0% and 24,5% in the day of production, which means that a small quantity of drug was incorporated (in relation to the quantity initially added in the formulation). Minoxidil is a hydrophilic drug – this behaviour does not favour the interaction of this drug with lipids – which explains these results.

After 13 and 28 days, there was a slight decrease in the percentages for NLC 2%, presumably, again, due to minoxidil hydrophilic character that explains the drug release into the aqueous media. Although, this decrease as well as the slight variations for NLC 3% are not significant. In this way, even though the low incorporated

quantities, a good chemical stability of minoxidil loaded-NLC was found for all formulation in storage and all concentrations tested.

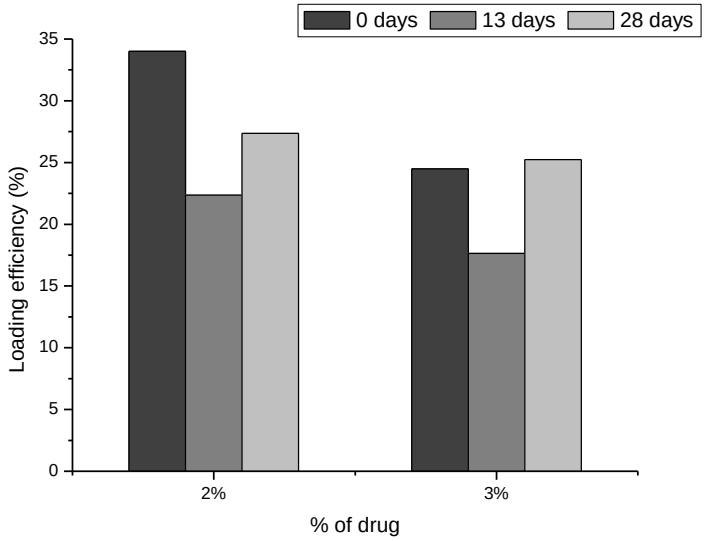

Figure 34: Minoxidil loading efficiency into different NLC produced (NLC 2% minoxidil and NLC 3% minoxidil) with time.

In order to be more perceptible, in **Figure 35** the same results presented above are represented in terms of minoxidil mass – the quantity of minoxidil loaded to each NLC formulation. Similarly, this quantity is in relation to the quantity initially added in the formulation – 20 mg for NLC 2%, and 30 mg for NLC 3%.

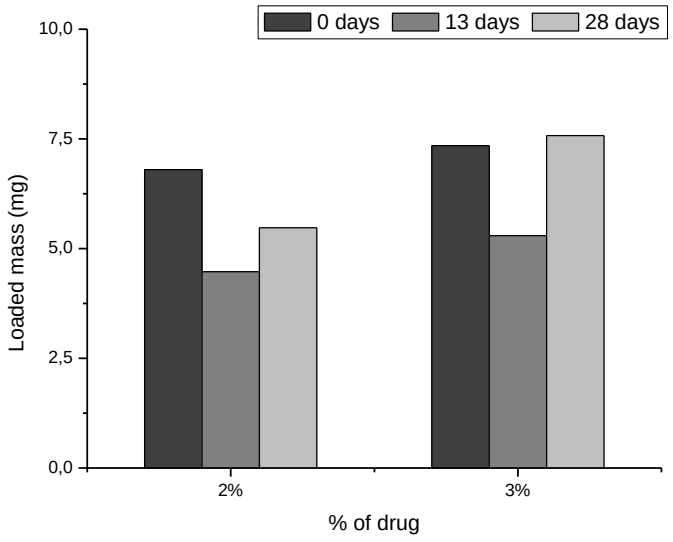

Figure 35: Minoxidil loaded mass into different NLC produced (NLC 2% minoxidil and NLC 3% minoxidil) with time.

3.3.2 Finasteride

The percentages of finasteride loaded into NLC (**Figure 36**) were of 85,8% and 96,2% in the day of production, which means that a great quantity of drug was incorporated (in relation to the quantity initially added in the formulation). Finasteride is a hydrophobic drug – this behaviour supports the interaction of this drug with lipids – which explains these results.

After 13 and 28 days, there was a slight decrease in the percentages for both NLC tested. However this decrease is not significant. In this way, apart from high incorporated quantities, a good chemical stability of finasteride loaded-NLC was found for all formulation in storage and all concentrations tested.

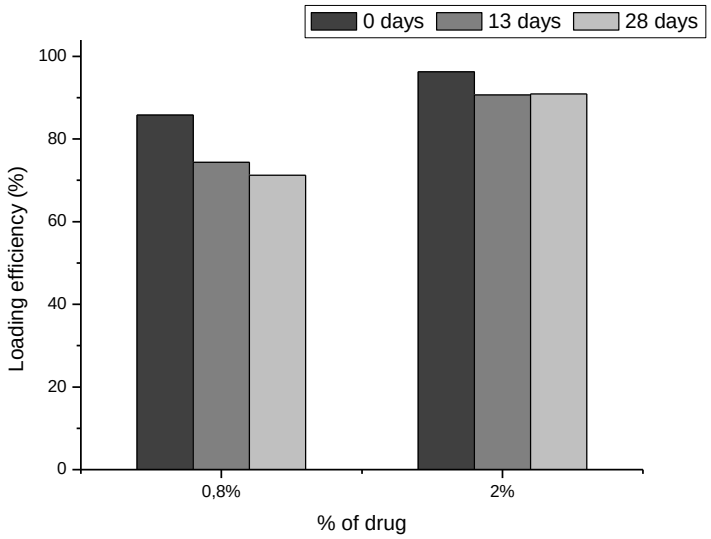

Figure 36: Finasteride loading efficiency into different NLC produced (NLC 0,8% finasteride and NLC 2% finasteride) with time.

In order to be more perceptible, in **Figure 37** the same results presented above are represented in terms of finasteride mass – the quantity of finasteride loaded to each NLC formulation. Similarly, this quantity is in relation to the quantity initially added in the formulation – 5 mg for NLC 0,8%, and 12,5 mg for NLC 2%.

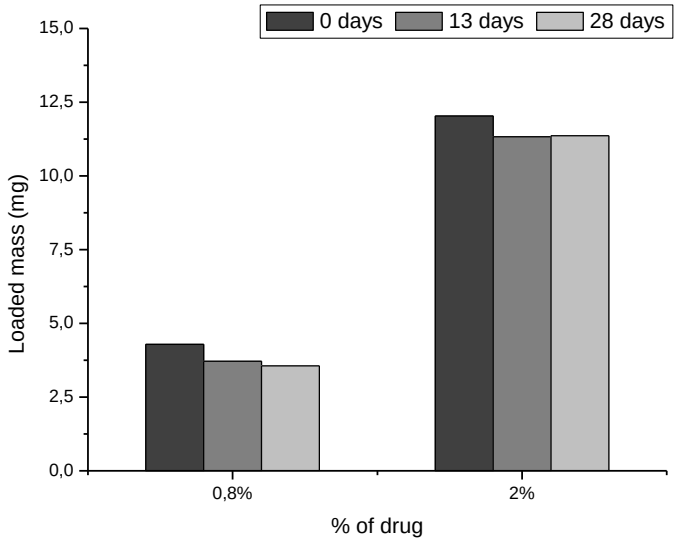

Figure 37: Finasteride loaded mass into different NLC produced (NLC 0,8% finasteride and NLC 2% finasteride) with time.

3.4 Evaluation of lipid nanoparticles stability

The purpose of stability tests is to provide evidence on how the quality of a formulation changes with time under the influence of a variety of conditions. Nanosuspensions are considered to be physically stable if the particle size distribution does not change within defined limits during the observation period under the storage conditions. Physical instabilities which may occur in nanosuspensions are agglomeration, aggregation, sedimentation, flotation, caking and crystal growth[70]. Several investigations indicate that no general statement over the physical stability with regards to particle size of lipid nanoparticles can be done and, because of that, each system needs to be investigated separately. As an example, *Saupe* and co-workers reported a constant particle size of SLN of cetyl palmitate stabilized with Tego Care 450 and NLC composed of cetyl palmitate and Miglyol 812 stabilized with Tego Care 450 over an observation period of one year at room temperature (25 °C) and 40 °C[58]. *Freitas and Müller* investigated the effect of light and temperature on the physical stability of SLN dispersions composed of 10% tribehenate and 1.2% poloxamer 188[71]. They found that particle growth could be induced by an input of kinetic energy (light, temperature) to the system. *Ruktanonchai et al.* showed that after 120 days of storage at room temperature (25°C), no significant changes were observed in particle size values for alpha-lipoic acid-loaded NLC, SLN and nanoemulsion[72].

Also aiming to access the stability of the developed formulations, measurements of particle size of drug-loaded lipid nanoparticles in study were performed over 28 days, at room temperature (25 °C): in the day of production, 7, 18 and 28 days later.

Another important parameter in the assessment of lipid nanoparticles stability is the zeta potential. As mentioned before, zeta potential is a useful tool to predict the physical long term stability of colloidal systems[15]. Zeta potential measurements were also performed, at room temperature, in the day of production, 7, 18 and 28 days after.

Next section presents the results on the stability evaluation, in the form of graphical representations, obtained for each parameter assessed.

3.4.1 Size

3.4.1.1 Minoxidil

The mean size, PI and SD of NLC loaded with minoxidil, of triplicate samples, over time are presented in **Figure 38**.

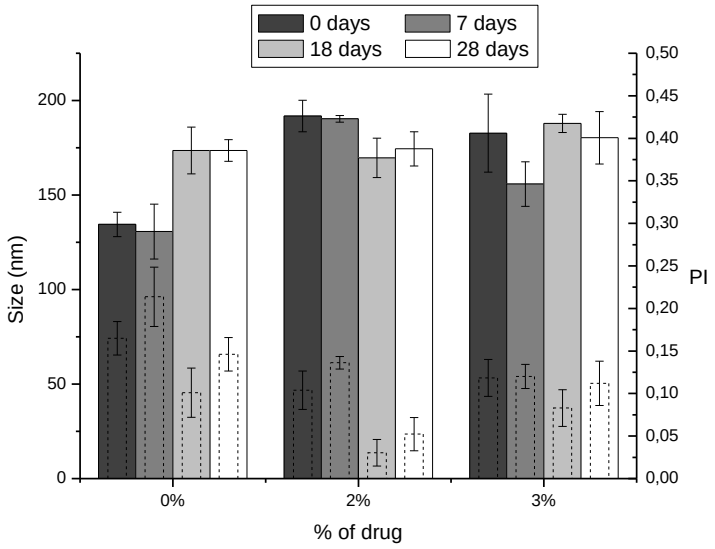

Figure 38: Mean size distribution and PI of triplicate samples of minoxidil-loaded NLC with different percentages, measured at different times.

The results show that, despite some variations, mean particle size and PI were kept constant over the observation period and at all minoxidil concentrations tested. The manual procedure of lipid nanoparticles production can introduce some errors: the movements of the arm and the positions of the tubes regarding the ultra-turrax and sonication tips are not exactly the same every time the formulations are produced, although an effort was made to eliminate these variations. Nevertheless, despite the variations due to systematic errors, it is possible to conclude, that all formulations (both loaded and unloaded) presented particles with sizes that are in the range of 131 to 192 nm. Therefore, the small variations in the values observed are only due to the intrinsic variability of the formulation procedure; and there was no direct relation between these size variations and the drug concentration in the formulation (as seen before in section *3.2.1.1*). Furthermore no significant size variations were observed in the time course where the nanoparticles where evaluated.

The mean size and PI of NLC were, over 28 days, bellow 200 nm and 0,250, respectively, as desired for dermal application.

These findings of particle size suggest a good physical stability of NLC loaded with minoxidil, over 28 days of storage.

3.4.1.2 Finasteride

The mean size, PI and SD of NLC loaded with finasteride, of triplicate samples, over time are presented in **Figure 39**.

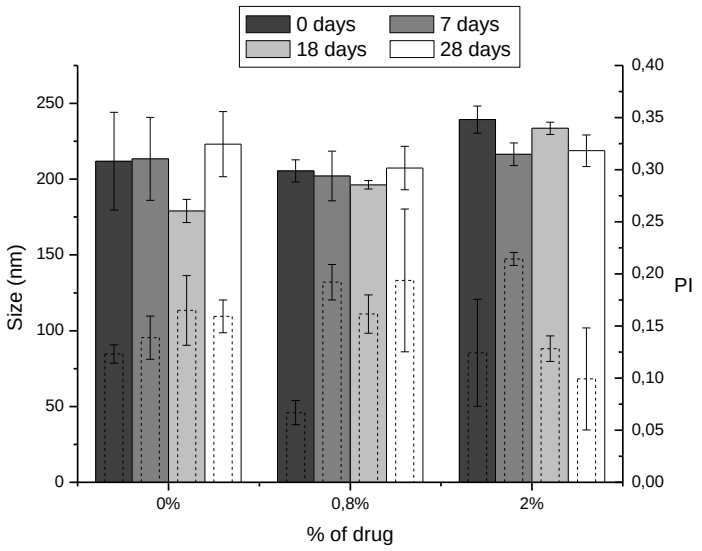

Figure 39: Mean size distribution and PI of triplicate samples of finasteride-loaded NLC with different percentages, measured at different times.

As with minoxidil, results show that, despite some variations, mean particle size and PI were kept constant over the observation period and at all finasteride concentrations tested. The manual procedure of lipid nanoparticles production, as it was already mentioned here, could be the only source of errors. Nevertheless, despite the variations due to systematic errors, it is possible to conclude, that all formulations (both loaded and unloaded) presented particles with sizes that are in the range of 179 to 240 nm. Therefore, the small variations in the values observed are only due to the intrinsic variability of the formulation procedure; and there was no direct relation between these size variations and the drug concentration in the formulation.

The mean size and PI of NLC were, over 28 days, around/a bit above 200 nm and below 0,250, respectively, which almost are the desired conditions for dermal application (size should be below 200 nm). Although, it is important to remind that all formulations have two populations – the main one, which is the one that mostly exists, has its mean size around 150-170 nm; the other population is present in a very low quantity but is the reason why nanoparticles' mean size increases to approximately 200 nm.

These findings of particle size suggest a good physical stability of NLC loaded with finasteride, over 28 days of storage.

In conclusion, both drugs-loaded NLC tested present a good physical stability with regards to particles size, which makes them appropriate to use.

3.4.2 Zeta Potential

3.4.2.1 Minoxidil

The mean zeta potential and SD of NLC loaded with minoxidil, of triplicate samples, over 28 days are shown in **Figure 40**.

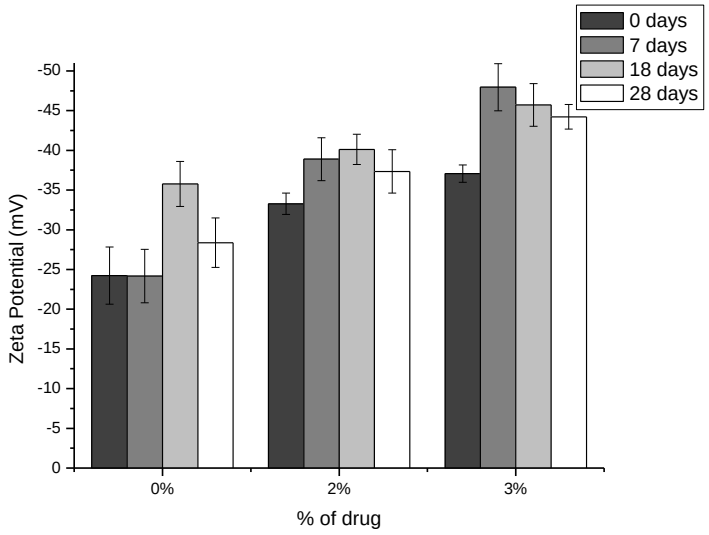

Figure 40: Mean zeta potential distribution of triplicate samples of minoxidil-loaded NLC with different percentages, at different times.

From the results obtained, it is possible to observe that zeta potential values were always negative and ranged from -24,2 mV to -48,0 mV. Some variations of zeta values with drug concentrations can be observed, and there seems to be a slight tendency of increase zeta potential absolute value when concentration of drug increases, but it is not clear – therefore, no relation between zeta potential values and drug concentrations can be established.

Over 28 days, for each formulation, there were no evident changes of the zeta potential values. As so, zeta potential measurements revealed that minoxidil-loaded NLC present good physical stability, in storage over a month, and particle aggregation and coalescence is unlikely to occur, due to the high electrostatic repulsion between the lipid nanoparticles. Hence, these findings support the conclusions of size measurements, suggesting good stability of NLC.

3.4.2.2 Finasteride

The mean zeta potential and SD of NLC loaded with finasteride, of triplicate samples, over 28 days are shown in **Figure 41**.

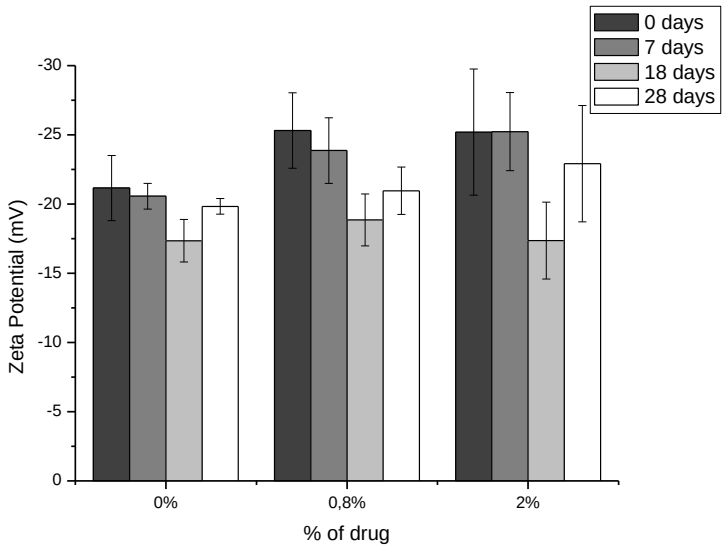

Figure 41: Mean zeta potential distribution of triplicate samples of finasteride-loaded NLC with different percentages, at different times.

From the results obtained, it is possible to observe that zeta potential values were always negative and ranged from -17,4 mV to -25,3 mV. Some variations of zeta values can be observed, but are not significant and, therefore, no relation between zeta potential values and drug concentrations can be established.

Over 28 days, for each formulation, there were no evident changes of the zeta potential values. As so, zeta potential measurements revealed that finasteride-loaded NLC present good physical stability, in storage over a month. Moreover and since zeta values are almost always above 20 mV, particle aggregation and coalescence is also unlikely to occur (not as much unlikely as for NLC of minoxidil), due to the relatively high electrostatic repulsion between the lipid nanoparticles. Hence, these findings support the conclusions of size measurements, suggesting good stability of NLC.

By combining results of particle size and zeta potential, it is clear that good physical stability of these drugs loaded-NLC could be obtained and particle aggregation during storage is not likely to occur.

3.5 Penetration assays

Penetration studies are important to assess the formulations ability to go through their barrier – skin – which is crucial to achieve their desired function. With these studies, therefore, it is possible to establish a penetration profile for drug formulation.

For all *in vitro* skin experiments, human skin is considered to be the "gold-standard". However, due to the limited availability of human skin, there are some alternatives as reconstructed human epidermis equivalents, reliable animal models for skin, as pig, and also biomimetic membranes which are easier to manipulate[73].

The first step to do these studies is the skin preparation. Skin is dissected, in this case from pig ear, and after excision it should quickly be stored deep frozen in tightly sealed plastic bags at -20 °C to -30 °C until use. It is important to pay attention to skin thickness – reducing the thickness will generally reduce experiment times/increase penetrated quantity. As well, long lag-times encountered with hydrophilic substances may require the further separation of the skin into its individual layers. Furthermore, care has to be taken to avoid any damage to the SC barrier[73].

Most publications in the field of skin penetration research are carried out using a large variety of set-ups and experimental protocols, both static and flow-through diffusion cells are approved. For *in vitro* penetration of drugs experiments, Franz diffusion cells (**Figure 42**) were largely used as they are two-compartment test system for the use of artificial membranes, reconstructed skin and excised skin. Basically, a donor and an acceptor compartment are separated by a membrane (skin); and sampling from the acceptor compartment is performed either continuously or at pre-determined time intervals[73]. Sampling of the experiments done in this work were at pre-determined times. Moreover, dosing is possible in infinite (dose that is large enough to maintain constant concentration in the donor during the course of an experiment) or finite manner (as permeation proceeds, a steady-state rate of absorption is not achieved)[73]. According to this classification, in this work dosing was infinite.

Control of temperature could be provided by a water jacket around each permeation cell, an external water bath or by warm air in a drying oven. Acceptor compartment should be at 37 °C, mimicking body temperature. Constant stirring of acceptor phase is also important in order to ensure diffusion and to homogenize acceptor solution. These solutions preferably comprise of buffer solutions of pH 7,4, mimicking physiological conditions[73].

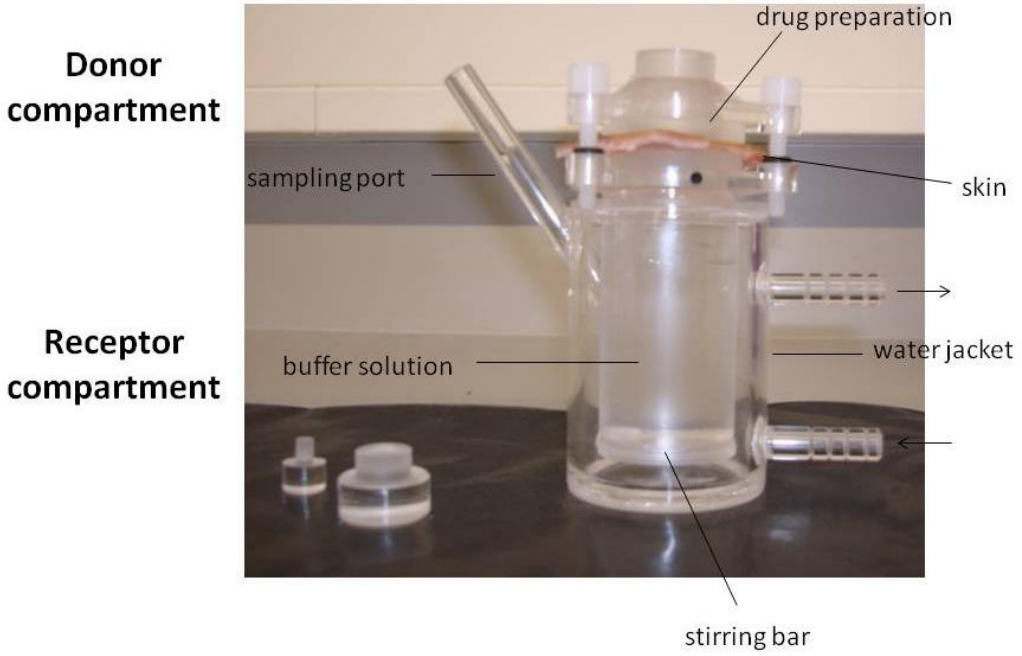

Figure 42: Vertical Franz diffusion cell used for penetration assays.

3.5.1 Methods

Initially, pig ear skin was excised and dissected. Skin surface was cleaned and hairs were removed. With a scalpel and a forceps to help, skin was excised. Then, skin was divided in pieces in order to be placed in Franz cells, and subcutaneous fatty tissue was removed. For storage, those pieces were frozen within plastic bags.

Franz diffusion cells experiments were made in triplicate for both formulations tested – NLC 2% minoxidil and NLC 2% finasteride. Penetration of both placebos were also analysed in order to discount their absorbance to drug-loaded NLC.

The receptor compartment was filled with phosphate buffer pH 7,4, and maintained at 37 °C and with stirring during all the experiment. When the skin is placed between the two compartments, is important to seal properly and to do not leave air bubbles between the skin and buffer. In the donor compartment 1 mL of NLC was placed. When the apparatus is ready the experiment begins and the time starts counting. Samples were taken at pre-determined time intervals (30 min, 1h, 1h30, 3h, 6h, 9h, 10h, 22h and 24h) from the sampling port; and the same volume removed is replaced with buffer. Again, air bubbles between skin and buffer need to me removed.

In the end, determination of the drug content in the samples was done using UV/VIS Spectrometer to minoxidil and high performance liquid chromatography (HPLC) to finasteride.

The concentration values obtained from these techniques need to be corrected according to the dilutions of receptor phase that were made after removing all the samples. This correction was made using the following equation[73]:

$$C_{cor} = C_{measured} + \frac{sample\ volume}{acceptor\ volume} \times (C_1 + C_2 + \cdots + C_{measured-1})$$

To minoxidil, PerkinElmer Lambda 45 UV/VIS Spectrometer was used to measure the absorbance of all samples obtained from experiments with NLC 2% minoxidil and NLC placebo. The spectrum of each NLC placebo sample was then subtracted to the spectrum of the corresponding NLC 2% minoxidil sample (the one taken at the same time interval). In the obtained spectra, absorbance values at 288 nm were read and, using the equation of the calibration curve made at this wavelength, minoxidil concentrations were calculated. As already mentioned above, these measured concentrations of the samples were then corrected. The penetration percentage was calculated by:

$$Penetration\ (\%) = \frac{[\text{Drug in the sample}] \times 100}{[\text{Drug in the formulation}]}$$

A spectrum of the phosphate buffer was also analyzed to establish the absorbance baseline.

To finasteride, HPLC method was used to determine concentrations of this drug in the samples. According to *Segall, et al.*[74], chromatographic determination was performed in a LC equipment using a MD-2015 multi-wavelength detector (Jasco, Japan) programmed for peak detection at 210 nm, a high-pressure pump (PU-2080) and a controller (LC-Net II/ADC) mastered by ChromNAV software. A reversed-phase monolithic column Chromolith RP-18e (100 × 4.6 mm i.d.) (Merck) connected to a guard column of the same material (5 × 4.6 mm i.d.) was used as stationary phase. Separation was conducted by isocratic mode (mobile phase containing 70% (v/v) methanol and 30% (v/v) water). Sample introduction was performed through a 20 µL loop assembled to a Rheodyne 7725i six-port manual injector. Chromatogram peak areas were related to concentrations by using standard solutions of finasteride. As already mentioned above, these measured concentrations of the samples were then corrected. The penetration percentage was also calculated using the same equation as for minoxidil.

3.5.2 Penetration of minoxidil

NLC 2% minoxidil was studied using Franz diffusion cells in order to assess the penetration of this drug through the skin (**Figure 43**).

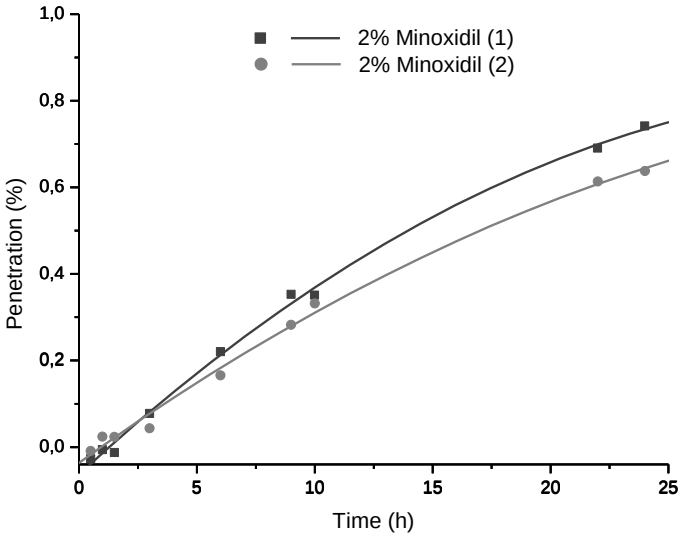

Figure 43: Penetration of minoxidil through the skin over 24 h. The two lines correspond to duplicate experiments.

It is important to note that three trials were made, but one of them was despised. Furthermore, a second order polynomial fit was used to draw the profile of penetration.

After 24 h, minoxidil penetration reached 0,74% and 0,64% of the quantity of drug initially placed in the donor compartment (4 mg). This means that only a very low quantity of minoxidil crossed the skin. Previous studies[13] indicate the difficulty that exists in this drug penetration through the skin. In a study, minoxidil-loaded SLN and pig ear skin were evaluated – after 24 h minoxidil had not crossed the skin; and in another study, penetration of minoxidil-loaded SLN through human epidermis was assessed – penetration occurs but exists a lag time of 6 h. Therefore, and since there are not many more experiments and values reported, the results obtained in this work were not different than what was expected according to the literature. A possibility to promote minoxidil penetration is the application of permeation enhancers like alcoholic solutions.

3.5.3 Penetration of finasteride

NLC 2% finasteride was studied using Franz diffusion cells in order to assess the penetration of this drug through the skin. Finasteride penetration was not possible to assess using UV/VIS Spectrometer since this drug has its maximum of absorption at 210 nm, which is the wavelength where skin constituents (which were released throughout the experiment) also largely absorb. Therefore, it was difficult and imprecise to measure finasteride with this method. For that reason, HPLC was used – thereby circumventing the problems related to the interference of the skin components released. Unfortunately, as only a small amount of finasteride crossed the skin, also HPLC did

not allow the quantification of the drug in all the samples over time, as almost all the obtained values were below the detection limit and quantification limit of the technique (**Table 17**).

Table 17: Penetration of finasteride through the skin over 24 h. The two columns correspond to duplicate experiments.

Time (hours)	Penetration (%) (1)	Penetration (%) (2)
≤ 10	0	0
22	0,00096	0,00041
24	0,0038	0,0037

It is important to note that three trials were made, but one of them was despised.

Only for the last samples – at 22 and 24h – the values obtained were quantifiable. After 24 h, finasteride penetration reached 0,0038% and 0,0037% of the quantity of drug initially placed in the donor compartment (2,5 mg). This means that only a very low quantity of finasteride crossed the skin.

Previous studies[17] indicate that the quantity of finasteride that crosses the skin is reduced. In a reported study, penetration of finasteride-loaded liposomes and niosomes through hamster ear skin was assessed – 24 h after topical application, quantity of finasteride that penetrates ranged from 5,5 to 13% of the initial dose. At first sight, these values seem to be much higher than those obtained here. However, by doing some calculations regarding these percentages and the initial dose placed in the donor compartment (which was 0,04 mL of a formulation with finasteride 0,53 mM) it is possible to reach values of penetrated mass of 0,0004 mg (5,5%) and 0,001 mg (13%). Comparing these values with the penetrated mass of 0,0001 mg (0,0038%) and 0,00009 mg (0,0037%), now they do not seem so different. Therefore, according to the literature, reduced penetration was expected and so the results obtained in this work were greatly low, but still not inappropriate. Moreover, in this described study, a 2 min massage was made after the formulation application – which promotes the penetration, and this was not done in this work.

4 Conclusions and future perspectives

Alopecia is a dermatological abnormality characterized by the reduction of visible hair. It has different types according to its cause, but one of the most common types – androgenic alopecia – affects up to half of the Caucasian male population by middle age, and almost all Caucasian men by old age (95%). Therefore, and since this disorder also affects psychologically, it is urgent to develop new drug delivery systems able to improve alopecia therapy.

The *stratum corneum* (SC) is known as the main physical barrier to most substances that come in contact with the skin. The success of dermatological products depends on the capability of the drug to overcome this barrier and to penetrate through skin in sufficient amounts to achieve the desired therapeutic effect. Bearing that in mind, several nanocarriers were developed to overcome this barrier. Among those nanocarriers, lipid nanoparticles exhibit many features for dermal application of cosmetic and pharmaceutical products, such as, the controlled release and targeting of drugs, occlusion associated with penetration enhancement, increase of skin hydration and excellent tolerability. As so, in this work NLC were chosen as systems with the ability to incorporate and deliver the anti-alopecia drugs, into the dermis and hair follicles.

From all the drugs used for alopecia therapy present in literature, in this work minoxidil and finasteride were chosen to be incorporated into lipid nanoparticles. Finasteride, an antiandrogen, is a synthetic steroid that selectively inhibits the action of the type II 5α-reductase enzyme. This enzyme converts T to DHT, which is an androgen involved in hair growth. Low levels of DHT/inhibition of 5α-reductase were already related to low levels of alopecia. On the other hand, minoxidil is a hydrophilic compound widely used to treat alopecia, but its mechanism of action is not so well known. It is a vasodilator initially approved as a drug to control hypertension – and this was the way to discover minoxidil ability to make hair growth. The effects of both drugs could be synergic and this could be an advantage to this formulation.

Lipid nanoparticles with anti-alopecia drugs were produced with success by ultrasonication method. It was possible to obtain lipid nanoparticles with size below 200 nm (some of them around 200 nm) as desired to achieve the dermis and hair follicles. Zeta potential values, in absolute values, were high enough to assure a good electrostatic stabilization for all NLC tested. Over one month of investigation, a constant particle size could be observed and zeta potential values stayed practically unchanged – which indicate a good physical stability in storage.

Beside a good physical stability, also a good chemical stability of anti-alopecia drugs-loaded NLC was observed when stored over one month: loading efficiency remained constant. This is important to avoid losing drugs during the production and

also to avoid the need of using higher concentration of drugs. However, for NLC of minoxidil, low values of loading efficiency were obtained.

After analyzing the physical and chemical stability of loaded LN for both drugs in storage, investigations about nanoparticles morphology, polymorphic modifications and *in vitro* drug penetration were performed.

Morphological investigations showed that all nanoparticles exhibit a spherical shape and a smooth surface independently of their composition.

Furthermore, DSC investigations showed that all loaded LN are solid for both body (37 ºC) and skin temperatures (32 ºC) since the onset temperature and the melting peak were above these temperatures, as desired for dermal application. The phase transition temperatures obtained by DSC were similar to those obtained by DLS – however, a discrepancy of approximately 5 °C between methods was detected (values obtained with DLS were lower than those obtained with DSC).

Penetration assays demonstrated that, mimicking physiological values of pH and temperature, NLC loaded with minoxidil and finasteride have low levels of penetration through pig ear skin. Finasteride had some problems to be detected and measured – this could be bypassed by improving quantification/detection limits of the method.

Before concluding about the real potentiality of these nanoformulations and the possibility of actually using these nanoparticles in anti-alopecia therapy, several experiments still need to be performed. First it is important to assure that all experiments are repeated at least three times, which did not happen because of the time restrictions to complete the most appropriated tests for a formulation development in the short time period given. DSC investigations should be done over time to evaluate the possible polymorphic modifications that can occur in storage. Drug release studies from the nanoparticles – that were not done for this work – should be done for all drugs used and in triplicate, at skin and plasma physiological conditions. Also more penetration studies should be done, for all drugs concentrations tested, and an evaluation of how the penetration varies with drug concentration should be done. Furthermore, despite this work involves various attempts to achieve a NLC of minoxidil with a good loading efficiency, future work could be focused on the best way to incorporate minoxidil in LNs, ensuring a higher loading efficiency. Still, the addition of another drug to LNs should be considered in order to create more effective LNs, with more ways to action.

Nevertheless, the combination of these two anti-alopecia drugs incorporated in NLC, have already proved to gather several good characteristics that indicate that the proposed novel formulation can be an excellent therapy for alopecia.

References

1. Forster, M., Bolzinger, M.-alexandrine, Fessi, H. & Briançon, S. Topical delivery of cosmetics and drugs. Molecular aspects of percutaneous absorption and delivery. *Eur J Dermatol* **19**, 309-323 (2009).

2. Baroli, B. Penetration of Nanoparticles and Nanomaterials in the Skin : Fiction or Reality ? *Structure* **99**, 21-50 (2010).

3. Agache, P. & Humbert, P. *Measuring the Skin*. 96 (Springer Berlin / Heidelberg: Berlin, 2004).

4. Naik, A., Kalia, Y.N. & Guy, R.H. Transdermal drug delivery: overcoming the skin's barrier function. *PSTT* **3**, 318-326 (2000).

5. Pouillot, A., Dayan, N., Polla, A.S., Polla, L.L. & Polla, B.S. The stratum corneum: a double paradox. *Journal of Cosmetic Dermatology* **7**, 143-148 (2008).

6. Desai, P., Patlolla, R.R. & Singh, M. Interaction of nanoparticles and cell-penetrating peptides with skin for transdermal drug delivery. *Mol Membr Biol* **27**, 247-259 (2010).

7. All Refer.com Health. at <http://health.allrefer.com/pictures-images/skin-layers.html, accessed on 10 March 2012>

8. Wosicka, H. & Cal, K. Targeting to the hair follicles: Current status and potential. *Journal of Dermatological Science* **57**, 83-89 (2010).

9. Chourasia, R. & Jain, S.K. Drug Targeting Through Pilosebaceous Route. *Current* 950-967 (2009).

10. Meidan, V.M., Bonner, M.C. & Michniak, B.B. Transfollicular drug delivery-is it a reality? *International journal of pharmaceutics* **306**, 1-14 (2005).

11. Li, L. & Hoffman, M. Topical liposome delivery of molecules t . o hair follicles in mice. *Journal of Dermatological Science* **14**, 101-108 (1997).

12. Lauer, A.C., Lieb, L.M., Ramachandran, C., Flynn, G.L. & Weiner, N.D. Transfollicular Drug Delivery. *Pharmaceutical Research* **12**, 179-186 (1995).

13. Padois, K. *et al.* Solid lipid nanoparticles suspension versus commercial solutions for dermal delivery of minoxidil. *International journal of pharmaceutics* **416**, 300-304 (2011).

14. Zhao, Y., Brown, M.B. & Jones, S. a The effects of particle properties on nanoparticle drug retention and release in dynamic minoxidil foams. *International journal of pharmaceutics* **383**, 277-84 (2010).

15. Schäfer-korting, M., Mehnert, W. & Korting, H.-christian Lipid nanoparticles for improved topical application of drugs for skin diseases ☆. *Advanced Drug Delivery Reviews* **59**, 427-443 (2007).

16. Kikwai, L. *et al.* In Vitro and In Vivo Evaluation of Topical Formulations of Spantide II. *Aaps Pharmscitech* **6**, 565-572 (2005).

17. Tabbakhian, M., Tavakoli, N., Jaafari, M.R. & Daneshamouz, S. Enhancement of follicular delivery of finasteride by liposomes and niosomes 1. In vitro permeation and in vivo deposition studies using hamster flank and ear models. *International journal of pharmaceutics* **323**, 1-10 (2006).

18. Barry, B.W. Drug delivery routes in skin: a novel approach. *Advanced drug delivery reviews* **54 Suppl 1**, S31-40 (2002).

19. Kwon, T.K. & Kim, J.C. In vitro skin permeation of monoolein nanoparticles containing hydroxypropyl beta-cyclodextrin/minoxidil complex. *International journal of pharmaceutics* **392**, 268-73 (2010).

20. Casagrande, R. *et al.* In vitro evaluation of quercetin cutaneous absorption from topical formulations and its functional stability by antioxidant activity. *International journal of pharmaceutics* **328**, 183-190 (2007).

21. Singh, H.P., Tiwary, A.K. & Jain, S. Preparation and in Vitro , in Vivo Characterization of Elastic Liposomes Encapsulating Cyclodextrin-Colchicine Complexes for Topical Delivery of Colchicine. *Pharmaceutical Sciences* **130**, 397-407 (2010).

22. Chambi, H.N.M., Alvim, I.D., Barrera-Arellano, D. & Grosso, C.R.F. Solid lipid microparticles containing water-soluble compounds of different molecular mass: Production, characterisation and release profiles. *Food Research International* **41**, 229-236 (2008).

23. Naisbitt, D.J. Drug hypersensitivity reactions in skin: understanding mechanisms and the development of diagnostic and predictive tests. *Toxicology* **194**, 179-196 (2004).

24. Kim, M.S., Na, C.H., Choi, H. & Shin, B.S. Prevalence and factors associated with neonatal occipital alopecia: a retrospective study. *Annals of dermatology* **23**, 288-92 (2011).

25. Ellis, J. a & Sinclair, R.D. Male pattern baldness: current treatments, future prospects. *Drug discovery today* **13**, 791-7 (2008).

26. Alzolibani, A.A. Epidemiologic and genetic characteristics of alopecia areata (part 1). *Acta Dermatoven APA* **20**, 191-198 (2011).

27. Coda, A.B. & Sinha, A. a Integration of genome-wide transcriptional and genetic profiles provides insights into disease development and clinical heterogeneity in alopecia areata. *Genomics* **98**, 431-9 (2011).

28. *Farmacopeia Portuguesa VIII. 8th ed*. (2007).

29. Sawaya, M.E. & Shapiro, J. Alopecia: unapproved treatments or indications. *Clinics in Dermatology* **18**, 177-186 (2000).

30. Neubert, R.H.H. Potentials of new nanocarriers for dermal and transdermal drug delivery. *European journal of pharmaceutics and biopharmaceutics* **77**, 1-2 (2011).

31. Pardeike, J., Hommoss, A. & Müller, R.H. Lipid nanoparticles (SLN, NLC) in cosmetic and pharmaceutical dermal products. *International journal of pharmaceutics* **366**, 170-84 (2009).

32. Beck, R., Guterres, S. & Pohlmann, A. *Nanocosmetics and Nanomedicines: New Approaches for Skin Care*. (Springer: 2011).

33. *European Pharmacopoeia. 6th ed*. (2007).

34. Chemical Book. at <http://www.chemicalbook.com/ChemicalProductProperty_EN_CB8749079.htm, accessed on 6 July 2012>

35. Rowe, R.C., Sheskey, P.J. & Quinn, M.E. *Handbook of Pharmaceutical Excipients*. (Pharmaceutical Press, 6th ed:).

36. Artfire. at <http://www.artfire.com/modules.php?name=Shop&op=listing&product_id=2615564, accessed on 6 July 2012>

37. chemBlink. at <http://www.chemblink.com/products/9005-67-8.htm, accessed on 6 July 2012>

38. Wissing, S.A., Kayser, O. & Muller, R.H. Solid lipid nanoparticles for parenteral drug delivery. *Advanced drug delivery reviews* **56**, 1257-72 (2004).

39. Potta, S.G. & et al Development of solid lipid nanoparticles for enhanced solubility of poorly soluble drugs. *J Biomed Nanotechnol* **6**, 634-40 (2010).

40. Priano, L. & et al Solid lipid nanoparticles incorporating melatonin as new model for sustained oral and transdermal delivery systems. *J Nanosci Nanotechnol* **7**, 3596-601 (2007).

41. Vitorino, C. & et al The size of solid lipid nanoparticles: an interpretation from experimental design. *Colloids Surf B Biointerfaces* **84**, 117-30 (2011).

42. Patel, S. & et al Brain targeting of risperidone-loaded solid lipid nanoparticles by intranasal route. *J Drug Target* (2010).

43. Shah, K.A. & et al Solid lipid nanoparticles (SLN) of tretinoin: potential in topical delivery. *Int J Pharm* **345**, 163-71 (2007).

44. Schubert, M.A. & Muller-Goymann, C.C. Solvent injection as a new approach for manufacturing lipid nanoparticles-evaluation of the method and process parameters. *Eur J Pharm Biopharm* **55**, 125-31 (2003).

45. Moddaresi, M. & et al Effects of lipid nanocarriers on the performance of topical vehicles in vivo. *Journal of Cosmetic Dermatology* **8**, 136-43 (2009).

46. Gallarate, M. & et al Preparation of solid lipid nanoparticles from W/O/W emulsions: preliminary studies on insulin encapsulation. *J Microencapsul* **26**, 394-402 (2009).

47. Wang, J.X., Sun, X. & Zhang, Z.R. Enhanced brain targeting by synthesis of 3',5'-dioctanoyl-5-fluoro-2'-deoxyuridine and incorporation into solid lipid nanoparticles. *Eur J Pharm Biopharm* **54**, 285-90 (2002).

48. Charcosset, C., El-Harati, A. & Fessi, H. Preparation of solid lipid nanoparticles using a membrana contactor. *J Control Release* **108**, 112-20 (2005).

49. Ricci, M. & et al Evaluation of indomethacin percutaneous absorption from nanostructured lipid carriers (NLC): in vitro and in vivo studies. *Journal of Pharmaceutical Sciences* **94**, 1149-1159 (2005).

50. Ujkeb. at <http://ujkeb.com/facilities.html, accessed on 7 July 2012>

51. Malvern. at <http://www.malvern.com/LabEng/technology/dynamic_light_scattering/dynamic_light_scattering.htm, accessed on 7 July 2012>

52. Bioresearch online. at <http://www.bioresearchonline.com/article.mvc/Automated-Protein-Characterization-With-The-M-0002, accessed on 7 July 2012>

53. Mohanraj, V. & Chen, Y. Nanoparticles - A Review. *Tropical Journal of Pharmaceutical Research* **5**, 561-573 (2006).

54. Mehnert, W. & Mader, K. Solid lipid nanoparticles: production, characterization and applications. *Advanced drug delivery reviews* **47**, 165-96 (2001).

55. Kaur, I.P. & et al Potential of solid lipid nanoparticles in brain targeting. *J Control Release* **127**, 97-109 (2008).

56. Souto, E.B. & et al Development of a controlled release formulation based on SLN and NLC for topical clotrimazole delivery. *Int J Pharm* **278**, 71-7 (2004).

57. Castelli, F. & et al Characterization of indomethacin-loaded lipid nanoparticles by differential scanning calorimetry. *Int J Pharm* **304**, 231-8 (2005).

58. Saupe, A. & et al Solid lipid nanoparticles (SLN) and nanostrucured lipid carriers (NLC) - structural investigations on two different carrier systems. *Bio-medical materials and engineering* **15**, 393-402 (2005).

59. Underwriters Laboratories. at <http://www.ulttc.com/en/methods/analysis/dsc.php, accessed on 11 July 2012>

60. Freitas, C. & Muller, R.H. Correlation between long-term stability of solid lipid nanoparticles (SLN) and crystallinity of the lipid phase. *Journal of Arbeitsgemeinschaft fur Pharmazeutische Verfahrenstechnik e V* **47**, 125-32 (1999).

61. Reitz, C. & Kleinebudde, P. Solid state characterization of sustained release lipid matrices prepared by solid lipid extrusion. 3-6 (2007).

62. Al-Bader, T. & et al Topical cosmetic compositions for treatng or preventing cellulite. *Oriflame Cosmetics SA* (2009).

63. D, G. Com posns. for removing subcutaneous fat - contg. coenzyme A, carnitine and caffeine. *Sederma SA*

64. Schafer-Korting, M. *Drug Delivery*. (Springer: 2010).

65. Bunjes, H., Koch, M.H. & Westesen, K. Influence of emulsifiers on the crystallization of solid lipid nanoparticles. *J Pharm Sci* **92**, 1509-20 (2003).

66. Zimmermann, E., Souto, E.B. & Muller, R.H. Physicochemical investigations on the structure of drug-free and drug-loaded solid lipid nanoparticles (SLN) by means of DSC and 1HNMR. *Pharmazie* **60**, 508-13 (2005).

67. Michel, N., Fabiano, A.-S., Polidori, A., Jack, R. & Pucci, B. Determination of phase transition temperatures of lipids by light scattering. *Chemistry and physics of lipids* **139**, 11-9 (2006).

68. Grancelli, A. *et al.* Interaction of 6-Fluoroquinolones with Dipalmitoylphosphatidylcholine Monolayers and Liposomes. *Langmuir* **18**, 9177-9182 (2002).

69. Encyclopedia Britannica. at <http://www.britannica.com/EBchecked/topic-art/526571/110970/Scanning-electron-microscope, accessed on 9 July 2012>

70. Heurtault, B. & et al Physico-chemical stability of colloidal lipid particles. *Biomaterials* **24**, 4283-300 (2003).

71. Freitas, C. & Muller, R.H. Effect of light and temperature on zeta potential and physical stability in solid lipid nanoparticle (SLN (TM)) dispersions. *International journal of pharmaceutics* **168**, 221-229 (1998).

72. Ruktanonchai, U. & et al Physicochemical characteristics, cytotoxicity, and antioxidant activity of three lipid nanoparticulate formulations of alpha-lipoic acid. *Aaps Pharmscitech* **10**, 227-34 (2009).

73. *Cell Course 2008*. (Saarland University: Saarbruecken, Germany, 2008).

74. Segall, A.I., Vitale, M.F., Perez, V.L., Palacios, M.L. & Pizzorno, M.T. A stability-indicating HPLC method to determine finasteride in a tablet formulation. *Journal of Liquid Chromatography & Related Technologies* **25**, 3167-3176 (2002).

Appendix I

Table 18: All nanoformulations done with minoxidil entrapped – to select the best according to its characteristics. Marked in red are the selected ones.

Formulation	Constitution					Characteristics			
	Drug (mg)	Solid lipid (mg)	Liquid lipid (mg)	Surfactant (mg)	Water (µL)	Loading efficiency (%)	Phase separation	Grumes	Appearance
1	30	320 Imwitor 308	150 Miglyol	100 Polysorbate 60	4400	15,5	Yes	No	Milky white + yellow oily
2	50	300 Imwitor 308	150 Miglyol	100 Polysorbate 60	4400	33,1	Yes	No	Milky white + yellow oily
3	30	350 Imwitor 308	120 Miglyol	100 Polysorbate 60	4400	5,3	Yes	No	Milky white + yellow oily
4	30	335 Imwitor 308	135 Miglyol	100 Polysorbate 60	4400	9,2	Yes	No	Milky white + yellow oily
5	60	290 Imwitor 308	150 Miglyol	100 Polysorbate 60	4400	23	Yes	No	Milky white + yellow oily
6	60	350 Imwitor 308	90 Miglyol	100 Polysorbate 60	4400	19,5	Yes	No	Milky white + yellow oily
7	60	320 Imwitor 308	120 Miglyol	100 Polysorbate 60	4400	8,8	Yes	No	Milky white + yellow oily
8	50	100 Cetyl palmitate	350 Imwitor 308	100 Polysorbate 60	4400	4,9	Yes	Yes	Milky white + translucent
9	50	300 Cetyl palmitate	150 Imwitor 308	100 Polysorbate 60	4400	11,1	No	Yes	Milky white + translucent
10	7,5	350 Cetyl palmitate	142,5 Imwitor 308	100 Polysorbate 60	4400	21	No	Yes	Milky white + translucent
11	7,5	350 Cetyl palmitate	142,5 Oleic acid	100 Polysorbate 60	4400	5,6	No	No	Milky white
12	5	863,5 Cetyl palmitate	91 Oleic acid	50,5 Polysorbate 60	3990	-	No	No	Solid after a night
13	10	767,5 Cetyl palmitate	182 Oleic acid	50,5 Polysorbate 60	3990	-	No	No	Solid after a night
14	15	671,5 Cetyl palmitate	273 Oleic acid	50,5 Polysorbate 60	3990	17	No	No	Milky white
15	20	671,5 Cetyl palmitate	268 Oleic acid	50,5 Polysorbate 60	3990	0,4	No	No	Solid after a night
16	30	671,5 Cetyl palmitate	258 Oleic acid	50,5 Polysorbate 60	3990	-2,7	No	No	Solid after a night
17	15	656,5 Cetyl palmitate	288 Oleic acid	50,5 Polysorbate 60	3990	16,6	No	No	Milky white
18	20	651,5 Cetyl palmitate	288 Oleic acid	50,5 Polysorbate 60	3990	34	No	No	Milky white
19	30	641,5 Cetyl palmitate	288 Oleic acid	50,5 Polysorbate 60	3990	24,5	No	No	Milky white
20	12	169 Cetyl palmitate + 169 Imwitor 308	150 Oleic acid	100 Polysorbate 60	4400	10	No	No	Milky white
21	30	160 Cetyl palmitate + 160 Imwitor 308	150 Oleic acid	100 Polysorbate 60	4400	9,2	No	No	Milky white
22	12	175 Cetyl palmitate + 175 Imwitor 308	138 Oleic acid	100 Polysorbate 60	4400	17,7	No	No	Milky white
23	30	175 Cetyl palmitate + 175 Imwitor 308	120 Oleic acid	100 Polysorbate 60	4400	-0,7	No	No	Milky white
24	30	1020 Cetyl palmitate	450 Oleic acid	250 Polysorbate 60	3250	20,9	No	No	Milky white
25	30	1020 Cetyl palmitate	450 Oleic acid	500 Polysorbate 60	3000	-2,9	No	No	Milky white
26	30	510 Cetyl palmitate + 510 Witepsol E85	450 Oleic acid	250 Polysorbate 60	3250	-0,9	No	No	Milky white
27	30	510 Cetyl palmitate + 510 Witepsol E85	450 Oleic acid	500 Polysorbate 60	3000	6,5	No	No	Milky white